DASA-2482

PIFR-137

DEVELOPMENT AND APPLICATIONS OF MYLAR STRIPLINES

by

S. Shope, I. Smith, G. Yonas, P. Spence, R. Ward, and B. Ecker

January 1970

This research has been sponsored
by the Defense Atomic Support Agency under
NWER Subtask LA013 Contract DASA 01-69-C-0016

Prepared by

Physics International Company
2700 Merced Street
San Leandro, California 94577

ABSTRACT

This report covers the development and application of Mylar striplines capable of producing currents in excess of 1 MA with pulse widths on the order of 50 nsec. The low-voltage line has a maximum operating voltage of 200 kV and a total impedance of 0.1 ohm. The high-voltage line can be operated up to 750 kV and has a total impedance of 1.8 ohms. Both lines use Mylar as the energy-storage medium and are switched with solid-dielectric switches. The low-voltage line drives a low-inductance diode that is used for the production of electron beams. The high-voltage line drives a double-sided diode with a line impedance of 3.6 ohms driving each side of the diode. The double-sided diode uses two opposing cathodes with a thin anode between them.

FOREWORD

This report presents the results of a program in which Mylar dielectric transmission lines were used to produce short pulses of extremely high current in electron-beam and X-ray generators. This report was written by S. Shope, R. Ward, P. Spence and B. Ecker, who performed the work; and I. Smith and G. Yonas, who supervised the program. The program was funded by the Defense Atomic Support Agency and conducted by Physics International Company under the guidance of project officers Lt. J. M. Wachtel and Major S. V. Gates.

CONTENTS

ILLUSTRATIONS

ILLUSTRATIONS (Cont.)

ILLUSTRATIONS (Cont.)

ILLUSTRATIONS (cont.)

TABLES

SECTION 1
INTRODUCTION

This report describes the work completed under Contract No. DASA 01-69-C-0016 to design, build, test, and operate two pulse generators using Mylar (polyethylene terephthalate) as a dielectric medium. These generators are often referred to as "low-impedance" machines. The two pulse generators are differentiated by their applications and their operating voltages. Both the high-voltage and low-voltage lines incorporate strip-transmission-line configurations.

The low-voltage line has been used to drive very low-impedance electron beam tubes. It is capable of producing currents of more than a million amperes (MA) in pulses lasting tens of nanoseconds. The goal of this development program has been to extract a beam of electrons having a mean energy of 100 kV and a current of more than 1 MA from the tube. We also wished to attempt some preliminary work in the kinds of beam control and diagnostics necessary to use such a beam to investigate the response of materials to extremely intense energy deposition. The low-voltage generator is an assembly of generator modules that are simultaneously pulse-charged, then triggered to feed a common load through several multichannel switches in each module. This report first discusses the design, construction, and testing of this system as a well-understood, reproducible and operational tool. Next follows the testing of the successful tube design. This design comprises an insulating envelope, low-inductance electrodes, and a low-impedance diode that has conducted about 1.5 MA at a peak electron energy of less than 100 kV.

The low-voltage line section concludes with a description of a series of experiments we performed to investigate the possibility of extracting the electrons in single or multiple beams.

The low-voltage line was designed to operate at charging voltages low enough that relatively familiar techniques would guarantee that little time would be spent in combating insulation breakdowns. The high-voltage line was, on the contrary, designed to be operated at between 500 kV and 1 MV. The main objective with this generator was to establish the design of a convenient module that would operate at as high a voltage as possible, generate about 1 MA, and be capable of forming the basic unit of a system comprising enough modules to generate currents of around 10 MA. These requirements have been met by a test program directed toward solving the problems in charging, insulation, switching, triggering, and diagnostics encountered in the routine operation of such a module. The high-voltage line section of this report discusses this test program and the results we obtained from it.

Using the results of this study, a generator was constructed to drive a two-sided X-ray tube. In this tube, the electrons are stopped in a high-Z foil target that is thin compared to an electron range. This is done by employing opposed electric fields to contain two initially opposed electron streams. The experiments defined the preliminary properties of such novel diodes, particularly the obtainable current densities and source geometries.

The body of this report comprises six sections. The first two of these are devoted to introduction, general topics, and experimental results pertaining to both generators. The other sections discuss in detail the experimental work on each of the two striplines and their respective tubes.

SECTION 2
GENERAL DISCUSSION

2.1 MYLAR STRIP TRANSMISSION LINES

The purpose of the Mylar stripline program is to develop modular pulse generators capable of producing either electron-beam or X-ray output levels not currently available. The major technical difficulty associated with both of these objectives is the generation of extremely large currents in the range of a few million amperes in short pulses lasting tens of nanoseconds and the concentration of these currents in useful areas in an X-ray tube or an electron beam accelerator.

Although other dielectrics, water particularly, are also candidates for constructing very high-current generators, or low-impedance machines as they are often called, Mylar was chosen as the subject for this study for several reasons. Data obtained in J. C. Martin's group at AWRE, Aldermaston, U.K., indicated that Mylar could be stressed under operational conditions to an electrical gradient of approximately 1.5 MV/cm. The energy density, W, in an electrostatic field is

$$W(\text{ergs/cm}^3) = \frac{\varepsilon E^2}{8} \quad (E \text{ in esu})$$

$$W(\text{J/cm}^3) = 0.044\ \varepsilon E^2 \quad (E \text{ in MV/cm})$$

For Mylar with a dielectric constant of 2.8, this energy density is approximately 0.25 J/cm^3. For water, the dielectric constant is

about 80 while the operational electric field is approximately 150 kV/cm. Since the energy density is only proportional to the dielectric constant and depends on the square of the electric field, the energy density in water is less than one-third of that in Mylar.

Another parameter of interest when comparing dielectrics is the linear current density that can be obtained from a transmission line. A strip transmission line of width w and separation s charged with an internal field E has an impedance, Z, of

$$Z = \frac{120\ \pi s}{\varepsilon^{1/2}\ w}\ \Omega$$

The voltage on such a transmission line is given by Es. The short-circuit current is therefore

$$I = \frac{Es}{Z} = \frac{\varepsilon^{1/2}\ Ew}{120\ \pi}$$

and the linear current density is

$$\frac{I}{w}\ (\text{MA/cm}) = \frac{\varepsilon^{1/2}\ E}{120\ \pi}\ (\text{E in MV/cm})$$

It is readily seen that the linear current density is proportional to the square root of the energy density, W, and is, of course, independent of the total voltage or thickness of the line. Since the current is proportional to the width w, for very high-current machines the width becomes the dominant dimension, and the size of the generator may be considered to be determined by the current rather than the voltage. Another corollary of the above results is that the current density from a Mylar line may be about twice that from a water line and this is the chief advantage of Mylar over water.

A charged Mylar strip transmission line of the type considered so far could be switched into another identical line of equal impedance (often called the series-switched mode); it could also be charged in the form of a Blumlein that would have the appearance of two transmission lines in series with the outer conductors continued to form a load line of matching impedance. These two possibilities are shown in Figures 1a and 1b. In either case the

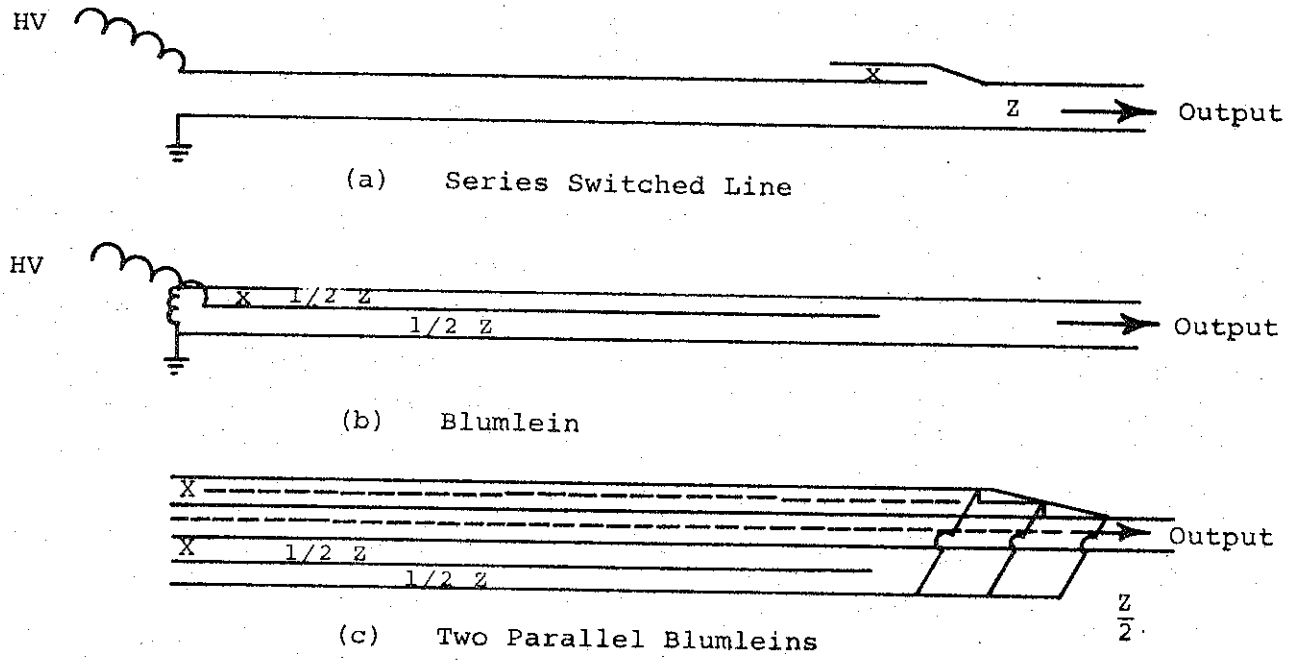

Figure 1 Mylar stripline configurations.

output pulse generated has a duration equal to twice the single transit time of the storage element. Consequently, once the line has been switched and the pulse has left the storage element and is propagating along an output line of the same impedance and the same width, the energy occupies twice the volume. In a propagating pulse of this kind, half of the energy is always in the magnetic field and only half the energy is still electrostatic, resulting in an electrostatic-energy density reduction to one-quarter of the initial value. The electrostatic field in the traveling wave is then half of the field in which the energy was stored. This phenomenon may also be seen from the fact that the

output voltages in each case are one-half of the open-circuit voltage. Thus, for a line in which the energy only propagates and is never stored, the linear short-circuit current density is

$$\frac{\varepsilon^{1/2} E}{60 \pi} \text{ (in MA/cm)}$$

The output transmission line could be tapered in width and insulation thickness by a factor of two before the electrostatic field exceeded the operational field of the generator. It is unwise to exceed this field because the breakdown strength of Mylar is time independent, which means that the output transmission line will not support more electric field than the generator just because the pulse is of brief duration. The tapering process clearly increases the linear current density by a factor of two.

A better scheme in practice is shown in Figure 1c. Adjacent to the first generator in this case, the Blumlein is a second identical generator connected in parallel at the output. In the case of the strip transmission lines, this connection would be made by folding metal around the edges of the Mylar. As the current feeds around progressively, the insulation thickness of the output line of the first generator is progressively decreased (as suggested in Figure 1c), but its width remains unchanged. The linear current density is doubled as before. Substituting the same values for ε and E used above, a current density of approximately 1.33 MA/m is obtained.

In practice, one may wish to apply to the generator a load considerably less than its own characteristic impedance without actually short circuiting the generator. If the generator is a Blumlein, the efficiency of energy transfer is given by G(2-G),

where G is the gain of the line into the load. If the load impedance is, for example, one-third of the generator impedance, then the gain is one-half. The energy-transfer efficiency may be seen to remain 75 percent and the load current is also 75 percent of the short-circuit current, or in the case considered, 1 MA/m.

Mylar can be purchased in 6-foot-wide rolls and, leaving a 6-inch clearance at the edge for tracking, gives a 60-inch or a 1.5-meter active width for the line. This width could be used efficiently at currents up to 1.5 MA.

So far the load voltage and charge voltage remain unspecified. In principle these can be chosen by correctly determining the thickness of the Mylar dielectric. In practice one is limited in charging voltage to something considerably less than 1 MV by problems of tracking, which will be considered later. If load voltages in excess of a few hundred kilovolts are required, it may be desirable to stack such modules in series to avoid inconveniently high charging voltages. A series configuration on two lines is shown in Figure 2. Apart from requiring twice as many switches, this arrangement is no different in principle from a single line charged to twice the voltage.

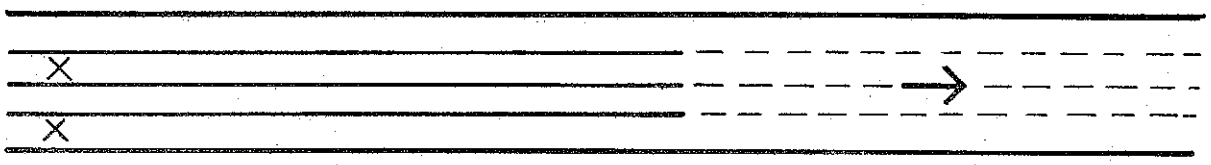

Figure 2 Two-element series Blumlein generator with output line.

2.2 COPPER SULFATE AS AN AMBIENT MEDIUM

One of the disadvantages of solid dielectrics, such as Mylar in the present application,is the problem of flashover at the edges of the conductors forming the striplines. The solution to this problem was developed at Aldermaston, U.K., and consisted of establishing a suitable liquid-immersion medium. For this medium, water is ideal because its high dielectric constant (80) protects it from electric fields high enough to cause breakdown; the field in a film of nonconducting water between a flat metal sheet and a flat Mylar sheet is only about one-thirtieth of the field in the Mylar, and if the latter is 1.5 MV/cm, the field in the water is only 50 kV/cm. This value is quite insufficient to break the water down. In this application the water does not store a significant amount of energy, but efficiently serves the purpose of applying the voltage to the Mylar itself, which is not possible using a low-dielectric-constant liquid such as oil (ε = 2.25),in which the corresponding electric field (1.8 MV/cm) far exceeds the breakdown strength. At much lower levels oil will initiate discharges that rapidly pass through the Mylar as well.

While the dielectric-constant mismatch reduces the fields in the water adjacent to the body of the Mylar dielectric, it only partly alleviates high electric fields that may occur at the edge of a sharp conductor. To prevent breakdown of the water at such an edge, and the consequent tracking, which can occur over long distances on the Mylar or eventually lead to the puncturing of the Mylar, the high field at the edges of the copper must be reduced to below 200 kV/cm, at most. This reduction can be achieved by decreasing the resistivity of the water--by adding copper sulfate, for example. Consider a sandwich of Mylar and copper (Figure 3) immersed in a copper-sulfate solution. The Mylar is of thickness D

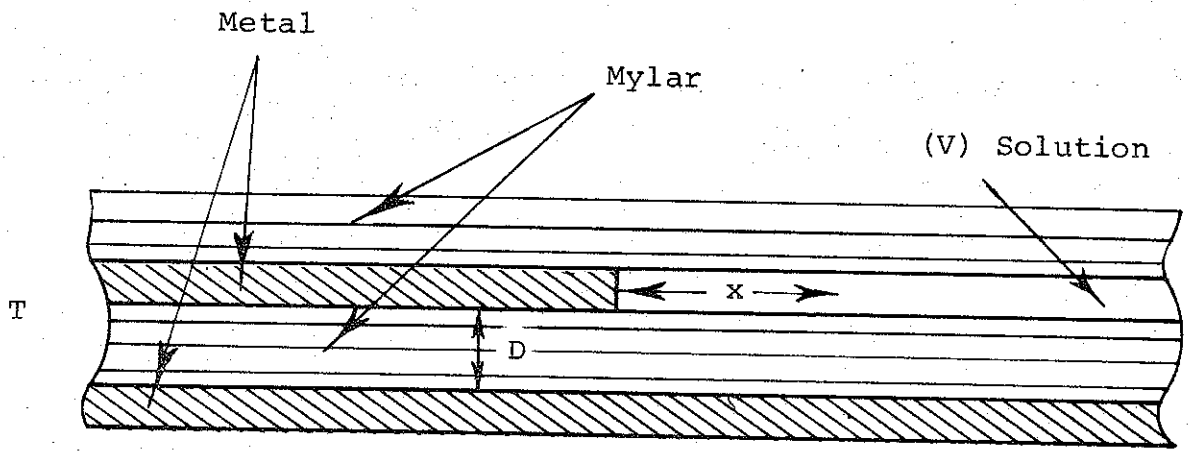

Figure 3 Pulse potential grading by conducting solution

and has a dielectric constant ε. The metal is of thickness T, and adjacent to the metal there is a film of copper sulfate of equal thickness. This film of copper sulfate acts as a resistor, and if a potential is applied to the metal edge with respect to the metal on the far side of the Mylar, conduction will take place in the copper sulfate, which will lead to this potential being transferred progressively farther away from the metal edge. This process relieves the field in the water (a certain amount of time-independent capacitive smearing of the potential also occurs but is generally insufficient to reduce the field below breakdown level).

The equations governing the spread of the potential may be derived (following J. C. Martin). If V is the potential at a distance x from the edge of the copper, the electric field in the water film is $\partial V/\partial x$. The current density j in the water film of resistivity ρ is given by

$$j = -\frac{1}{\rho}\frac{\partial V}{\partial x}$$

and hence the current per unit length in the direction of the edge is given by

$$jT = -\frac{T}{\rho}\frac{\partial V}{\partial x}$$

The difference in current per unit length at two points separated by a distance Δx is

$$-\frac{T}{\rho}\frac{\partial^2 V}{\partial x^2}\Delta x$$

This difference in current charges the capacity of an element of Mylar whose area per unit length of edge is Δx. If the capacity per square centimeter of Mylar is C_s, then the capacity of this element is $C_s \Delta x$ and its rate of charging $\partial V/\partial t$ is given by the equation

$$C_s \Delta x \frac{\partial V}{\partial t} = -\frac{T}{\rho}\frac{\partial^2 V}{\partial x^2}\Delta x$$

Let $\rho/T = R_s$, the resistance per square unit of the film of copper sulfate. Then the equation becomes

$$\frac{\partial V}{\partial t} = -\frac{1}{R_s C_s} \cdot \frac{\partial^2 V}{\partial x^2}$$

which is the familiar diffusion equation with a diffusion constant equal to $1/(R_s C_s)$. Hence, the smearing of the potential will progress in proportion to the square root of the time. If τ is the risetime of the voltage, then the peak field will be of the order of the potential divided by the diffusion distance

$$2\left(\frac{\tau}{R_s C_s}\right)^{\frac{1}{2}}$$

As an example, if the Mylar thickness is 0.5 cm, the risetime is 1.5 μsec, and the water-film thickness is 0.025 cm, a resistivity of about 7.5 kΩ/cm will reduce the peak field below 200 kV/cm. This value for resistivity corresponds to a relatively diluted solution of copper sulfate and water. This treatment may readily be applied to the case in which two copper edges line up on either side of the Mylar. This case requires only about 70 percent of the conductivity in the water. However, in a large machine there will always be edge regions of the first kind and the conductivity of the copper-sulfate solution should be low enough to compensate for this worst case.

It is also necessary to consider the effects occurring in the water when the line discharges. Generally, the sequence of events is that the voltage is applied quite gradually to the Mylar by pulse charging in a time of the order of microseconds, and then the potential is switched off in a much shorter time--approximately 10 nsec--when the line is discharged. The charge transferred by the solution to the Mylar dielectric beyond the edges of the metal must flow back through the solution and cannot do so in such a short time. This charge creates much higher fields in the liquid, and sparking can occur. Initially it was believed the sparks did not generally damage the Mylar and that the duration of the fields was so brief that long tracks would not occur. During the latter part of the program it was discovered that at the highest operating fields the fast-rising transient eventually caused line damage; the effect was remedied by improving grading. This mode of line failure and the necessary corrective measures will be discussed in a later section.

If great care is not taken when assembling the Mylar line, air bubbles may be entrapped between Mylar sheets or between Mylar

and copper. If these bubbles are within the body of the line, that is, totally between the copper electrodes and well inside their edges, the air will break down when the line is charged and discharged, but the spark is not sufficiently energetic to break down the Mylar except possibly by long-term erosion over the course of many shots. Bubbles outside the edges of the copper will also break down from the electric fields along the sheets of Mylar. The breakdown of such a bubble in this position can initiate tracks in the water, either because additional field enhancement is associated with the shape of the bubble or because the breakdown is fast and the new potentials created cannot be graded with sufficient speed.

To eliminate air bubbles in the lines, it is necessary to assemble them under degassed water. (A preferable alternative to this method is the vacuum impregnation of the lines after first assembling them completely in the dry state.) The first technique used to assemble the line was to pass each sheet of Mylar or copper slowly through the surface of the water and then immediately between neoprene squeegees to remove residual air adhering to the Mylar. This method proved unsatisfactory--air bubbles remained. After several days they would agglomerate and become visible between each layer of Mylar. It was found that the addition of a wetting solution, Emcol 4150, in a concentration of one part in 500 sufficiently wetted the Mylar to eliminate the air bubbles.*

*After assembly of the line it was necessary to recycle the water and remove the majority of the wetting solution, which not only made the water cloudy but produced a rash on hands immersed in the solution. In routine operation it is found that the chilling effect of having to work with one's hands under even a small depth of water slows such procedures as replacing solid-dielectric switches or checking connections. To help overcome this, immersion heaters were provided to raise the temperature somewhat closer to that of bath water.

2.3 DIELECTRIC CONSTANT OF MYLAR

When dry Mylar (with a dielectric constant of 2.75) is submerged in water, which has a dielectric constant of 80, it absorbs in time a certain quantity of liquid, and thus its dielectric constant might be expected to change. Workers at the Cornell University Plasma Physics Laboratory have reported observing a possible increase in dielectric constant by as much as a factor of two,as evidenced by increasing pulse duration or transit time of Mylar transmission lines. However, J. C. Martin at AWRE, Aldermaston, England, reported that he could not detect an increase of capacity in a parallel-plate Mylar capacitor after soaking it in warm copper-sulfate solution.

Such an increase in dielectric constant will obviously make Mylar a still more useful dielectric. It is important to know the dielectric constant in order to be able to design a generator of given required impedance. The impedance of the transmission line is well defined if the thickness, width, and dielectric constant are known. Also,given the impedance of an operating line, the current in the load can be deduced from the voltage gain of the line. This technique gives an important cross check for the other types of current monitoring that may be employed.

Measurements of dielectric constant were first performed using parallel-plate Mylar capacitors. It was then decided to adopt the approach of measuring the transit time of a small sample in a strip transmission line under precise conditions. In the transmission line, which was approximately a meter long, mercury was used as the metal electrodes to ensure that contact with the Mylar was virtually perfect (Figure 4). A repetitive cable pulser sent a fast-rising pulse into one end of the line. The voltage monitor at the injection

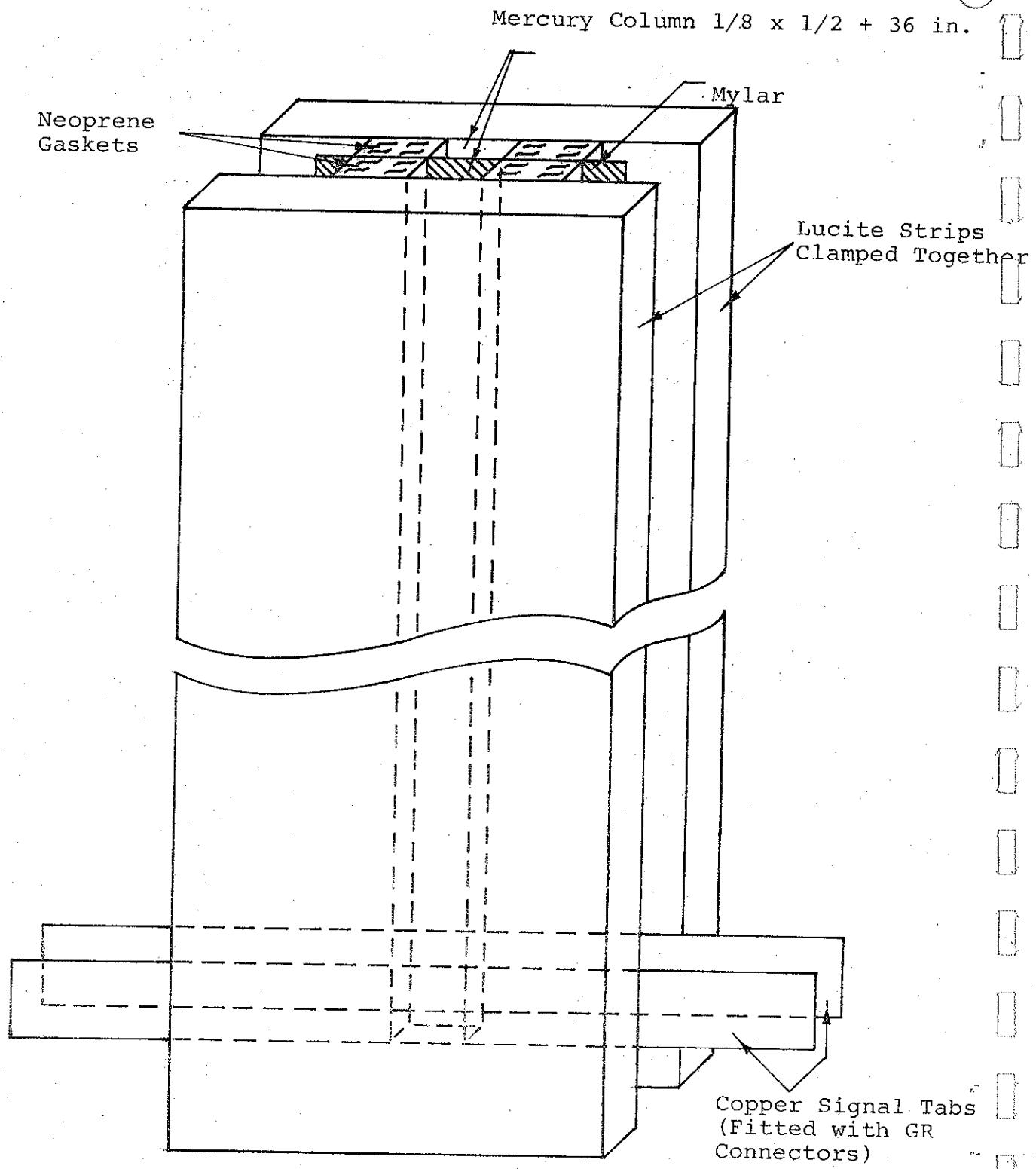

5340

Figure 4 Mercury transmission line.

point was used to display the pulse on a Model 519 Tektronix oscilloscope. The reflection from the other end of the Mylar transmission line was used to measure the double transit time.

The transmission line was vertical and the pulse was injected at the bottom. The sheet of Mylar dielectric ended at approximately the surface level of the mercury and by slightly changing the height of the mercury column it was possible to cause it to flow around the edge of the Mylar and short circuit the line or remain just below the edge and thus cause the line to be an open circuit while leaving its length essentially unchanged. Pulse traces in the conditions of open and short circuit were overlayed on the same photograph and the time of arrival of the reflection was defined very clearly (Figure 5). The double transit time and the distance between the injection point and the other end of the transmission line were used to derive the wave velocity in the Mylar and hence its dielectric constant.

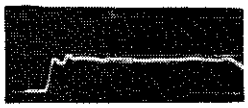

Shorted

Overlay

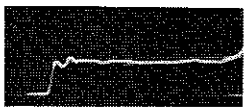

Open
Circuit

Figure 5 Ten-mil Mylar transit time.

To achieve saturation of the Mylar with water in as short a time as possible, it was desirable to use a thin sheet of Mylar. Three-mil Mylar was eventually chosen. The water diffused to the middle in approximately one-tenth the time taken to reach the middle of a sheet of 10-mil Mylar.

When thinner sheets of Mylar were employed, the risetime of the reflection became longer due to resistive losses in the mercury. The risetime τ of a pulse which has executed two transits of the transmission line may be considered to be inversely proportional to that frequency f which is attenuated by a factor of e in this distance. The frequency f may be shown to be that frequency for which the resistance R of the transmission-line electrodes from end to end is equal to twice the characteristic impedance Z of the line. In terms of the skin depth, δ

$$R \propto \delta^{-1}$$

while

$$\delta \propto f^{-\frac{1}{2}}$$

It follows that $\tau \propto f^{-1} \propto \delta^{2} \propto R^{-2} = Z^{-2} \propto d^{-2}$, where d is the thickness of the Mylar film.

With thicknesses of less than about 3 mils, the risetime, using mercury electrodes (resistivity approximately 10^{-4} Ω/cm), was so long that the pulse-reflection point was no longer well defined.

Samples of 3-mil Mylar were kept permanently immersed in warm water. At intervals of a few days the double transit time of pieces of dry Mylar was measured in the transmission line, which could be rapidly disassembled. A wet sample was then immediately compared.

In no case was a significant difference of transit time detected. The dielectric constant of Mylar is not believed to change by more than a few percent when soaked in water. Several wet samples were measured on each of the tests.

These experiments provided an excellent basis for comparison of the dielectric constants of samples of wet and dry Mylar, but did not in general yield credible results for the absolute dielectric constants of either Mylar or polyethylene, which was used as a standard. Using an oscilloscope that was apparently calibrated for a 2-nsec/cm sweep, the dielectric constant of polyethylene appeared to be 2.84, as opposed to the well-established value of 2.2, which appears in the literature. Using the value of 2.2 to provide, in effect, a calibration of the time base and the transmission-line length, the dielectric constant of Mylar appeared to be 3.0, which is within 7 percent of the usually accepted value of 2.8. We have used the value 2.8 in our calculations of the impedance of the Mylar lines subsequently built, and in terms of line impedance and short-circuit current, the error in this assumption would appear to be at most a few percent.

2.4 FAULT MODES IN MULTIPLE-LINE ASSEMBLIES

When a generator is fabricated with a number of parallel or series modules, or a series-parallel combination, there is always a possibility that one or more modules will not switch or will fire late. This possibility becomes more probable when a greater number of modules are used. An analysis has been performed to determine when this condition can lead to overvoltage of the errant modules and to determine design criteria for future generators. There are three cases of interest: parallel Blumlein, series Blumlein, and parallel-series Blumlein. Each case is analyzed for open-circuit, short-circuit, and matched-load firings.

2.4.1 Case I: Parallel Blumlein. If all the conductors of each Blumlein are strapped hard in parallel with all those of the other Blumleins, there is no overvoltaging of an unswitched line because the lines that do switch can communicate with the unswitched modules. Such design is especially attractive if many lines can be fired with one set of switches. In many cases the Blumleins are physically too far apart to permit the connections to be of sufficiently low inductance, and the only interconnection is between the uncharged output conductors at the common load. Overvoltage may then result if the switches are poorly synchronized.

Consider the case of n Blumleins (Figure 6a) connected in parallel at their output ends. Each Blumlein has unit impedance and is charged to unit voltage. Let the generator be driving a load impedance $Z_L = m/n$, where m is an arbitrary number (the degree of the mismatch). If all lines switch simultaneously, the assembly acts as a single Blumlein. The pulses traveling in component lines always tend to decrease the initial charging voltage, and though overshoot always occurs in the switched line and also in the unswitched line if $m < 1$, the voltage and field in any line never exceed the charging value, no matter what the load.

If x lines do not switch, the unswitched lines may be replaced by one Blumlein whose impedance is $1/x$, and the switched modules may be replaced by a Blumlein whose impedance is $1/n-x$ (Figure 6b shows the equivalent circuit). The unswitched Blumlein equivalent will parallel the load Z_L for the switched Blumlein, resulting in a new load impedance Z_L'.

$$Z_L' = \frac{m}{n + mx}$$

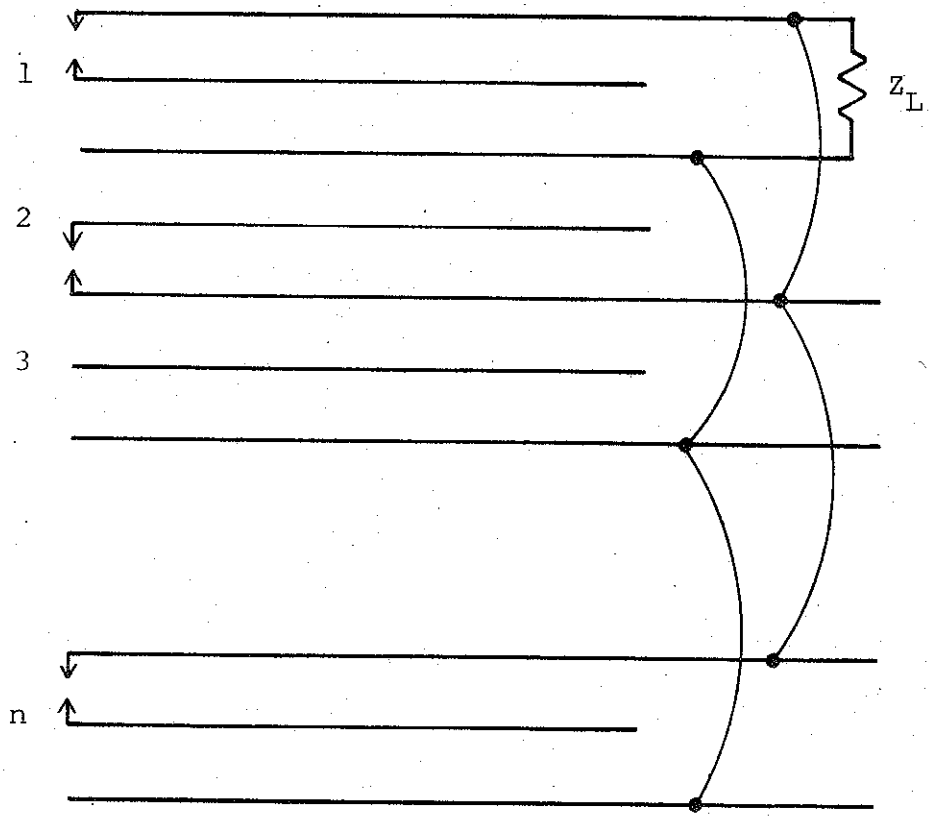

n Parallel Lines

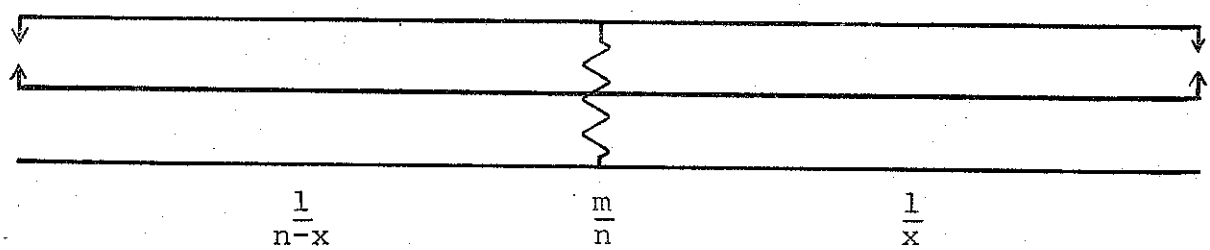

Equivalent of n Parallel Lines

Figure 6 Parallel lines.

7298

The voltage V_τ developing across the unswitched Blumlein is given by

$$V_\tau = \frac{2 Z_L'}{Z_L' + Z_o} = \frac{2 m (n - x)}{n (m + 1)}$$

where

$$Z_o = \frac{1}{n - x}$$

Examination of this equation shows that V_τ is maximum for $x = 1$; therefore, this case is the only one that will be considered.

The voltage V_τ will be divided equally between the two component lines of the unswitched Blumlein. This voltage will add to the original charge voltage in the line containing no switch and subtract in the other line. The overvoltage in the first case will be

$$V_1 = 1 + \frac{m (n - 1)}{n (m + 1)}$$

This propagates toward an open circuit, reflects, and results in a voltage

$$V_2 = 1 + \frac{2 m (n - 1)}{n (m + 1)}$$

For a large n, one finds

$$\lim_{n \to \infty} V_2 = 1 + \frac{2 m}{m + 1}$$

Consider the three representative modes of operation--short circuit, matched load, and open circuit. For these cases $m = 0$, 1, and ∞, respectively. The results are:

$$(V_2)_{m = 0} = 1$$

$$(V_2)_{m = 1} = 2$$

$$(V_2)_{m = \infty} = 3$$

2.4.2 Case II: Series Lines. Consider n Blumleins of unit impedance and charge voltage driving a load impedance m' n', where m' is an arbitrary impedance (Figure 7). If x Blumleins do not switch, the impedance of the driving source is (n' - x), which will be driving an impedance Z_L' that is the sum of the load impedance m' n' and the sum of the impedances x of the unswitched Blumleins. Thévenin's theorem may be used to find the voltage V_1 applied to the unswitched Blumleins:

$$V_1 = \frac{2x\ (n' - x)}{n'\ (m' + 1)}$$

This voltage is distributed among the x unswitched Blumleins, resulting in a voltage of

$$\frac{2\ (n' - x)}{n'(m' + 1)}$$

on each Blumlein. Each line receives half of this voltage. In the line that contains the unfired switch, this added voltage to the original charge voltage results in a voltage of

$$1 + \frac{n' - x}{n'\ (m' + 1)}$$

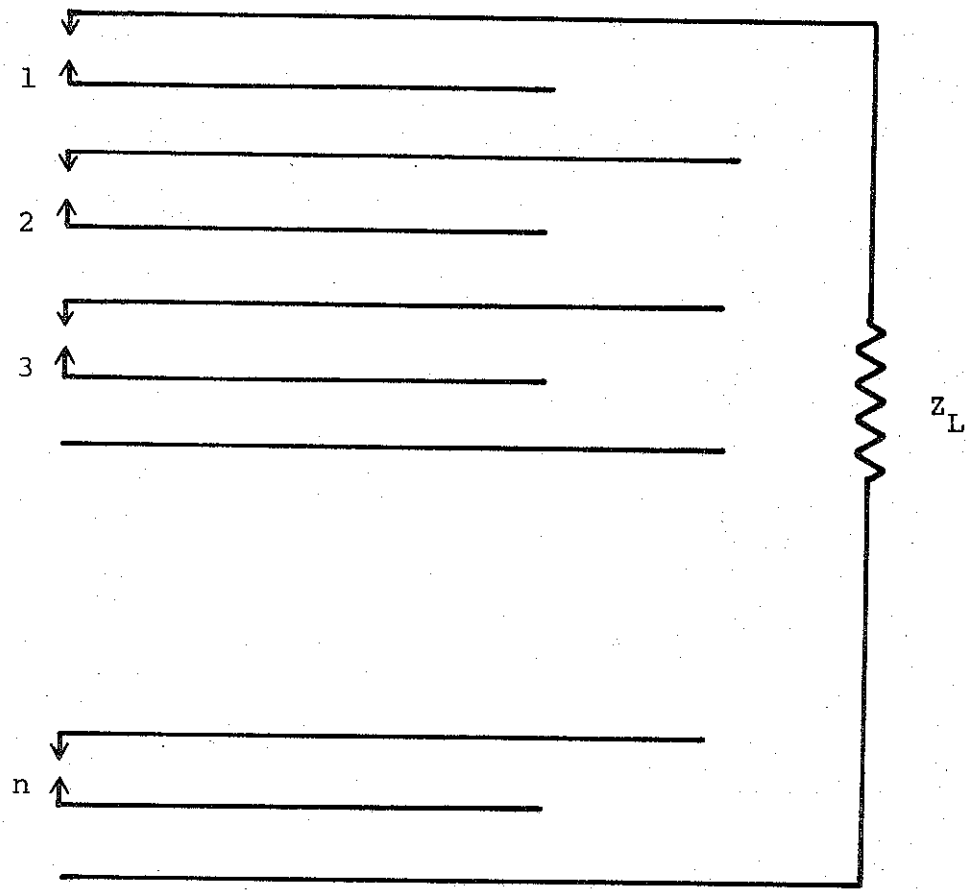

Figure 7 n' series lines.

This voltage propagates toward an open circuit and results in a voltage

$$V_2 = 1 + \frac{2\,(n' - x)}{n'(m' + 1)}$$

upon reflection. The voltage is a maximum for x = 1. Taking the limit, one finds

$$\lim_{n \to \infty} V_2 = 1 + \frac{2}{m' + 1}$$

For the short-circuit case m' = 0, matched m' = 1, and open m' = ∞

$$(V_2)_{m' = 0} = 3$$

$$(V_2)_{m' = 1} = 2$$

$$(V_2)_{m' = \infty} = 1$$

This is the same as the n parallel Blumleins except m is replaced by 1/m'.

2.4.3 Case III: Parallel-Series Modules. For this case, a generator is fabricated from n parallel modules, each comprised of two series Blumleins with unit impedance and charge voltage, driving a load 2 m/n (Figure 8a). If one module completely fails to switch, the result is the same as in the parallel-line analysis. The case of most interest is that of one Blumlein in a module not switching (Figure 8b). The resultant voltage on the unswitched Blumlein can be analyzed from results obtained from the parallel and series analyses. A voltage V_p will be induced on each line of the unswitched Blumlein from the parallel modules where

$$V_P = \frac{m\ (n - 1)}{n\ (m + 1)}$$

The results of the series analysis may be used to obtain the effect of the switched Blumlein if the load impedance m' n' in the series analysis is replaced by

$$m'\ n' = \frac{2\ m}{mn - m+n}$$

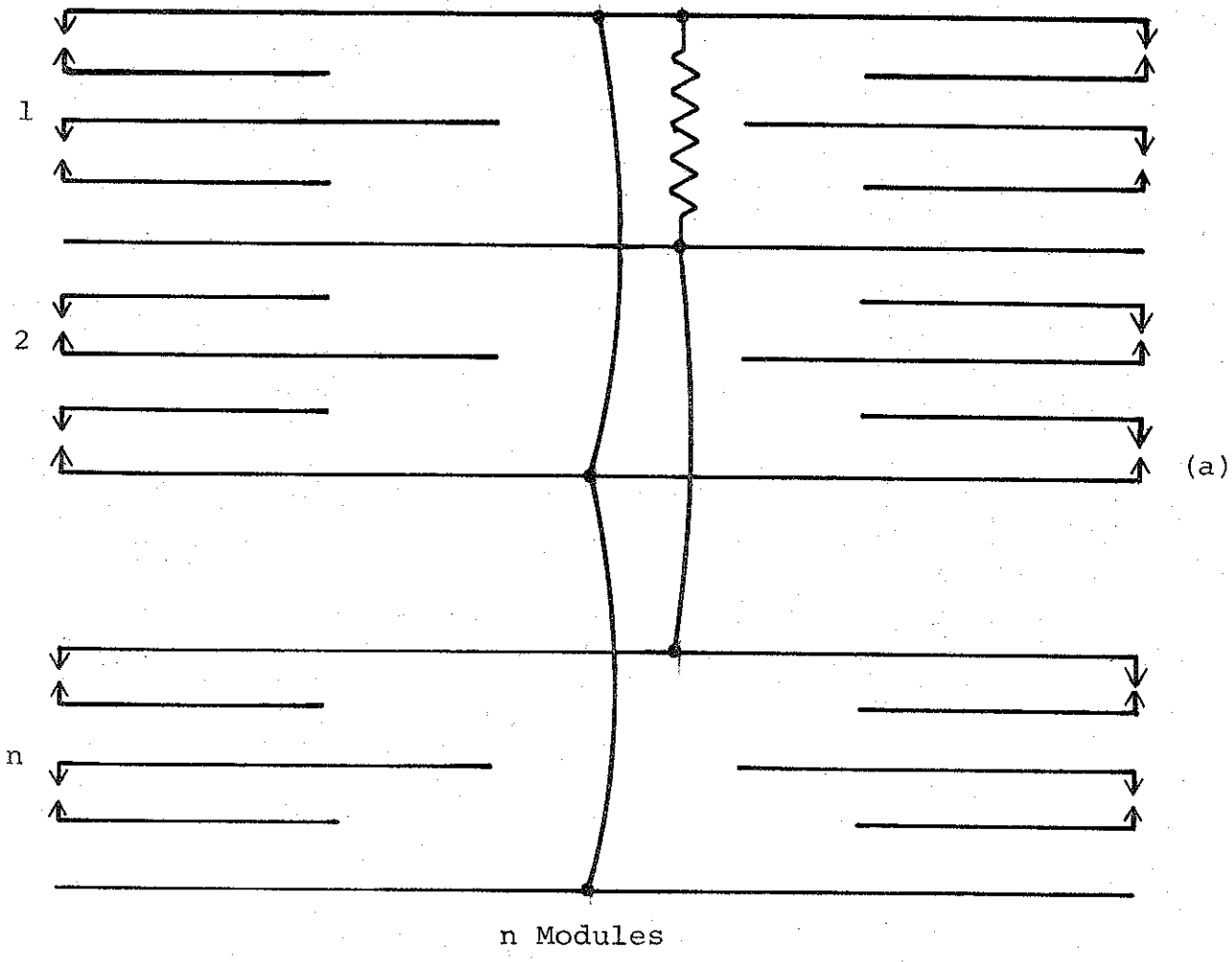

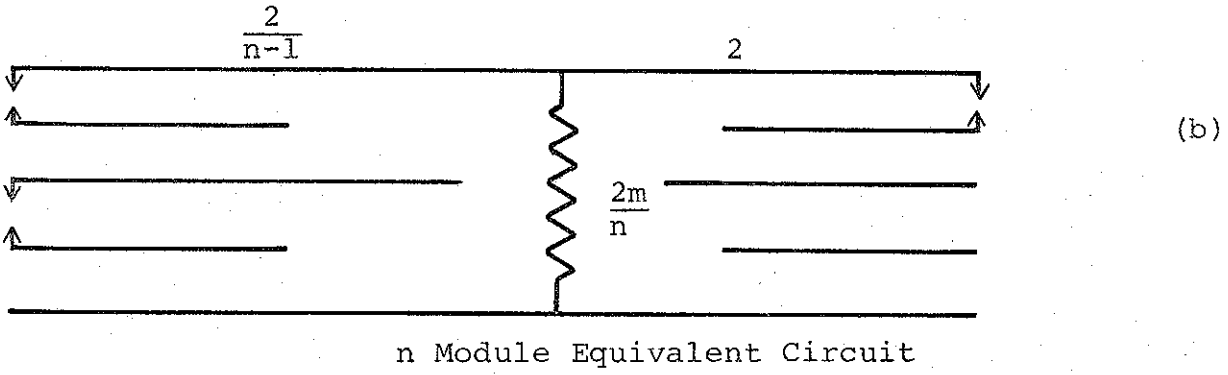

7300

Figure 8 n parallel modules of two series Blumleins

Since n' and 2, m' $= \frac{m}{m\,n - m + n}$, which results in a voltage of

$$V_s = \frac{m\,n - m + n}{2\,n\,(1 + m)}$$

induced on each line of the unfired Blumlein.

The induced voltages from the parallel and series cases are opposite in polarity so the resultant voltage on the line with no switch is

$$V_p - V_s = \frac{m\,n - m - n}{2\,n\,(1 + m)}$$

The voltage adds to the original charge voltage, propagates toward an open circuit, reflects and results in a voltage V_x of

$$V_x = 1 + \frac{m\,n - m - n}{n\,(1 + m)} = \frac{m\,(2n-1)}{n\,(1+m)}$$

$$\lim_{n \to \infty} V_x = \frac{2\,m}{1+m}$$

The voltage in the line with the unfired switch is being reduced by $V_p - V_s$ and results in a voltage V_y upon reflection, where

$$V_y = 1 - V_p + V_s$$

$$= \frac{m + n}{n\,(1 + m)}$$

$$\lim_{n \to \infty} V_y = \frac{1}{1 + m}$$

For a short circuit

$$(V_x)_{m = 0} = 0$$

$$(V_y)_{m = 0} = 1$$

For a matched load

$$(V_x)_{m = 1} = 1 - \frac{1}{2n} V_x \to 1 \text{ as } n \to \infty$$

$$(V_y)_{m = 1} = \tfrac{1}{2} + \frac{1}{2n} V_y \to \tfrac{1}{2} \text{ as } n \to \infty$$

$(V_x)_{m = 1}$ has a maximum value of one when $n = \infty$, and $(V_y)_{m + 1}$ has a maximum value of one when $n = 1$.

For an open circuit

$$(V_x)_{m = \infty} = 2 - \frac{1}{n} V_x \to 2 \text{ as } n \to \infty$$

$$(V_y)_{m = \infty} = \frac{1}{n} V_y \to 0 \text{ as } n \to \infty$$

$(V_y)_{m = \infty}$ is largest for small n and has a maximum value of $\tfrac{1}{2}$ for $n = 2$.

2.4.4 Late-Time Voltages. If the load impedance does not change with time and the initially unfired switches never close, damping effects ensure that after the first pulse the degree of overvoltage is successively reduced. If the unfired switches close less than a pulse duration after the others, the overvoltage is thereby removed. If these switches fire later still, when the

other lines are still ringing, further overvoltages that are very tedious to analyze could conceivably be developed. However, because of risetime effects and other losses, these probably will not be worse than the cases that have been treated.

2.4.5 Conclusions. If Blumleins are combined in series or in parallel, the failure of one Blumlein to switch results in one of its component lines being exposed during the first output pulse to a voltage greater than that to which it was initially charged.

For Blumleins in series, the component line bearing the switch is overvoltaged, and for parallel lines, the line without a switch is overvoltaged.

The magnitude of the overvoltage increases with the number of lines and depends upon the load impedance. It increases with decreasing load impedance for series Blumleins and increasing load impedance for parallel Blumleins. In both cases the total range of overvoltage for very large n is from 1:1 to 3:1, with 2:1 applying in the matched cases.

In practice, the purpose of series configurations has been to obtain high voltages, and therefore they have been matched high. Parallel configurations are designed to produce high currents and are matched low; therefore, the worst conditions are not usually encountered. Risetime effects and the finite value of n help to ensure that the overvoltage is considerably less than 2:1. This value is unlikely to produce breakdown of the dielectric, because the generator is usually operated at a voltage not exceeding half the single-shot voltage of a single component line in order to have a satisfactory operating life, even in the absence of all fault conditions.

Precautions to further reduce the possibility of damage from such fault conditions in which lines are operated in parallel are (1) connecting the Blumleins in parallel at the switch end whenever possible; (2) avoiding open circuit firings (e.g., to cross-calibrate monitors) at near maximum charge voltage; (3) incorporating more than one switch in each line to increase the probability that at least one will fire; and (4) using the series-parallel configuration, which is inherently safer.

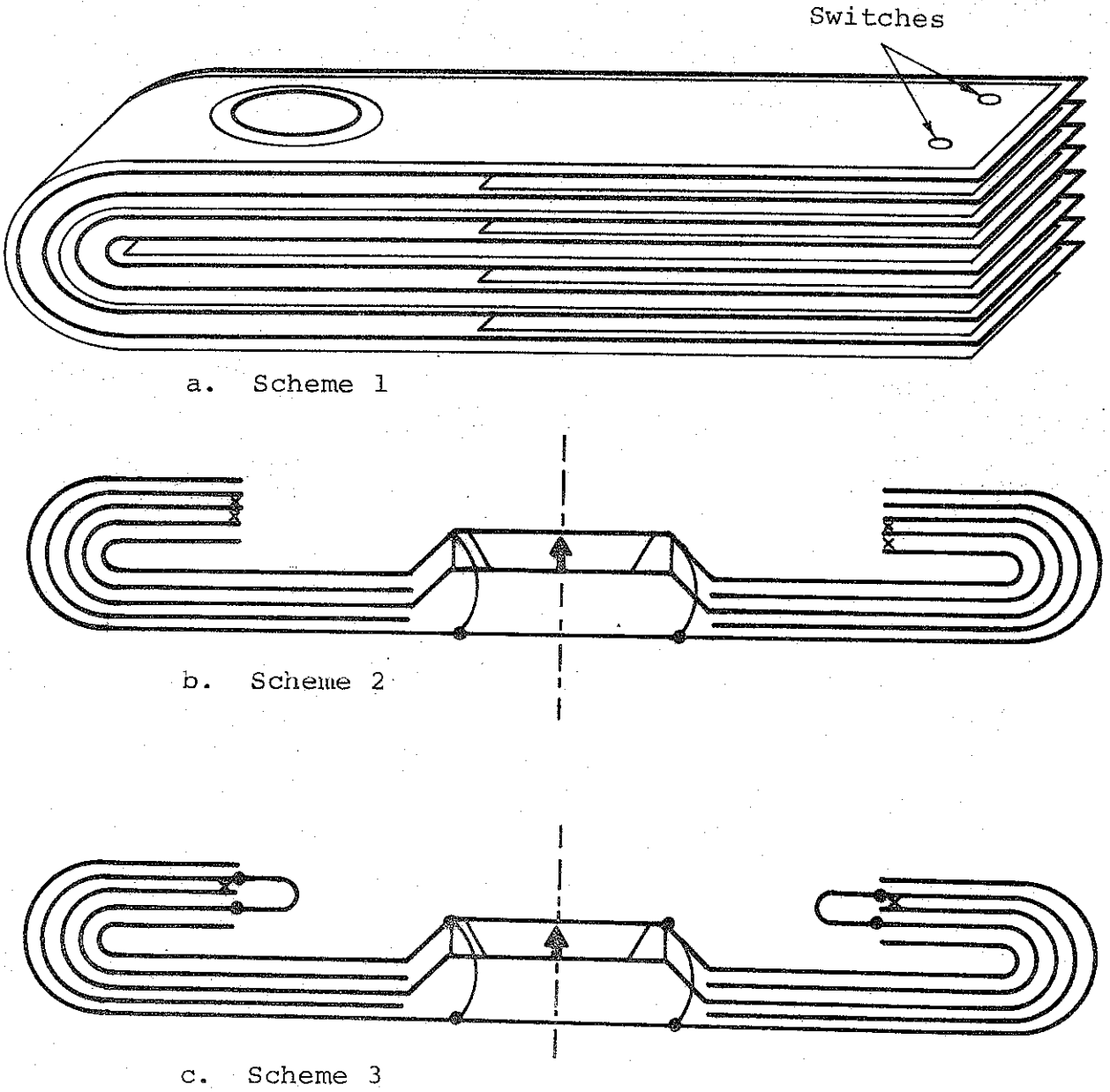

Figure 9 Three schemes considered for assembling and switching Mylar lines.

5352

on which it occurs; (2) no special triggering sequence is required (unless current symmetry in a pinching diode is so critical that the lines that feed the tube from the side should require that they be triggered 2 to 3 nsec early because of the extra transit time and inductance in their output leads; (3) more space is available for switches and their electrodes even while these remain reasonably close together; and (4) paralleling the outputs of the modules at the tube is very easy.

The generator was assembled in a steel tank (on wheels) 20 feet long, 7 feet wide, and about 1 foot deep (Figure 10). In Figure 11, the generator configuration is that used later in the program, when the number of Blumleins was reduced to two and the tube was situated at one end.

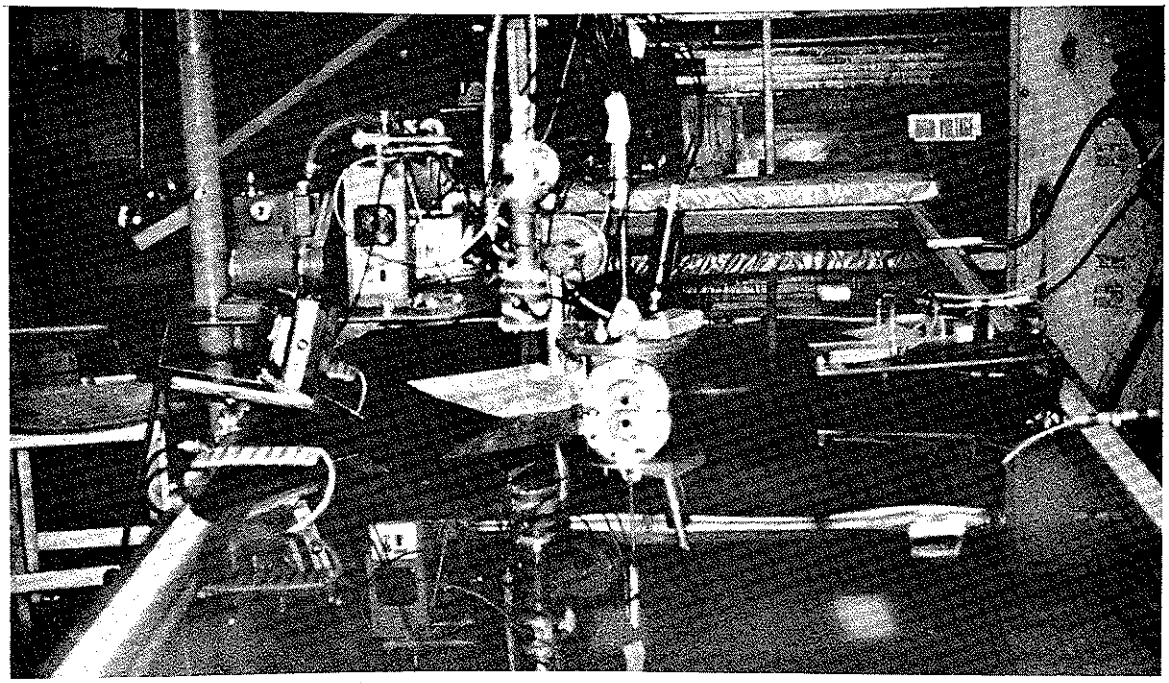

Figure 10 Generator configuration, 0.1 ohm line.

3.2 SWITCHING

The component strip transmission lines of the low-voltage generator have a characteristic impedance of about one-fifth of an ohm. To produce a pulse with a risetime of approximately 10 nsec

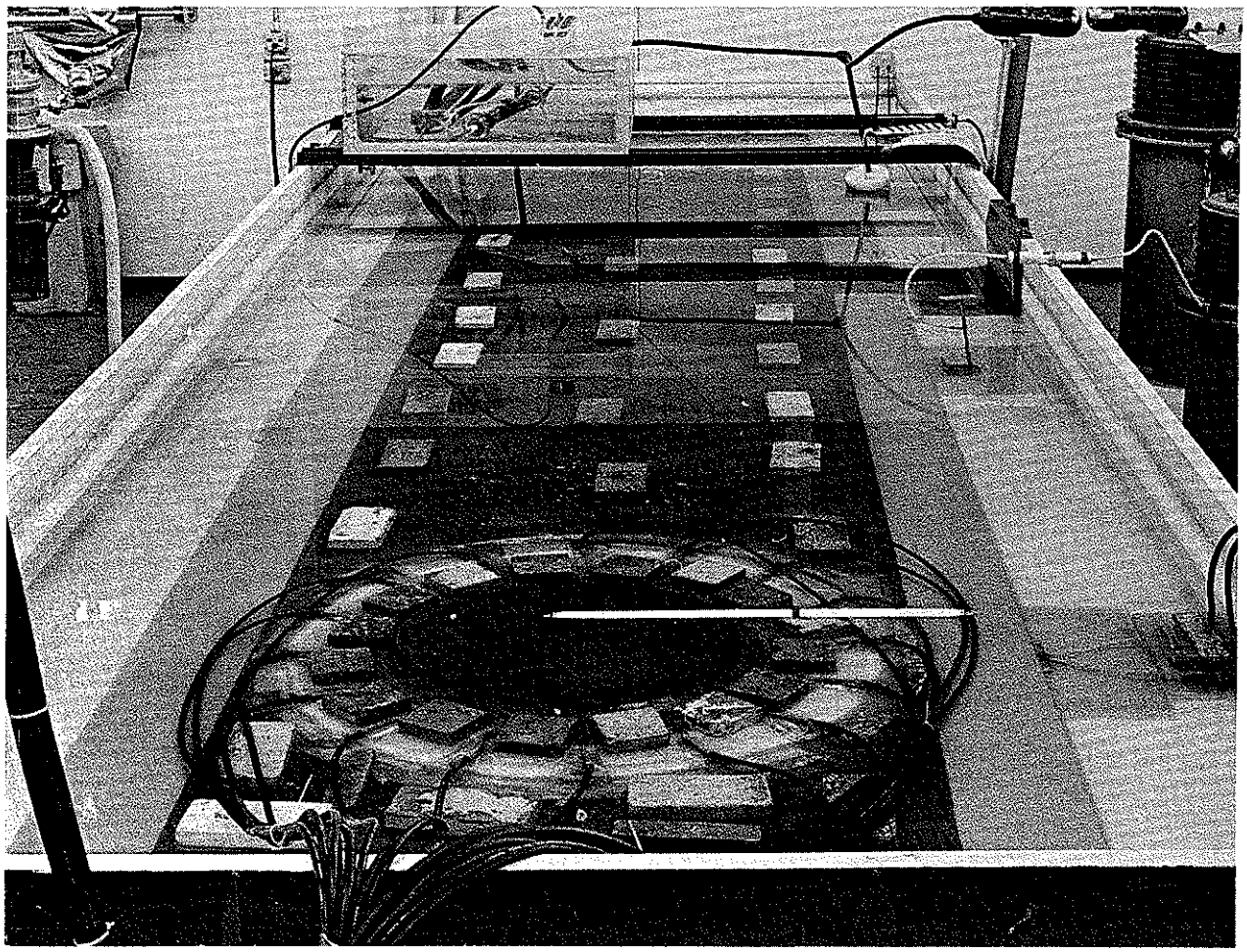

Figure 11 Generator configuration, 0.3-ohm line.

in such a line, a switch inductance of about 1 nH is required. At the beginning of the program this risetime was considered to be feasible only with the use of the solid-dielectric switches developed at Aldermaston. As a result of work under the Defense Atomic Support Agency Contract DASA 01-68-C-0136 and the Siege Phase II study, Contract F 29601-69-C09957, with the Air Force Special Weapons Center, it now appears that pressurized three-electrode SF_6 switches could be developed to provide an alternative. These switches would not need replacement after each shot and would therefore speed operations considerably. Several channels would be needed in parallel for each line because the inductance of a single channel would be excessive, but since the switches can be synchronized with jitters of a few tenths of a nanosecond or less, this degree of multichanneling should present little difficulty.

The line was switched initially using three-electrode, field-enhanced Mylar switches (Figure 12). These consisted of two sheets of Mylar whose total thickness was determined by the voltage at which the switch was required to operate. The trigger electrode, consisting of a ½-inch-wide aluminum finger either 1 mil or ½ mil thick, is placed between the two Mylar sheets in a thin film of unpolymerized epoxy resin. When this switch has been inserted in the line, the trigger electrode is connected to the center of a 50-ohm cable. There are eight such cables, one for each of the switches in the generator. The ends of the cables are remote from the switches and are connected in parallel in a low-inductance configuration at the master trigger switch, for which a stabbed polyethylene card was used. The voltage on the cable center conductors, and hence on the trigger electrodes of the switches, was maintained at half the total charging voltage during pulse charge by a resistive divider adjacent to the master switch assembly. This assembly was kept out of the water to avoid stray conduction. When the polyethylene master-switch broke down (by simple overvoltage), it generated a pulse that rose in a few nanoseconds in

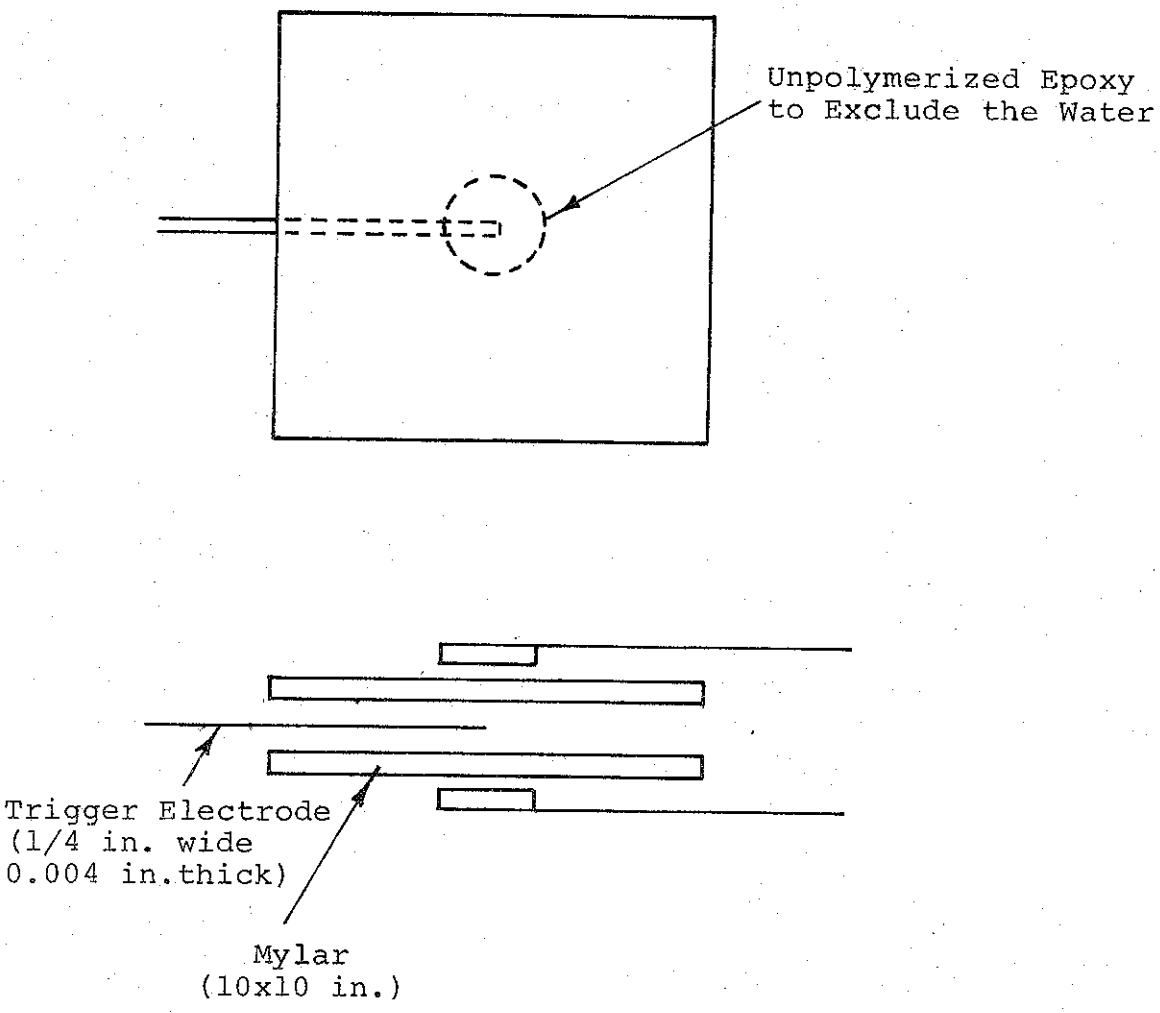

NOTE: No attempt was made to remove the sharp edges.

5348

Figure 12 Typical switch tested in the low-voltage stripline.

each of the cables. The cables are of equal length--approximately 3 feet--and the trigger electrodes represent to each cable a small capacitance, which is in effect an open circuit. Thus, simultaneous pulses of amplitude equal to the total charging voltage are applied to the eight trigger electrodes. These pulses result in a very high electric field in the epoxy at the sharp edge of the trigger electrode, and the breakdown of the epoxy is immediately followed by the breakdown of the Mylar itself. This breakdown generally occurs in a number of channels, and since Mylar is the strongest dielectric known, each channel is, for the voltage applied, the shortest and least-inductance channel that can be obtained.

Because the breakdown of the epoxy initiates the breakdown of the Mylar, this switch might really be considered a liquid-dielectric switch with accurate spacing maintained with thin plastic film. The choice of the medium in which the trigger electrode is immersed is dictated by the fact that liquids will not withstand anything approaching the same fields during the charge as Mylar, and the switch will not achieve its full operating electric field--and hence its minimum inductance--unless a means is found to reduce the field in the liquid. In dc-charged switches, a charge transfer in the liquid has ample time to remove the field almost entirely and apply the voltage to the Mylar; but in the case of pulse charging, a dielectric-constant mismatch must be used. The dielectric constant of the unpolymerized-epoxy version is approximately 10 and, hence, the field in the epoxy is reduced to a few hundred kilovolts per centimeter. The sandwich of epoxy and Mylar consequently has almost the same dielectric strength as the Mylar itself, whereas, if transformer oil were used, it would appear to severely degrade the breakdown strength of the Mylar. If a liquid of higher dielectric constant than epoxy were employed, such as glycerine ($\varepsilon = 40$) or water itself, it is certain that the breakdown strength of the Mylar would again be unimpaired, but in this case the field produced by the trigger pulse in the liquid would be of lower value and the switch would have poorer triggering characteristics. Epoxy, therefore, represents the best compromise.

Some experiments were also carried out in which water was used in the place of the epoxy, and the switches still triggered. In fact, the trigger pulse was fast enough that they triggered at the edge of the trigger electrode. However, they did not form multichannels as did the epoxy switches. A typical fired epoxy switch is shown in Figure 13.

The breakdown channels in the solid dielectric switch inflict some damage on the nearby metal electrodes, and it is highly desirable to attach thin electrodes to the switch so that the part which is most damaged is replaced every time. Some form of adhesive to attach this electrode to the switch is highly desirable. Otherwise, insertion of the switch into the line is a very difficult process, and the electrodes are occasionally lost inside the line. Almost every adhesive tried had a breakdown strength lower than that of the Mylar and reduced the work field and degraded the switch operation.

Eventually a 3M brand No. 8044 Spray Disk Adhesive was found to give satisfactory results. A satisfactory adhesive may be very useful when extremely fast risetimes--and hence the lowest possible switch inductance--are required, such as in generators in producing very short pulses of 10 nsec or less. However, in the meantime, experiments had shown that the alternative form of a solid dielectric switch (which used stabbed polyethylene to form two-series elements that are simply overvolted in turn by the same triggering system previously described) regularly broke down in enough channels to compensate for the increased thickness of the switches and hence the larger inductance of a single channel. At 150 kV, for example, two sheets of 10-mil Mylar would suffice for the switch, but a total of 60 mils of polyethylene would generally be used.

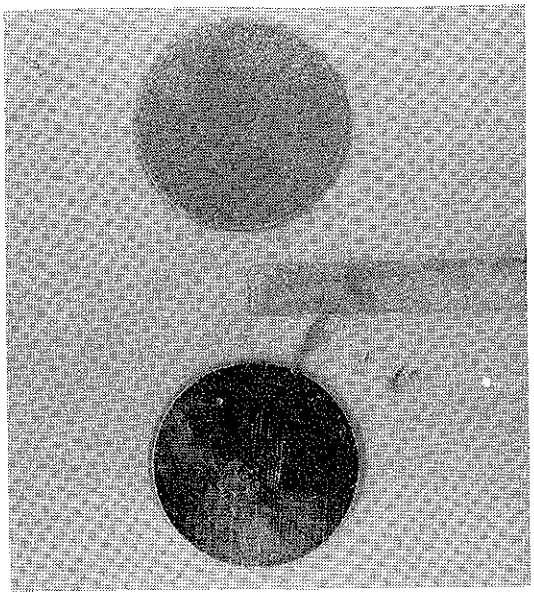

a. Unfired Switch

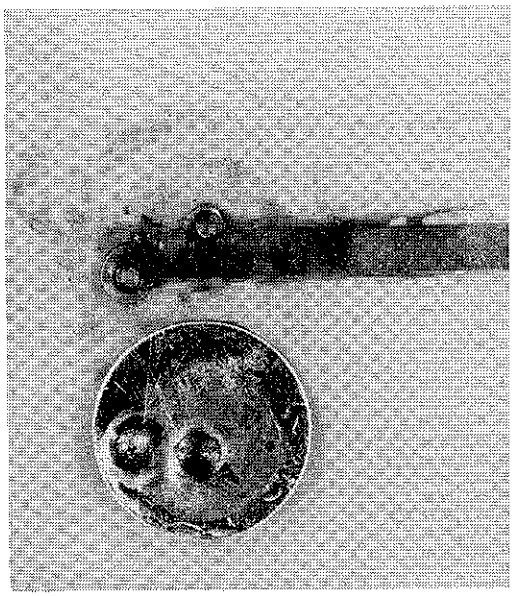

b. Switch that Double-Channeled

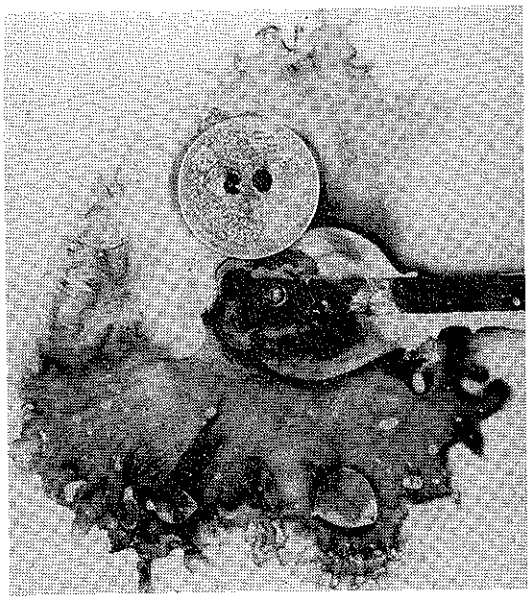

c. Switch that Multi-Channeled

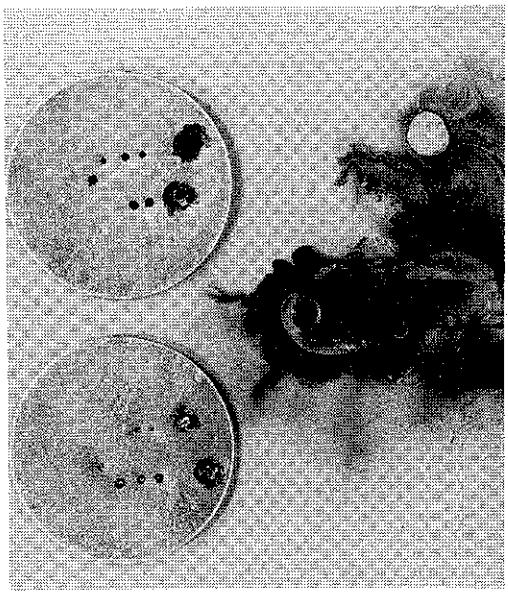

d. Switch that Multi-Channeled

Figure 13 Mylar switches with epoxy-coated triggers before and after firing.

Figure 14 shows the cross section of a polyethylene switch which again followed that developed at AWRE. Each switch card is stabbed to a predetermined depth by an array of 45 needles with their points all lying in one plane. When the needles are withdrawn, an air-filled indentation with a sharp point results. When a high voltage is applied to the switch, the air breaks down so that the voids may be regarded essentially as conductors having at the point a field high enough to break down the polyethylene. The self-breaking voltage of these switches, which is independent of time down to a few nanoseconds, has a scatter of only a few percent. When triggered at 30 percent below the self-breakdown voltage, the switches were found to fire consistently with enough channels to produce a risetime considerably less than 10 nsec. Typically, the side of the switch that is overvolted initially by the trigger pulse arriving from the cable would break in three to seven channels and the second part of the switch, which is overvolted more rapidly by the breakdown of the first part, would break in 20 to 40 (Figure 15). Enlargements of a line switch fired at 30 percent below self-fire appear in Figures 16 and 17.

Figure 18 shows the device used to stab the polyethylene. A pneumatic mechanism ensures reproducible and consistent stabbing by applying a constant force to the needles. The stab depth is controlled by means of shim stock, and a dial gauge gives visual confirmation of the depth of stab.

Sheets of 30-, 60- and 80-mil polyethylene were used in the low-voltage line. A calibration curve of self-breakdown voltage as a function of stab depth was obtained by charging a small capacitor and discharging it into untriggered switches (Figure 19).

Note: Stabs start from the positive electrode

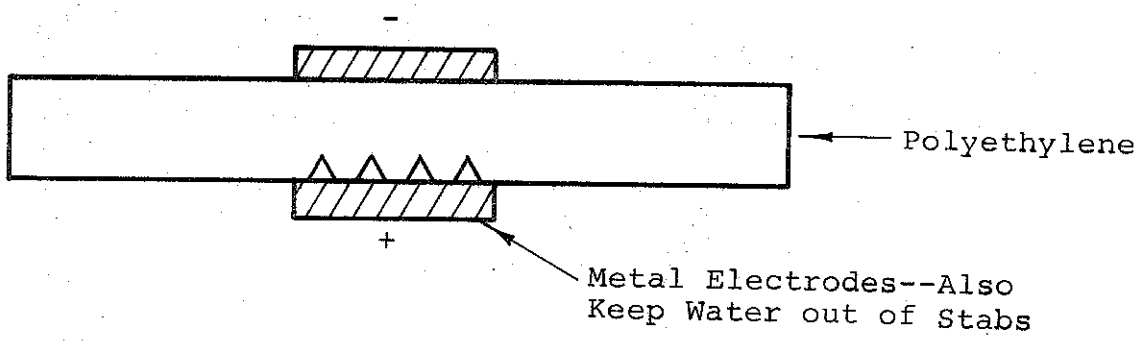

a. Master Switch

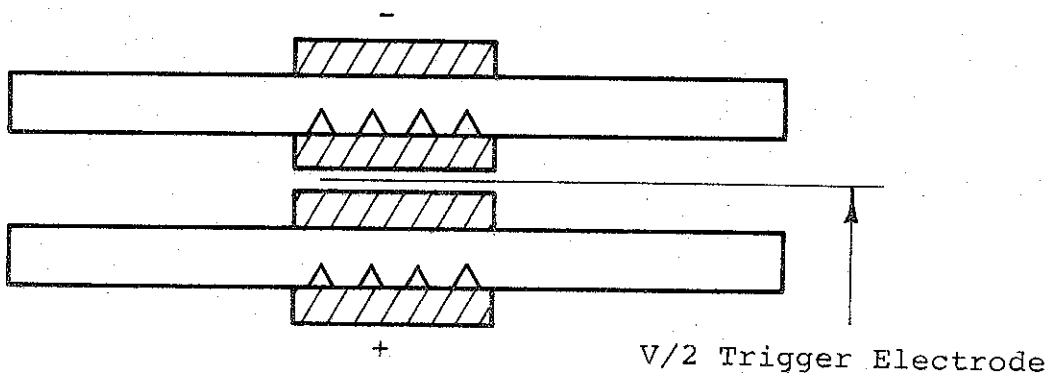

b. Line Switch

Figure 14 Cross section of stabbed polyethylene switches.

8498

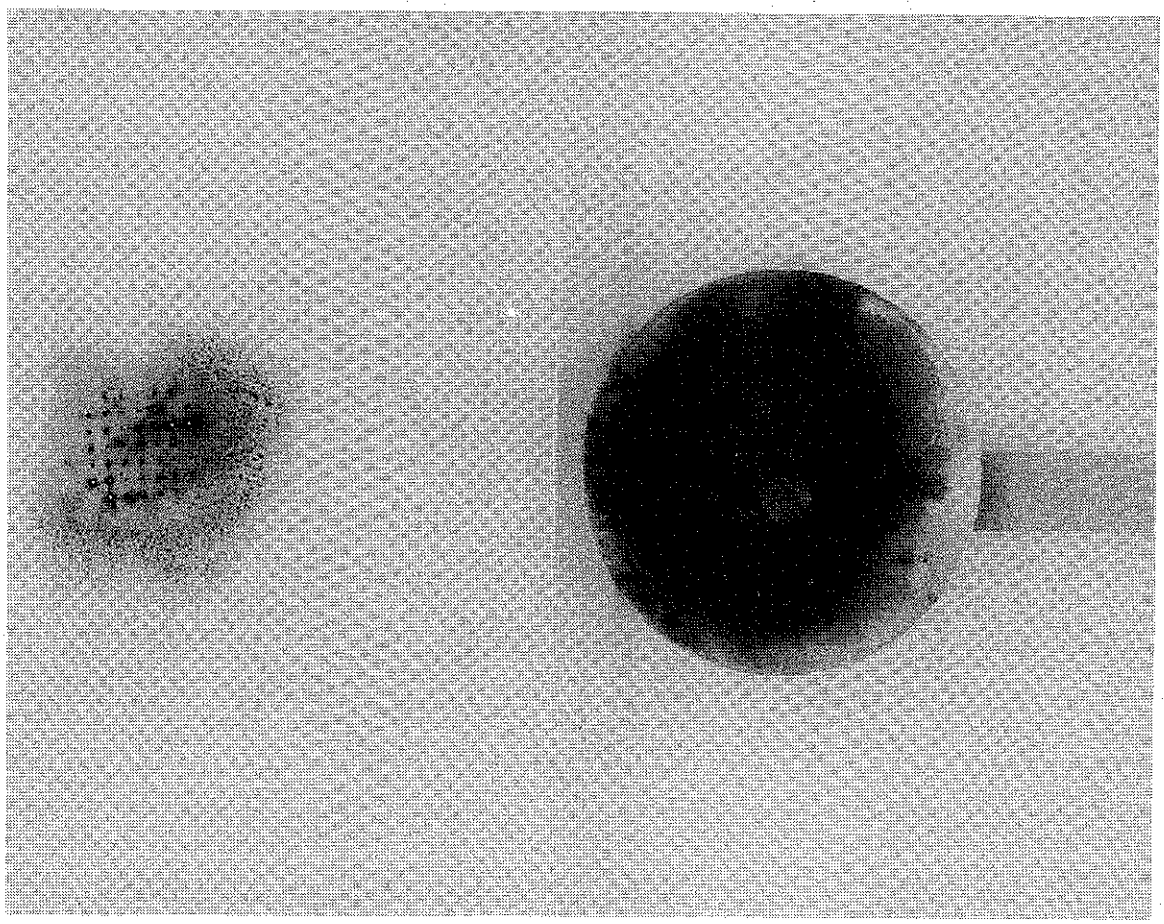

Figure 15 Multichanneling at 30 percent below self-fire.

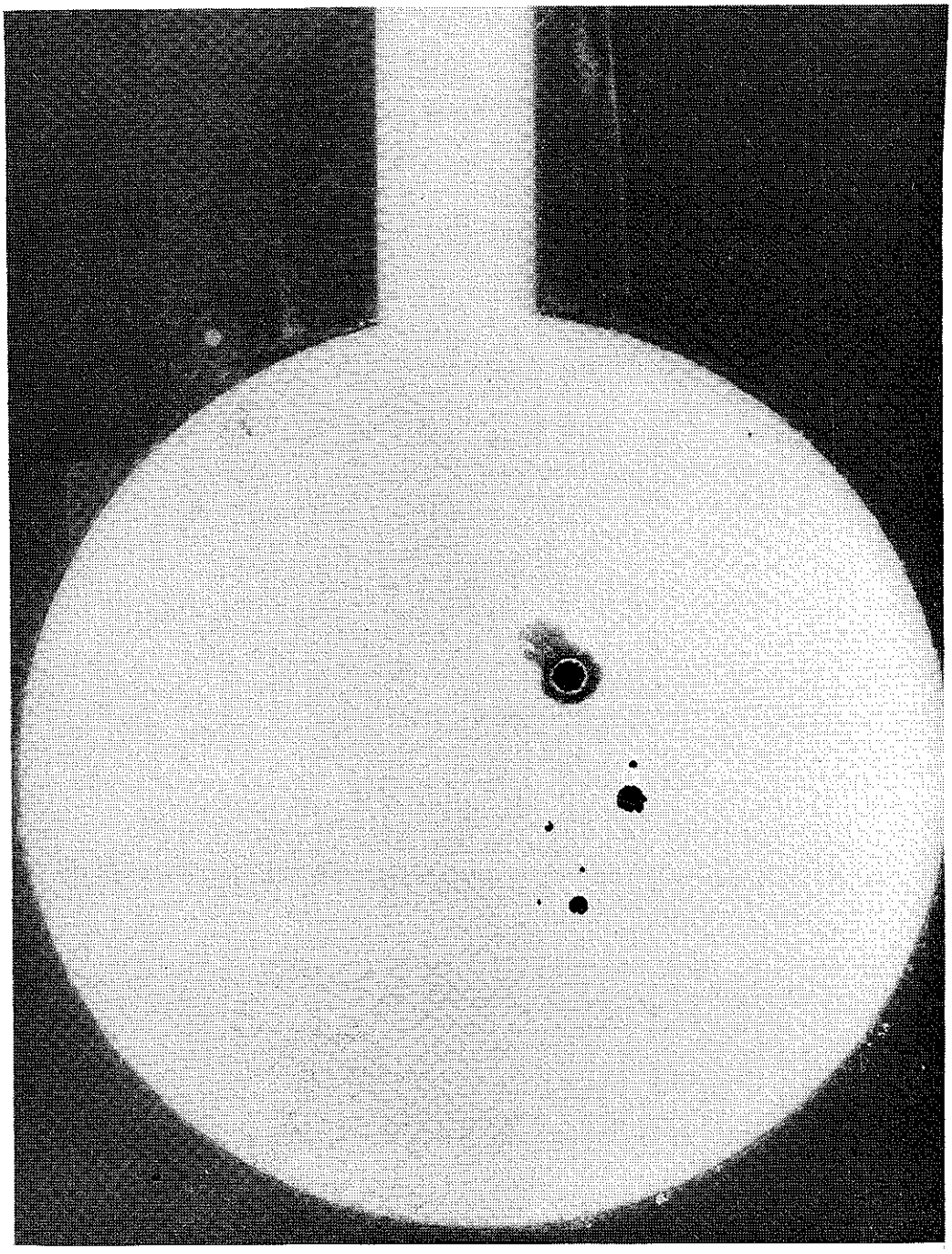

Figure 16 Magnified trigger tab.

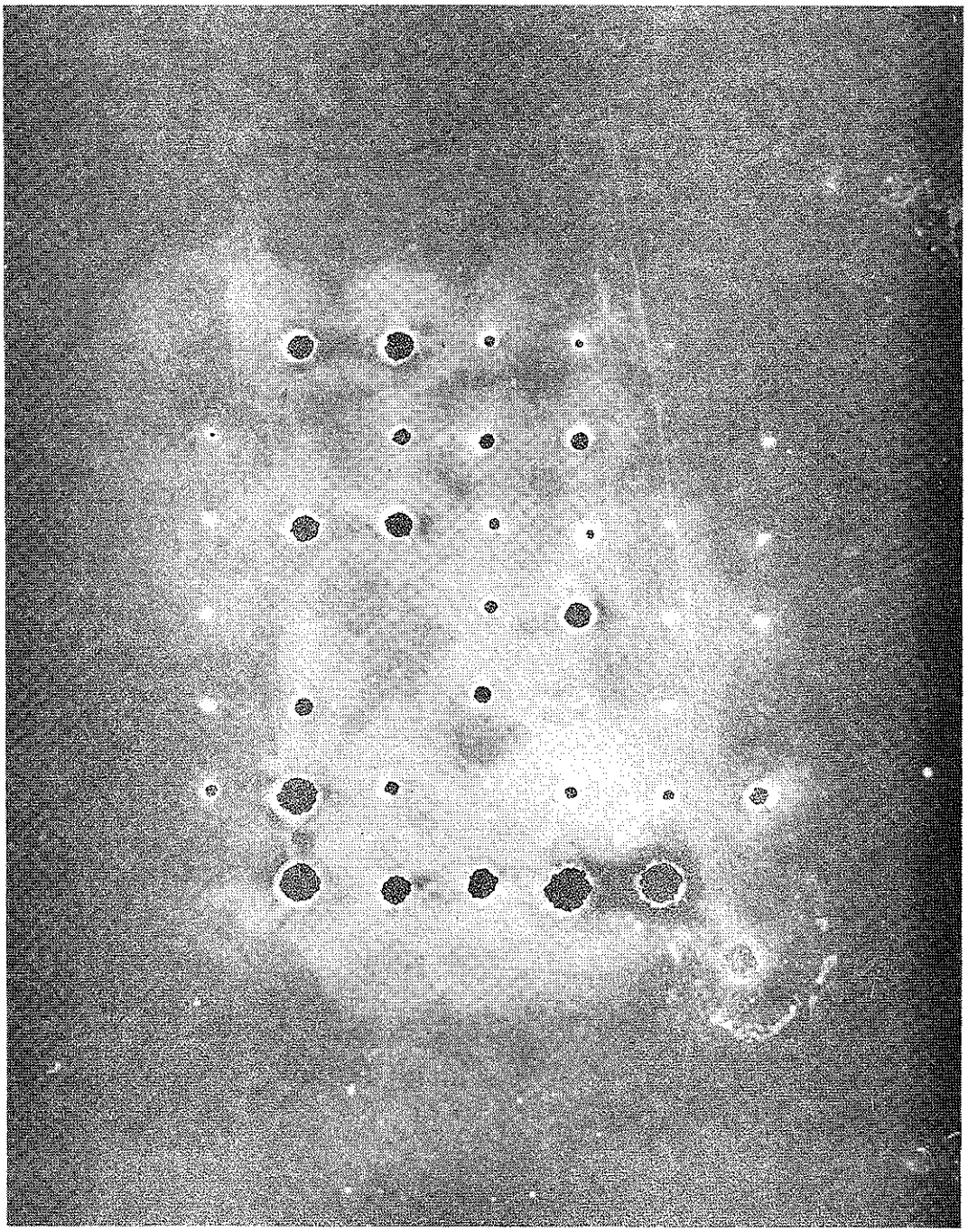

Figure 17 Magnified triggered line switch.

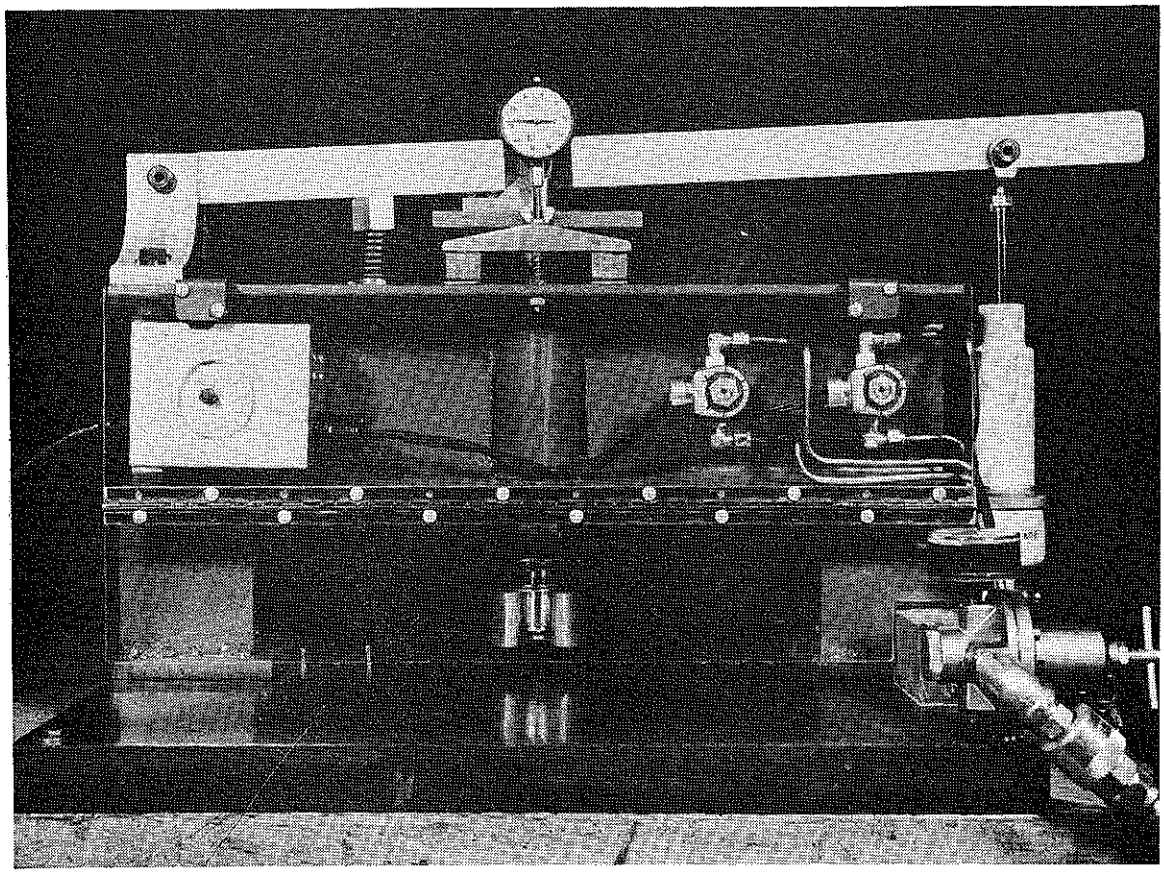

Figure 18 Automatic stabbing machine for polyethylene switches.

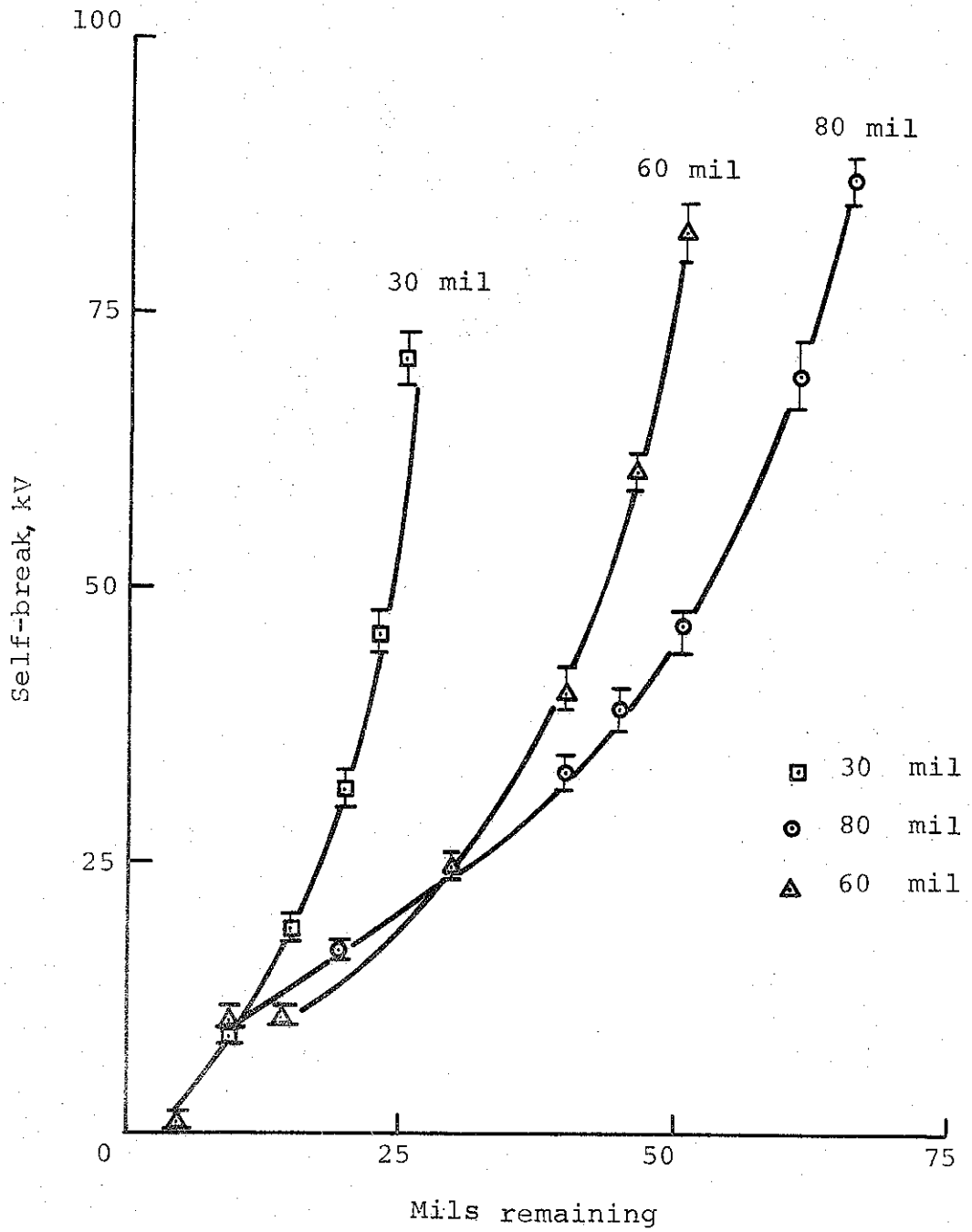

Figure 19 Self-break curve for polyethylene switches.

8448

As previously described, each Blumlein was switched at two locations on the end electrically remote from the tube. There are several reasons for this, apart from the desire to guarantee an adequate risetime. The aspect ratio of the line, 14 feet long by more than 4 feet wide, indicates that the wave diverging from a single switch is not planar, especially since some of the switches are displaced from the center of the lines. Probably more important, should one switch fail to fire, the other one will ensure that most of the output of that Blumlein is still obtained while, as discussed above, the possibility of a portion of that Blumlein being overvoltaged by pulses from the remainder of the modules is avoided.

In practice the failure of a switch to fire has been very rare, and the current flowing in any Blumlein is very evenly divided between the two switch locations.

3.3 PULSER DIAGNOSTICS

3.3.1 Voltage Monitors. To monitor the input and output voltages, resistive dividers were assembled in the form of chains of 2-watt carbon resistors. At the low voltages at which this line operates, it was perfectly possible, and indeed was found very convenient, that both these monitors be positioned just outside the water with the full voltage brought out to them by a short polyethylene-insulated lead. The risetime of the monitors in such a configuration is only a few nanoseconds, which is quite adequate. In the case of the higher-voltage line, similar techniques were employed, except that capacitive division was employed to reduce the voltage transmitted to the carbon divider to an acceptable level. This capacitive division was simply achieved by sliding a large sheet of copper into the Blumlein in such a way that it divides in the appropriate ratio the number of Mylar sheets between the two copper conductors whose potential difference is to be monitored.

3.3.2 Current Monitor. An output current monitor was constructed of an annulus of 1/2-mil stainless steel 1 to 5 cm wide and 2-1/2 feet in diameter. This annulus was placed in the top conductor between the line connections and the load. Provision was made for measuring at a number of places the voltage developed across it and mixing the signals to take into account possible azimuthal asymmetries in the current. The requirements on this resistor are that it be thin compared with the skin depth, but thick enough or of sufficient circumference that it is not warmed substantially in a single pulse. Its resistance should also, of course, be much less than that of the generator or it will reduce the efficiency of the system. These conditions were all satisfied, though in all cases the margin was not very great. The resistance was initially one-tenth of a milliohm; to improve the signal-to-noise ratio, the resistance was later increased to half a milliohm. The skin depth for the highest frequencies of interest is approximately 3 mils. The temperature rise at the maximum available current of about 3 MA is about 20 degrees.

3.4 PREPULSE ELIMINATION

Before the line was connected to an X-ray tube, it was considered desirable to minimize the prepulse.* Even prepulses of the order of 10 kV have been shown to impair the operation of low-impedance diodes in which the anode-cathode spacing is very small. The production of plasmas in this region before the pulse arrives can lead to very erratic performance in terms of a variable impedance and location for the beam pinch and eventually to total shorting of the diode during or before the pulse.

---

*Prepulse is the voltage appearing on the output of the line during pulse charge before the line is switched.

Careful positioning of the low-voltage feed from the capacitor bank on the isolating inductor (used to charge the two low-voltage sides of the Blumleins) would in theory eliminate the prepulse completely if there were not stray capacities in the system (see Figure 20). Because of the very low impedance of the low-voltage line,

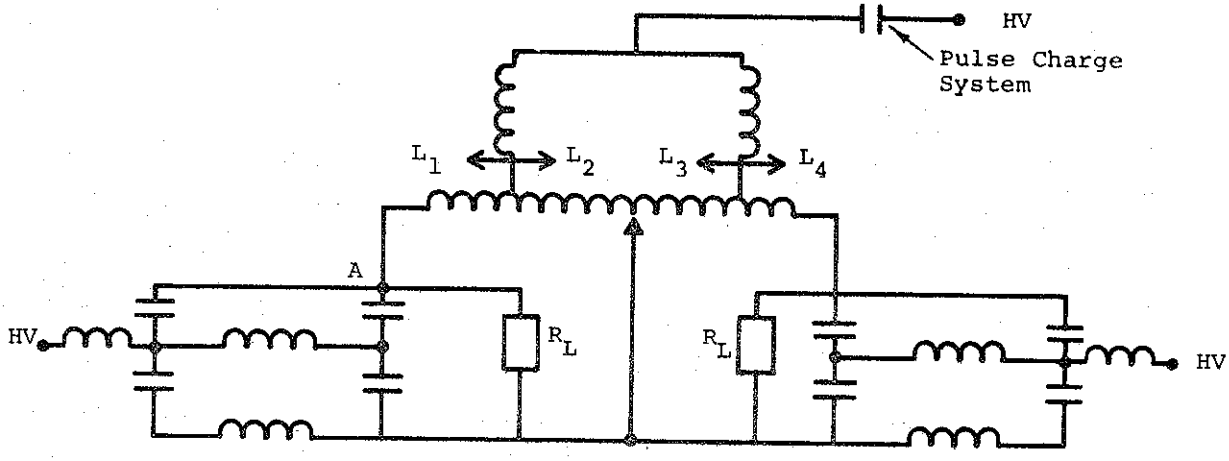

NOTE: Stray capacitances have been eliminated from the circuit.

Figure 20 Stripline circuit.

very little isolating inductance is required and is provided simply by 3-foot-long metal rods immersed in the water. These are only a few inches from the grounded tank but are insulated from it by sheets of plastic. Tuning is done by a sliding contact between the low-voltage feed from the capacitor bank and these metal rods. Tuning is performed on both the generator modules. The fact that the generator is charged by a single-element capacitor bank in air, having very low capacity to ground, made it possible to tune the prepulse to a very low level indeed, about 0.2 percent of the pulse-charge voltage. Tuning was repeated occasionally to ensure that no circuits had changed.

The residual prepulse is probably associated with distributed stray capacities in the water itself. Full operational voltage is only a few hundred volts, not much more than the minimum of the Paschen curve. Hence, it was regarded as unlikely that, having achieved such a low prepulse, it would be necessary to use a prepulse isolation switch in the tube. This, in fact, proved to be the case.

Though the prepulse switch first developed and tested on the Model 730 Pulserad is a passive device with vacuum flashover, a long life, and very low inductance, it was nevertheless felt desirable to be able to eliminate the switch if possible. The criterion used was that the asymmetry in its breakdown might give rise to asymmetries in the diode region, which in turn could cause instabilities in the diode pinch. Instabilities had been observed in a few cases on the Model 730 Pulserad in the form of radial motion of the pinch during the pulse, though this pinch was not necessarily a result of the prepulse switch.

3.5 GENERATOR TESTING AND DEVELOPMENT

In this section the testing, operation, and problems encountered with the generators during the performance of the contract will be discussed. No attempt will be made to include any experimental data unless it is directly related to the operation of the pulser itself. All experimental tube data generated from each of the lines to be discussed is presented in another section.

Experiments on the first low-voltage line included diagnostic calibration and balancing V/2 for the switch triggers. A preliminary check was also made to ensure that the prepulse could be balanced to a low level, though it was necessary to repeat this check when the

tube was installed; therefore, the process will be described later. At first it was attempted to maintain the V/2 trigger voltage by capacity division, using Mylar sheets and copper sheets to form a capacitor. This method proved to be unsatisfactory because the capacity divider being submerged in water was unbalanced by stray capacity and resistance. A relatively low-impedance resistive divider (made up of a number of tubes of copper sulfate) outside the generator was then used. The overall resistance (100 ohms) was low compared with that of the stray resistances in the water in the generator tank and could not be neglected, and since the resistance in the tank tended to change occasionally, the ratio was adjusted at intervals to ensure that no significant departure occurred. Tuning was carried out by ringing the capacitor bank--charged to as much as 10 or 20 kV--into the line and observing both the charging voltage and the V/2 trigger voltage with identical monitors on a twin-beam oscilloscope. After the initial tuning of the line, the line was switched with a copper-sulfate load on the line.

Once the switching system was established, the voltage was successfully raised to almost 150 kV. Thus, the electric field of 1.5 MV/cm, for which the system was designed, was demonstrated under appropriate operating conditions. The matched output current was about 1-1/2 MA.

Because of the success of these tests, the belief that the line could operate with a considerable lifetime at somewhat higher fields, and the desire to cross-check input and output monitors at the highest possible voltage, an open-circuit firing at about this level (150 kV) was attempted. An open-circuit shot in which the voltage on the switched lines reverses a number of times is somewhat more of a strain on the generator than firing into a matched load, but in principle not excessively so. However, in

fact, the line broke down electrically in the pulse-charge region. The specific cause of failure cannot be definitely identified, but was believed to be nonsimultaneous switching (see Section 2.4).

Because of the extent and location of the damage and because of the wear sustained by the switching region of the line during the initial switching tests, it was decided to assemble a new line of similar design rather than repairing the damaged one.

When the new line was completed, it was successfully fired at a 200-kV open-circuit voltage. It was decided that 65 to 85 kV into the low-impedance diode would be a very safe voltage to be tested on the tube.

During this set of experiments, difficulties occurred with the switching. The switches failed to fire consistently and often fired at voltages other than those predicted by the previous voltage-stab-depth calibration curve. The problem was traced to the needles in the stabber, which were originally secured with Woods metal. Enough switches had been stabbed that the needles were loose. A new stabber was fabricated with the needles soldered in place, which produced very consistent switching. Self-breakdown switch data agree within 5 percent of the previous set of data.

Testing continued after the switching was improved. During the testing, a loose lead caused a spark that damaged the line. This failure was clearly not associated with normal electrical operation. The line was satisfactorily repaired by merely cutting out the damaged sections and interleaving Mylar and copper.

After continued testing, the switching again showed signs of becoming erratic. An examination of the switch area showed severe damage to both the Mylar and the copper of the line. Four-mil-thick electro-deposited, unannealed copper had been used. The hard copper in the switch area had been badly broken, even though backup plates and sheets of weighted polyethylene had been used to prevent mechanical damage. Most of this damage resulted from single-channel prefires caused by the malfunction of the stabber.

A new line was again fabricated in preference to making further repairs. This action was influenced by the fact that new and more suitable copper was available (10 mils thick, annealed, and 4 inches wider than the copper previously used). Besides making it possible to add more dielectric in the line and improving the regularity of the field grading at the edges because of the increased copper thickness, the annealed copper was more resistant to mechanical damage.

At this point a new current-viewing resistor was also installed. It had a value of 0.5 milliohm as opposed to 0.1 milliohm used previously. The necessity for this change was indicated by an increase in the background noise associated with this signal, which could not be reduced by careful and systematic rerouting of cables or the addition of an extra copper shield around the cable joining the current-viewing resistor to the screened-room housing the oscilloscopes. After reassembling the generator, short-circuit shots were fired to check the new current-viewing resistor. Figure 21 shows the traces from these shots. The output-voltage waveform shows an inductive voltage signal from the tube, which was not provided with a very low-inductance short. The traces are synchronized and the output voltage is zero when the current peaks.

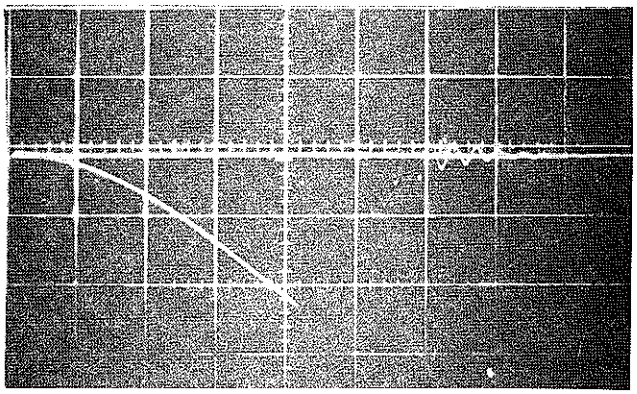

Pulse Charge
22 kV/cm
1 μsec/cm

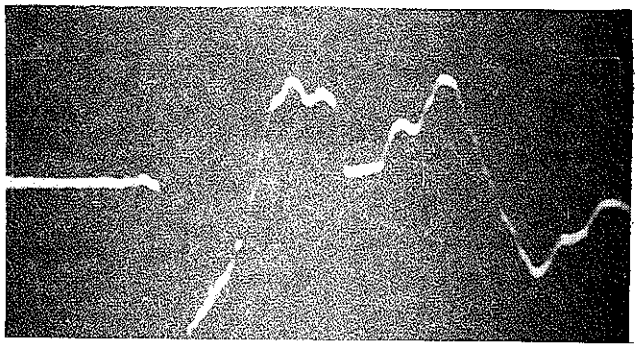

Output Voltage
22 kV/cm
50 nsec/cm

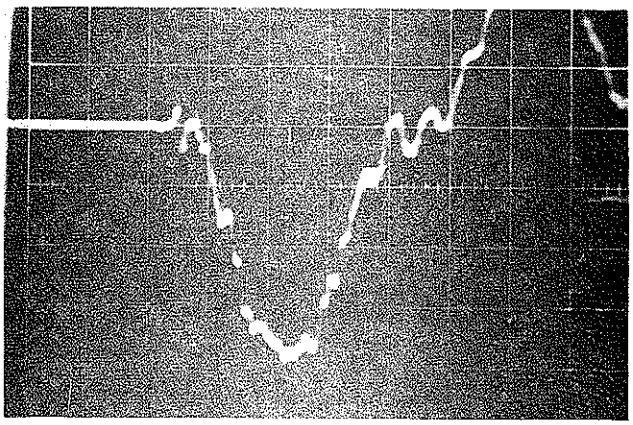

Output Current
200 kA/cm
50 nsec/cm

Figure 21 Short-circuit shot.

A calculated shorted output current from the pulse-charge voltage and the known line impedance were once again in excellent agreement with the current calculated from the resistance of the current-viewing resistor. Experiments were then resumed.

Later in the program the line voltage was increased to an average of about 125 kV. Previous lines had been operated at these voltages and higher, but not for any substantial number of discharges. Continuous operation at the higher voltages revealed several effects associated with long-term wear.

The symptom of the first problem was again erratic switching. Much more energy was being deposited in the switches, and the metal at the switch site was being progressively damaged. The problem was corrected by using 1/8-inch stainless-steel backing at the switch sites. The life of these new switch conductors appears to be indefinite.

There were also failures of the trigger cables. These failures were possibly induced by transients reflected down the cables where the switching was erratic. The trigger cables were changed from RG-217 to the larger RG-17.

Several line failures also occurred at the increased voltage. These were at the edges of the line. Several times the failure site was easily repaired by cutting away damaged Mylar and interleaving new material. Eventually it was decided to renew the dielectric completely.

It was not at first understood why the failure rate had increased so rapidly at the higher operating stress, since fields were still much less than the breakdown data indicated as a useful

limit. Prior to increasing the voltage, several hundred shots had been fired at between 75 to 110 kV, and it was unlikely that these had degraded the Mylar life.

A new line was fabricated in the form of two parallel Blumleins rather than four, resulting in an impedance of 0.30 ohm. This decision was made when the likely requirements for successful tube operation, based on the results with the tube to that date, were reviewed.

The new line operated satisfactorily at the higher voltages for a considerable number of shots. However, similar failures eventually began to recur at the edge of the line. Examination revealed that numerous air bubbles had formed in the line, and it was decided to remove the air by unstacking and reassembling. In the course of this task, tracks were noticed on the Mylar, 1/4 to 1 inch long, just outside the perimeter of the copper that formed the output conductor. The tracks were confined to the pulse-charged portion of the line, but since no voltage is applied to the output conductor during pulse charge, the evidence suggested that the tracks were caused by the high-speed output transient. The streamers caused progressive degradation into the Mylar, leading to eventual failure.

It was concluded that one could not ignore the high-speed transient voltage when designing the resistive grading. Examination of Figure 22 shows that the stress caused by the high-speed transient is indeed greatest at the edge of the uncharged output conductor (the center conductor in the stack) where this lies alongside of the charged or high-voltage conductor.

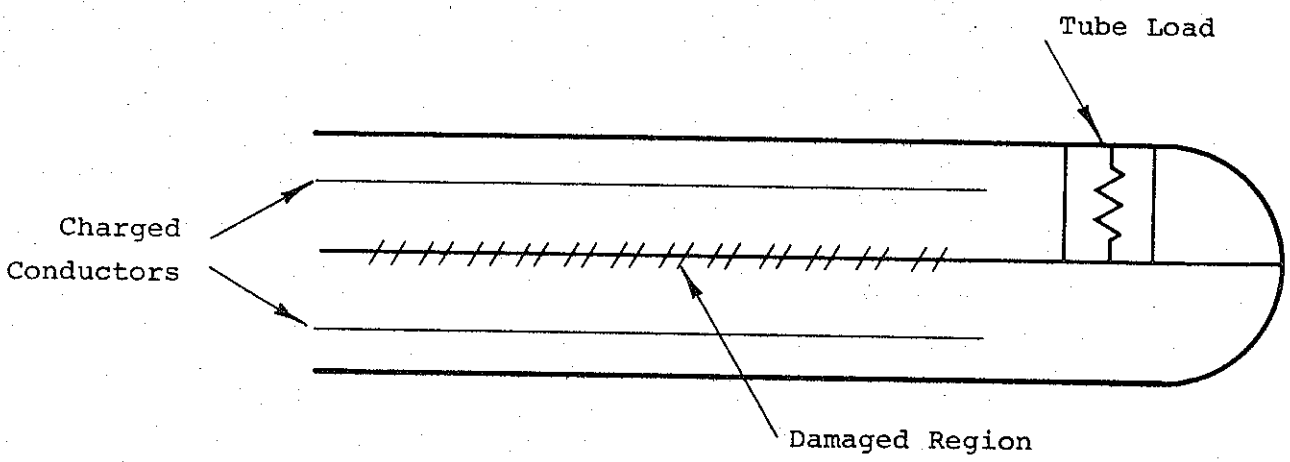

Figure 22 Blumlein transit damage.

Except when the Blumlein feeds a nearly short-circuit load, the discharge transient in the switched lines exceeds those in the unswitched lines. In the matched case, for example, the switched line experiences a transient V propagated from switch to load, where V is the charging voltage; and then a further transient of the same size, V/2, propagating back towards the switch. The peak field generated in the copper sulfate at the line edges varies with position, being greatest near the output end where the reflection produces its effect without giving time for the field from the first transient to diffuse away. In the unswitched line (in the matched case), a transient V/2 is injected when the switch transient reaches the load, and in this case the second transient, which is the reflection from the open circuit at the far end of the unswitched line, has the same magnitude as the first. Thus, it is hard to compare quantitatively the transients in the two lines, but at the weak points, the total "instantaneous" transients are V/2 in the switched line and V in the unswitched. For higher impedance loads, the ratio is greater, and this was usually the case, especially

considering the effect of the load inductance, which was considerable in reducing the rate of change of voltage in the unswitched line and, hence, the peak field in the liquid.

Figure 22 shows that the uncharged middle conductor is common to two switched transmission lines and the charged conductors are common to one switched and one unswitched line. The transient induced field at the edge of one of these conductors is largely produced by the sum of the transients in the lines on either side. Thus, the stress in the copper sulfate due to the fast transient is greatest on the uncharged center conductor, which was the damaged region. Where the center conductor has emerged from the charged region of the line, the transient voltage with respect to the surrounding conductor is likely to be similar, but they are twice as far away. Note that this analysis would yield a different result if the outer pair of lines were switched, when no conductor should experience such a high transient stress. This would entail charging the line positive instead of negative, and this change was avoided because positive electrodes in water have been shown to initiate breakdown streamers in lower fields than negative electrodes by about a factor of two. In the case of the present line it is significant that the center conductor experiences a negative discharge transient which is greater than the positive transient experienced by the charged conductors by not more than about 1.5:1, in effect, but no damage was ever observed near the charged conductor. This suggests that the polarity effects found for pure water do not apply to the Mylar/water interface, which is consistent with breakdown tests performed at Aldermaston on high-voltage transformers employing a similar construction.

In summary, the generator operated reliably and reproducibly at gradients in the Mylar in excess of 1 MV/cm. In fact, no intrinsic dielectric failure of the Mylar has ever been observed with the possible exception of the open-circuit test described earlier. In routine operation, control over the output characteristics is very precise, with only a few percent less on switching voltage. A small amount of routine preventive maintenance or inspection is required (as with most generators). Chiefly, the copper-sulfate solution must be cleaned by filtering and its resistivity and accuracy of the trigger voltage divider must be checked. The firing rate with five to nine replaceable switches is controlled almost entirely by the handling time of the tube, where components are replaced on each shot as in all high-current applications. The charging and switching techniques used demonstrate that an almost arbitrary number of similar Blumlein could be operated simultaneously in parallel to generate much higher currents.

Re

SECTION 4

LOW-VOLTAGE TUBE

4.1 TUBE DESIGN

If the 1/10-ohm generator is operating into a matched tube, the inductance of the tube is in series with a 1/5-ohm resistance, and this leads to a very stringent requirement on the inductance of the tube if the risetime of the current is not to be excessively

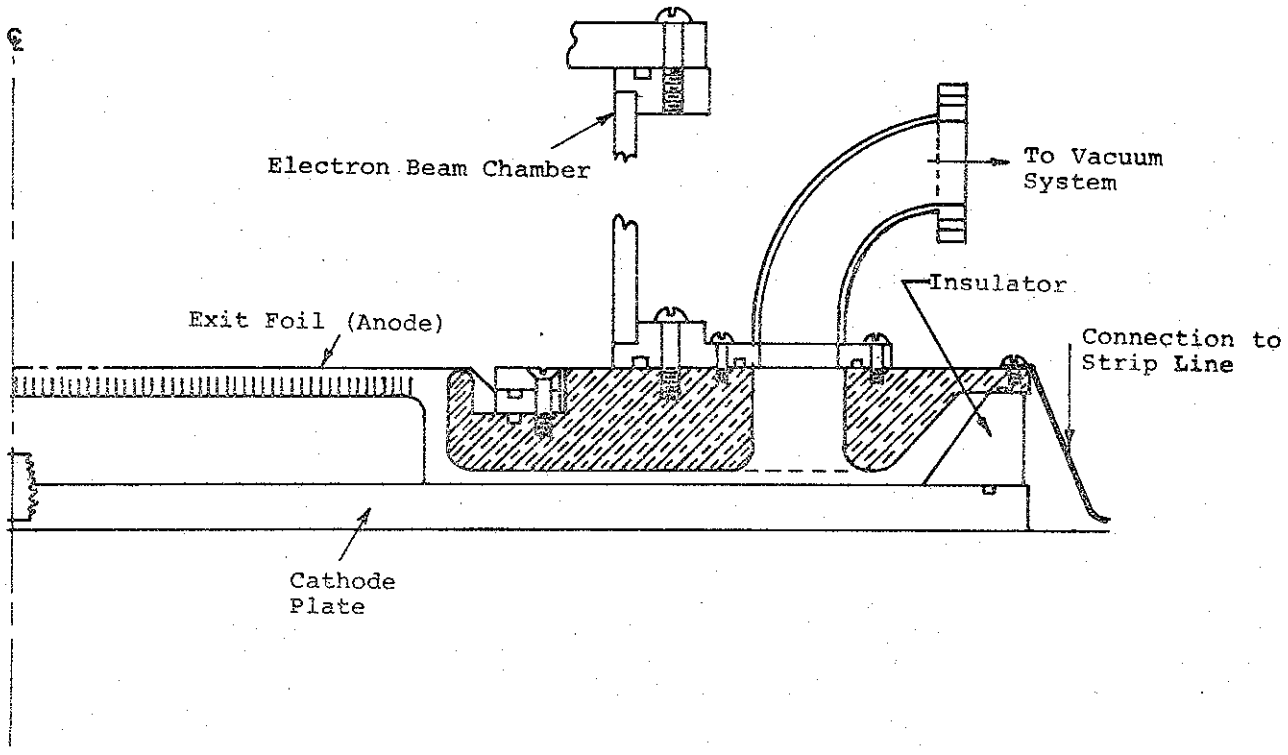

Figure 23 Half-sectional view of the low-voltage tube.

long. The inductance of the initial tube design is just over 3 nH, which corresponds to an e-folding risetime of 15 nsec. It is believed that careful design could reduce this inductance to between 1 and 2 nH while keeping the same tube size. However, the rate of current rise is clearly limited by the tube inductance and not by the risetime of the switching. The tube used on the low-voltage line is shown in Figure 23 in cross section.

If the risetime of the generator as defined by the switches is very much less than the risetime of the tube circuit, then the inductance of the tube will initially appear as an open circuit to the generator, which will deliver twice its matched voltage. The initial inductive-voltage transient appears on the tube and, though brief, may cause the insulator to flash over since the breakdown strength of the insulator in this mode is not very time dependent. The tube insulator must then be made longer, which increases the inductance of the tube and, in general, increases both the amplitude and the duration of the inductive-voltage transient. This solution is therefore self-defeating to some extent. The conclusion to be drawn is that when the output-current risetime is limited by the inductance of the tube, that inductance is very critical. Much effort should be devoted to reducing it as far as possible. Also, a fast risetime from the generator, which is of very little benefit because it is not transmitted to the cathode, should be avoided in order not to overstress the tube. In fact, the generator should have a risetime not very much less than that of the tube itself. For example, if the risetimes of the generator and of a matching tube are both equal to τ, then the time history of the cathode voltage is described by

$$1 - \exp\left(-\frac{t}{\tau}\right) - t \exp\left(-\frac{t}{\tau}\right)$$

To find the voltage on the tube envelope, one adds the cathode voltage to the inductive drop $2t \exp\left(-\frac{t}{\tau}\right)$, obtaining

$$1 - \exp\left(-\frac{t}{\tau}\right) + t \exp\left(-\frac{t}{\tau}\right)$$

which gives a maximum of only 1.14 at $t = 2\ \tau$, and therefore the peak tube voltage does not exceed the final cathode voltage by more than 14 percent.

Comparable contributions to the inductance of the low-voltage line tube are made by the outer insulator region, the vacuum between the large anode and cathode plates, and the cathode region, which is in effect a short stub of coaxial cable. Outside of the tube insulator a short, hollow, truncated metal cone connects the anode plate to the positive output side (which is ground) of the generator. Pressure loading ensures a good contact, and the conical shape minimizes the inductance while avoiding flashover of the residual water-immersed Mylar dielectric.

The inductance of the region formed by the insulator and the junction with the generator can be reduced simply by increasing the diameter of the tube. This increase would, however, slightly increase the inductance of the vacuum region inside the tube between the anode and cathode. In the present tube, the spacing employed here is 1/8 to 1/4 inch. At a voltage of 150 kV, the field on the lower surface, which is the cathode, is as high as 500 kV/cm. This value is certainly enough energy density to draw copious quantities of electrons from a bare metal surface. To avoid this, the cathode plate is kept covered by a thin but continuous film of silicone diffusion-pump oil. It was shown in experiments under the AURORA program that an oiled cathode surface

emits less than an ampere per square centimeter under a field of a million volts per centimeter. In fact, the limitation on this field remains to be established; the inductance of this region and, therefore, the tube as a whole can probably be again reduced. There is reason to believe that the silicone oil film will fail electrically in fields not much higher than a few million volts per centimeter in the vacuum. However, other liquids with an adequately low vapor pressure and a high dielectric constant, which will result in their being exposed to a field considerably less than that of the oil, have been discovered and investigated. The possibility also exists of using a slightly chilled layer of extremely clean mercury as the cathode conductor inside the tube. Magnetic isolation between anode and cathode plate is a final possibility, which was demonstrated in coaxial geometry at high voltages (1 to 5 MV) under the AURORA program, but it has yet to be shown that it is not subject to instabilities if closely spaced, flat electrodes are used.

It should be noted that all of these schemes except the last rely upon having a cathode-conductor surface forming the lower electrode on the horizontal tube. In our experiments the tube must be opened, inspected, cleaned, and refurbished with a new anode after each shot, a process which necessitates its removal from the generator tank. After it is reassembled and pumped down on an adjacent bench (the tube is held together by the vacuum only), the tube is slowly moved back to its position in the line with the aid of a hoist and swivel to maintain its horizontal attitude, preventing silicone oil from running off the surface or from forming a bridge between anode and cathode plate, which would readily flash over when the tube was pulsed.

The initial tube was designed to accommodate cathodes up to 20 cm in diameter. It was felt that with such a large cathode very low impedances could be maintained at moderately large spacings and that this would provide a good method for checking out the tube at high currents. It was hoped that, in spite of the large diameter of the cathode, the beam would pinch to a considerable extent as in the Model 730 Pulserad.

Provisions were also made for using smaller diameter cathodes in the same anode plate by having adapter plugs that insert into the anode plate and reduce the diameter of the hole. This provision is necessary to maintain the low inductance.

4.2 DIAGNOSTICS

The same generator diagnostics used when the line was discharged into a copper-sulfate resistor were employed during the first tube tests. These were a pulse-charge monitor, an output-voltage monitor, and a stainless-steel current-viewing resistor. Figure 24 shows typical traces from each of these three monitors. They are independently calibrated before insertion in the line. Their calibrations are checked against theory and, after installation in the line, are also checked by firing a series of open- and short-circuit shots. In addition, a number of diagnostics appropriate to the tube itself were employed.

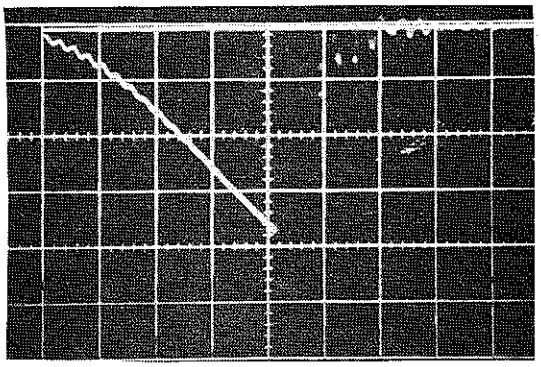

Pulse Charge
22 kV/cm

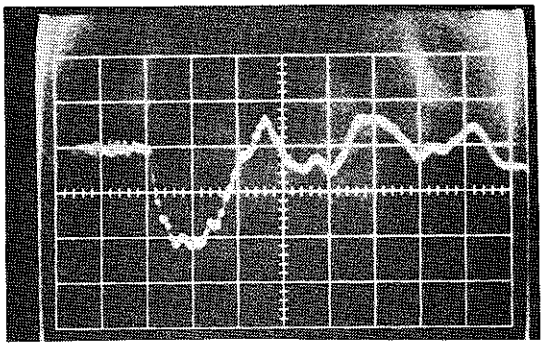

Output Voltage
55 kV/cm
50 nsec/cm

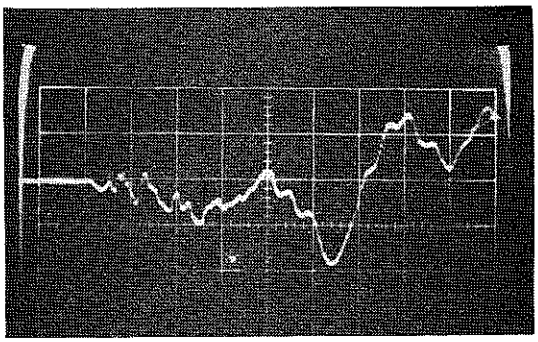

Output Current
0.55 MA/cm

Figure 24 Tube in place and 3-mm A-K spacing.

4.2.1 Faraday Cup. A Faraday cup constructed during a previous program was used to cross-check the current-viewing resistor in terms of total current delivered to the anode. The Faraday cup is a short 3-1/2-inch-diameter coaxial with a 0.001-inch stainless-steel outer conductor separated from a carbon inner conductor by four turns of 0.01-inch Mylar.* A new Faraday cup similar to the old one just described and large enough for use with the 20-cm-diameter cathode was also fabricated and cross-checked with the current-viewing resistor.

4.2.2 Pinhole Camera. An X-ray pinhole camera was used to take radiographs of the various cathodes tested. The camera was constructed of 1/8-inch lead sheets with a 1-mm pinhole, resulting in a magnification of 1/3 X.

4.2.3 Photodiode. The photodiode is an ITT with pilot B scintillation plastic. The low energy of photons produced by electron-beam irradiation of high-Z materials requires placing the scintillator-photodiode detector inside the drift chamber to avoid attenuation of the photon flux by the drift chamber walls. But problems are presented because the drift chamber is often operated at breakdown pressures as predicted by the Paschen curve, which means that the photodiode bias usually must be 300 volts, at which point saturation occurs at comparatively low dose rates. However,the photodiode output is used primarily in the beam work as a measure of the pulse duration. Figure 25 shows typical photodiode records for a short pulse (diode flashover midway during the pulse) and for a normal pulse (diode voltage held for full pulse duration).

*Details of this cup are given in "High ν/γ Experiments," PIFR-106, DASA 2175 (December 1968) SRD report.

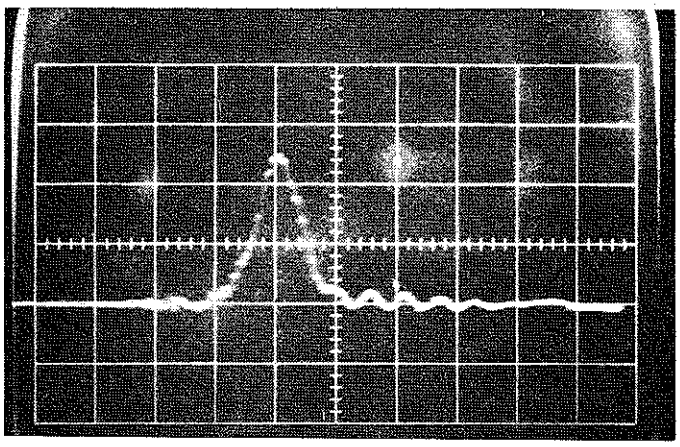

Photodiode--Pulse Width Normal
50 nsec/cm

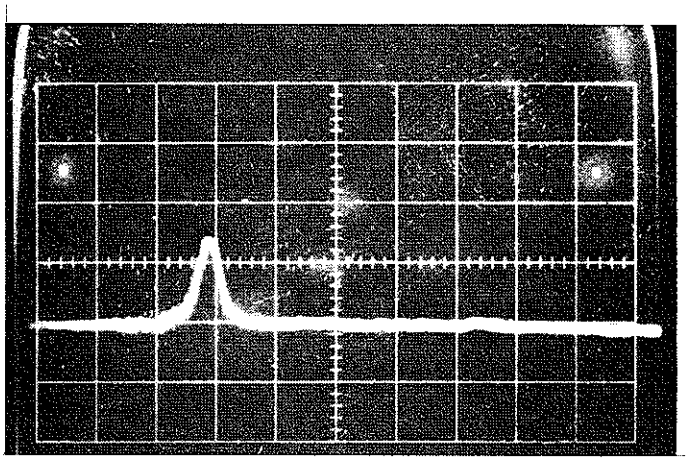

Photodiode -- Tube Arced
Pulse Width Narrow
50 nsec/cm

Figure 25 Photodiode traces.

4.2.4 Calorimetry. Calorimeter blocks were constructed from a 0.030-inch-thick layer of graphite bonded with thermal-conducting epoxy to a 0.100-inch-thick copper backing plate to which a thermocouple was attached. Temperature rise of the blocks was monitored with a Bausch and Lomb chart recorder. The useful range of graphite calorimeters is limited to low fluence levels, because front surface dose levels close to the anode are high enough to remove material from the calorimeter block. Qualitative fluence information at high fluence was obtained from damage in aluminum and red cinemoid foils.

4.3 DIODE EXPERIMENTS

4.3.1 Initial Tests. The insulating properties of the tube in the absence of current and magnetic field were verified by removing the cathode and allowing the tube to present an open circuit to the Blumlein, which then generated a peak voltage of up to 200 kV. The current monitor trace, which was synchronized with the tube voltage and photodiode traces by a common oscilloscope trigger, showed that no current flowed in the tube for the first two pulses of the Blumlein output train, but on the third pulse and subsequent pulses the tube impedance became progressively lower. Inspection of the tube showed that the arcing had occurred between the parallel anode and cathode conductors at many points over the large area that they present to each other. The experiment, however, showed clearly that any current that was observed to flow with the cathode in place must almost certainly be flowing between the cathode and the anode at least for the first pulse or two. This was important because it was impossible to use the Faraday cup in all tests.

The first tube tests with a diode also incorporated a 20-cm diameter cathode, comprising a large number of roll pins inserted individually into holes drilled in a brass block and then machined to form a planar cathode surface. The advantages of the roll pins are that they have two electron-emitting edges each and, in addition, can be individially removed and replaced in regions where cathode wear is greatest. The anode was sufficient to stop the electron beam almost completely in all cases, i.e., about 4-mil-thick stainless steel or copper.

The cathode was operated with various anode-cathode spacings. As with previously operated systems, the impedance seemed approximately to obey the formula of Child's law

$$Z \text{ (ohms)} = \frac{136\ d^2}{r^2\ V^{1/2}}$$

where d and r are the cathode radius in centimeters and V is in megavolts except that the constant was once more in the region of 80. Diode impedances as low as 0.05 ohm were obtained with anode-cathode spacings of about 1 mm, and currents up to almost 1.5 MA were recorded in the diode. This initial series of tests satisfactorily demonstrated the capability of the machine and of the low-inductance-tube diode system.

4.3.2 Beam Pinching in the Diode. During the program several different cathodes were used and these are referred to in the succeeding sections:

1. An 18-cm-diameter array of roll pins with a minimum spacing of about 2-1/2 mm
2. An 8.3-cm-diameter array of needle tips spaced about 2 mm apart
3. A 6.2-cm-diameter array of needle tips spaced about 2 mm apart

4. A 6.2-cm-diameter array of 7000 close-packed needles
5. A plasma cathode with a diameter of 6.7 cm

Measurements were next made of the current density at the anode. Observations of plane-parallel diode behavior in earlier high-current machines, such as the 730 Pulserad, had shown that at low values of diode impedance a strong pinch occurred, with a large fraction of the electrons reaching the anode near the center of the diode. The pinch is almost certainly a result of the self-magnetic interaction of the beam. It has been widely suggested that such a pinch should be expected to occur whenever the individual electron trajectories at the edge of the beam become so strongly curved that electrons lose all forward motion to inward radial motion before reaching the anode plane. Attempts at a self-consistent calculation of the electron flow that then results have so far been unsuccessful because of the complicated nature of the particle trajectories.

An exact criterion for pinching has not been well established. One appropriate form can be postulated by assuming that the cathode is a planar emitting surface; that there is a uniform electric field (V/d in the nomenclature of the preceding section) between the anode and cathode; and that the impedance is given by an expression of the form

$$Z_1 = \frac{kd^2}{r^2 V^{1/2}} \text{ ohms}$$

where k is an experimentally determined replacement for the usual Child's law constant.

The distance in the direction of E traveled by an electron released from rest in a crossed E-H field is given by

$$x = \frac{2mc^2 E}{e (H^2 - E^2)}$$

where E and e are in electrostatic units (esu) and H is in electromagnetic units (emu). This formula is valid for $H \geqslant E$, which corresponds to a drift velocity less than c. Substituting for E and H the values V/d and $2i/10r = 2V/10\ Zr$, respectively (which correspond to the magnetic field near the edge of the cathode), the criterion for pinching, $x < d$ becomes

$$\left(\frac{kd}{61rV}\right)^2 \quad \frac{1}{1 - \left(\frac{kd}{60rV^{1/2}}\right)^2} < 1$$

or assuming $k \cong 60$,

$$\frac{d}{rV\left(1 - \frac{d^2}{r^2 V}\right)^{1/2}} < 1$$

In the present case of interest one can simply write

$$\frac{d}{rV} \leqslant 1,$$

since if this condition is satisfied with $V \cong 0.1$ MV, then

$$\frac{d^2}{r^2 V} << 1$$

Electron space charge may be expected to reduce the field near the cathode and, hence, increase the tendency to pinch over that predicted in this treatment. In practice, field enhancement is often found at the edge of the cathode (and also near individual emitters) and this may have the reverse effect.

Work on the 730 Pulserad had previously shown that pinching certainly occurred with $d/rV \cong 1/2$. The algebraic form of the criterion suggests that in the preliminary experiments with the roll-pin cathode ($r \cong 10$, $V \cong 0.1$, $d = 0.2$ to 0.3 cm) strong pinching should certainly occur, which was not the case, however.

Figures 26 and 27 show the target damage of the anode at different currents. It can be seen that at higher current levels the beam shows a definite tendency to converge towards the anode without ever pinching tightly. In particular, Figure 26 shows the anode damage with a 4-mm anode-cathode spacing with a beam current of about 0.5 MA; Figure 27 shows the damage with a spacing of 2 mm and a current of rather less than 1 MA. Current distributions at the anode were also observed with pinhole cameras and faceplate thermoluminescent dosimeter (TLD) maps. Dose levels of up to 70 R were detected at 10 cm from a 4-mil copper anode with peak photon energies of less than 100 kV. Radiation outside the tube and beam chamber was at a high enough level to require external lead shielding.

In view of these results it was decided to investigate in the next set of experiments to determine whether the failure to pinch was a result of a difference between conditions in the Mylar-line tube and those in other low-impedance machines, such as risetime, prepulse, or residual gas. A 6.2-cm-diameter, multiple-needle cathode, identical to those used in the Model 730 Pulserad and the

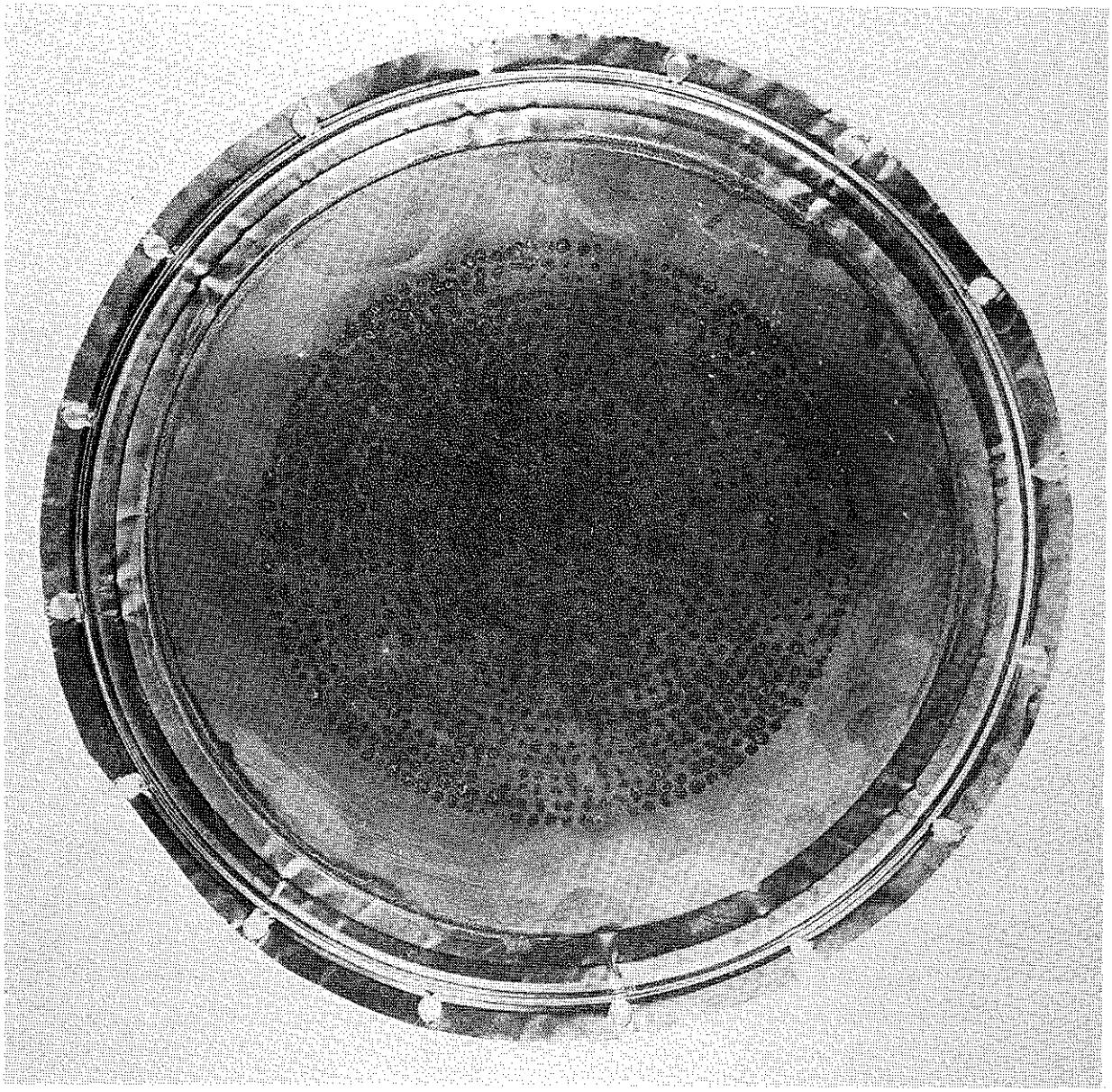

Figure 26 Anode damage from a 18-cm-diameter cathode at 4 mm with a current of 0.5 MA and voltage of 130 kV.

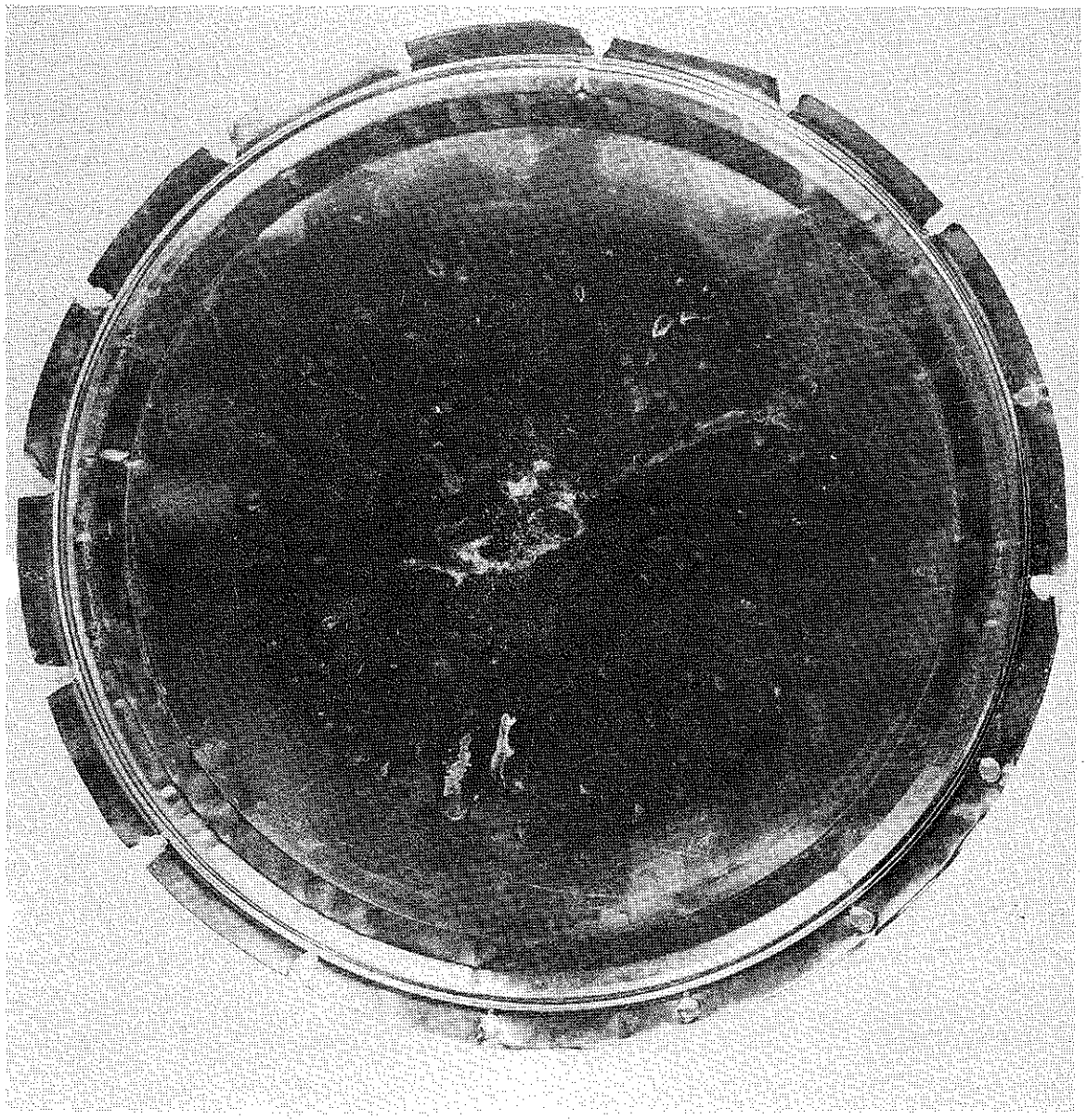

Figure 27 Anode damage from a 18-cm-diameter cathode at 2 mm with a current of 0.8 MA and a voltage of 100 kV.

low-impedance Model 1150 Pulserad (in which a strong electron-beam pinching in the diode was observed), was installed with an adapter in the anode plate to reduce the size of the anode aperture from just over 8 inches to about 3 inches. With this cathode, strong beam pinching was immediately observed. Figures 28 and 29 show the center section of 4-mil-thick copper anodes ruptured in the center by the pinched beam. Damage to each anode can be seen to increase from the edge of the cathode outline toward the center. TLDs were again used to map the X-ray dose on the anode for each shot. A typical map is shown in Figure 30. The current on this pulse was about 450 kA. Figure 31 shows an accompanying photodiode trace and the output voltage trace. The photodiode pulse width confirms that the impedance of the diode is relatively stable during the entire first voltage pulse.

Pinhole radiographs of the anode were also made using the 6.2-cm-diameter, 600-needle cathode. An anode of 1-mil aluminum was used with the pinhole camera set back 6 inches from the anode. The radiographs confirmed a pinched beam at AK spacings of 1.5 to 3.0 mm (see Figure 32). Radiographs at 1-mm AK, however, showed a uniform beam with no evidence of a pinch (see Figure 33).

The next cathode tested was the 8.3-cm-diameter needle cathode. Figures 34 to 36 show the damage to 4-mil copper anodes at various AK gaps. As with the 6.2-cm-diameter needle cathode, the 8.3-cm-diameter cathode will not produce a pinched beam at an AK gap of 1 mm, but will at increasing AK spacings. The AK settings used for the plasma cathode of 1.75 and 2.0 mm similarly pinched; a typical radiograph is shown in Figure 37.

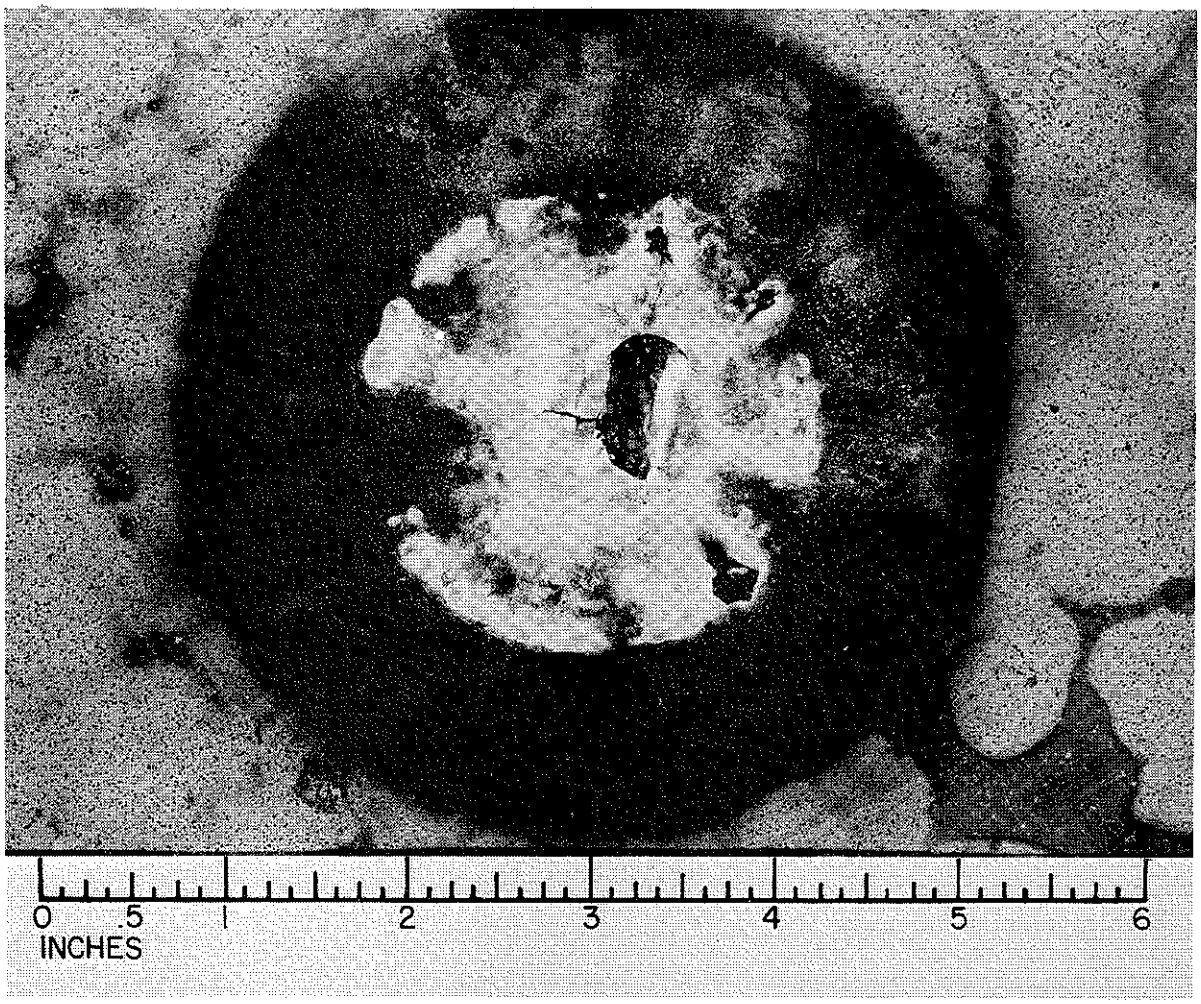

Figure 28 Anode damage from a 6.2-cm-diameter needle cathode at 2.25 mm with a current of 100 kA and a voltage of 120 kV.

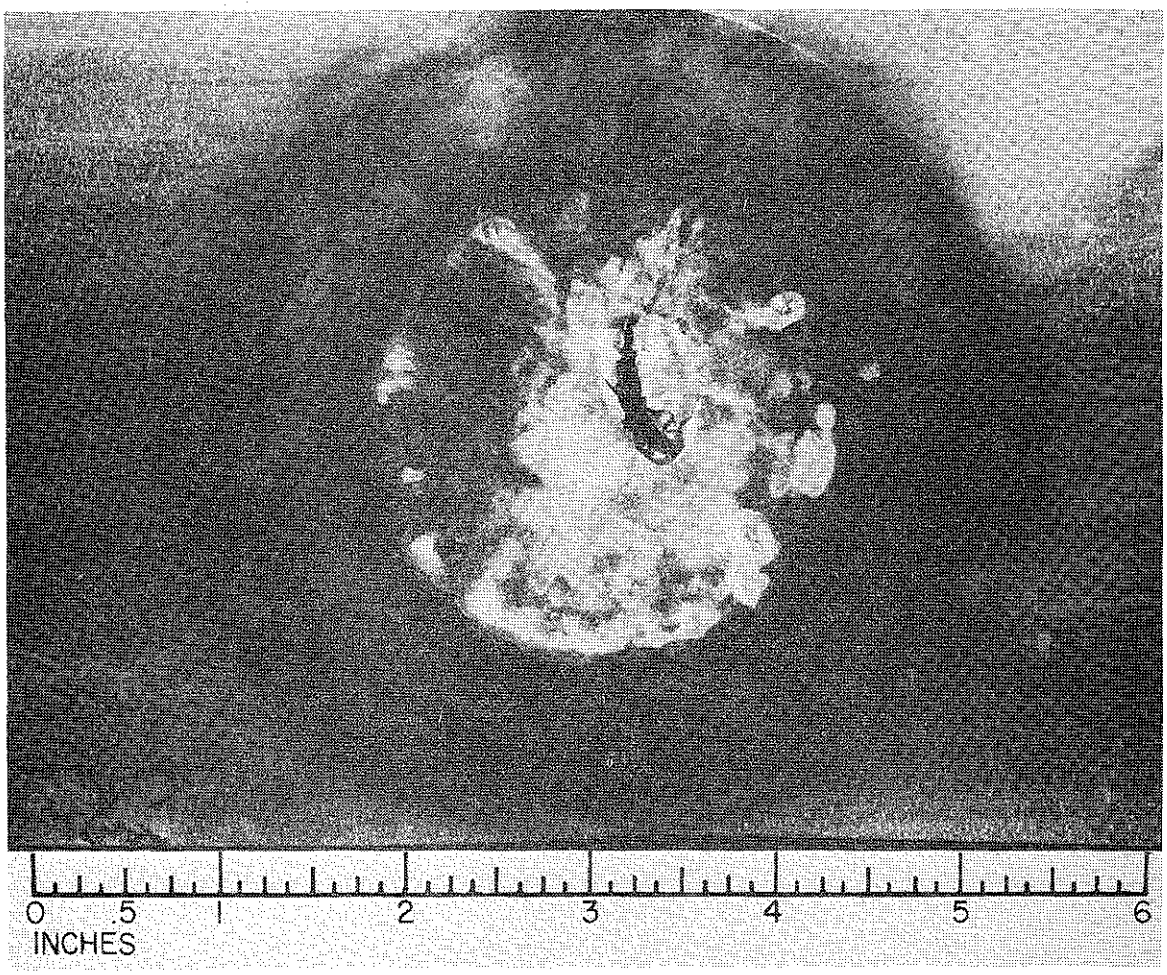

Figure 29 Anode damage from a 6.2-cm-diameter needle cathode at 3 mm with a current of 80 kA and a voltage of 130 kV.

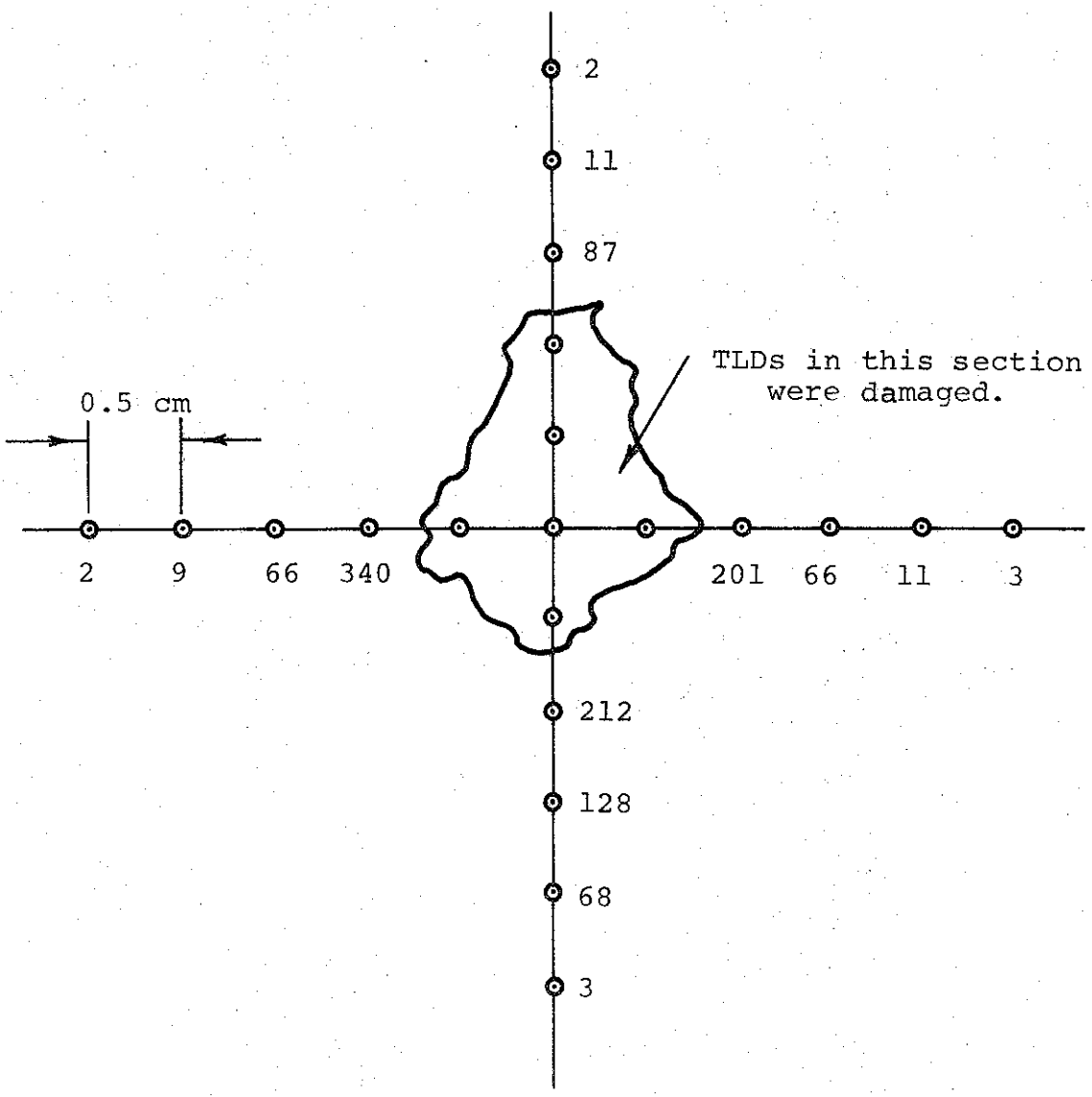

Figure 30 Dose distribution (roentgens) from an anode TLD map on the low-voltage Mylar line.

5923

Pinch behavior of the 2-1/2-inch-diameter 7000-needle cathode followed that of the 6.2-cm needle cathode (Figure 38). It would not pinch at 1 mm but would at larger AK gaps--at least up to 3 mm. When the pinch did occur it was not well defined or symmetric. Figure 39 shows a typical pinch. It is somewhat elongated and there appears to be an additional "hot spot" near the cathode edge. Hot spots occurred on numerous shots and were not always in the same location. The close spacing of the needles, made by reducing the field enhancement at the tips, probably caused emission less regular and more sensitive to needle position.

The results suggest the possibility that pinching in plane parallel diodes has a low-impedance limit (perhaps when the spacing becomes less than 3 to 5 percent of the radius), as well as a high-impedance limit. The results are not conclusive, however.

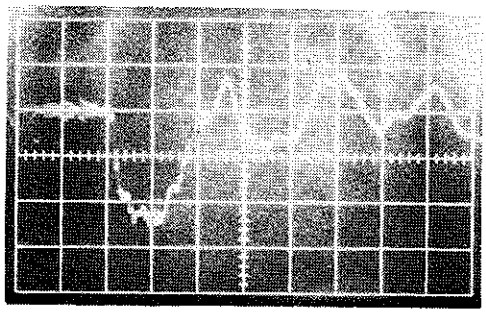

Output Voltage
(t_o--2 cm from left)
50 nsec/cm
55 kV/cm

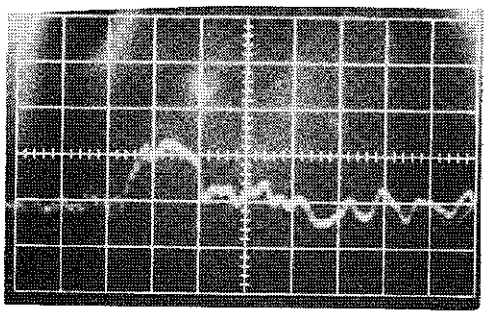

Photodiode
(t_o--2 cm from left)
50 nsec/cm

Figure 31 Output voltage and photodiode waveforms from low-voltage Mylar line.

R9688

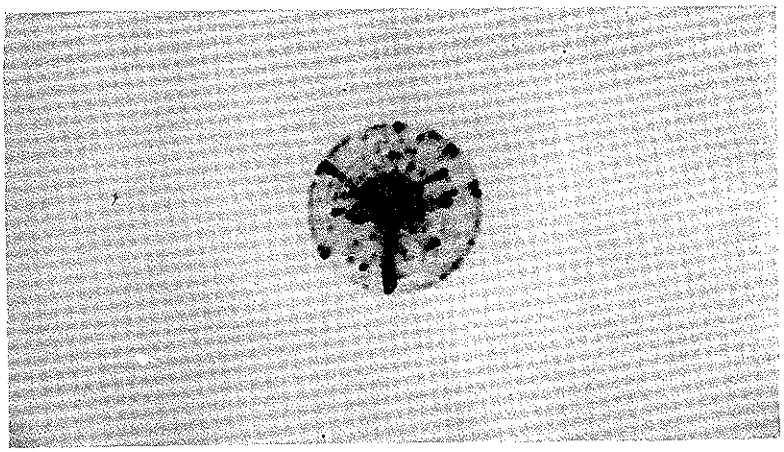

Figure 32 Radiograph with a 6.2-cm-diameter needle cathode at 1.5 mm with a current of 300 kA and a voltage of 140 kV.

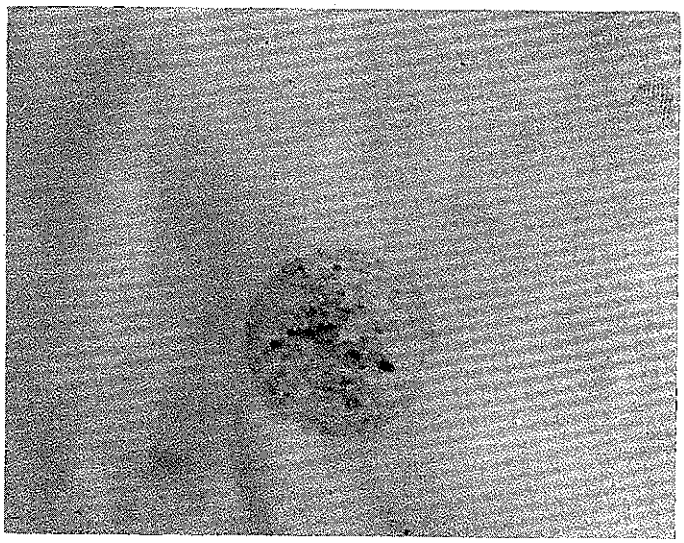

Figure 33 Radiograph with a 6.2-cm-diameter needle cathode at 1 mm with a current of 500 kA and a voltage of 110 kV.

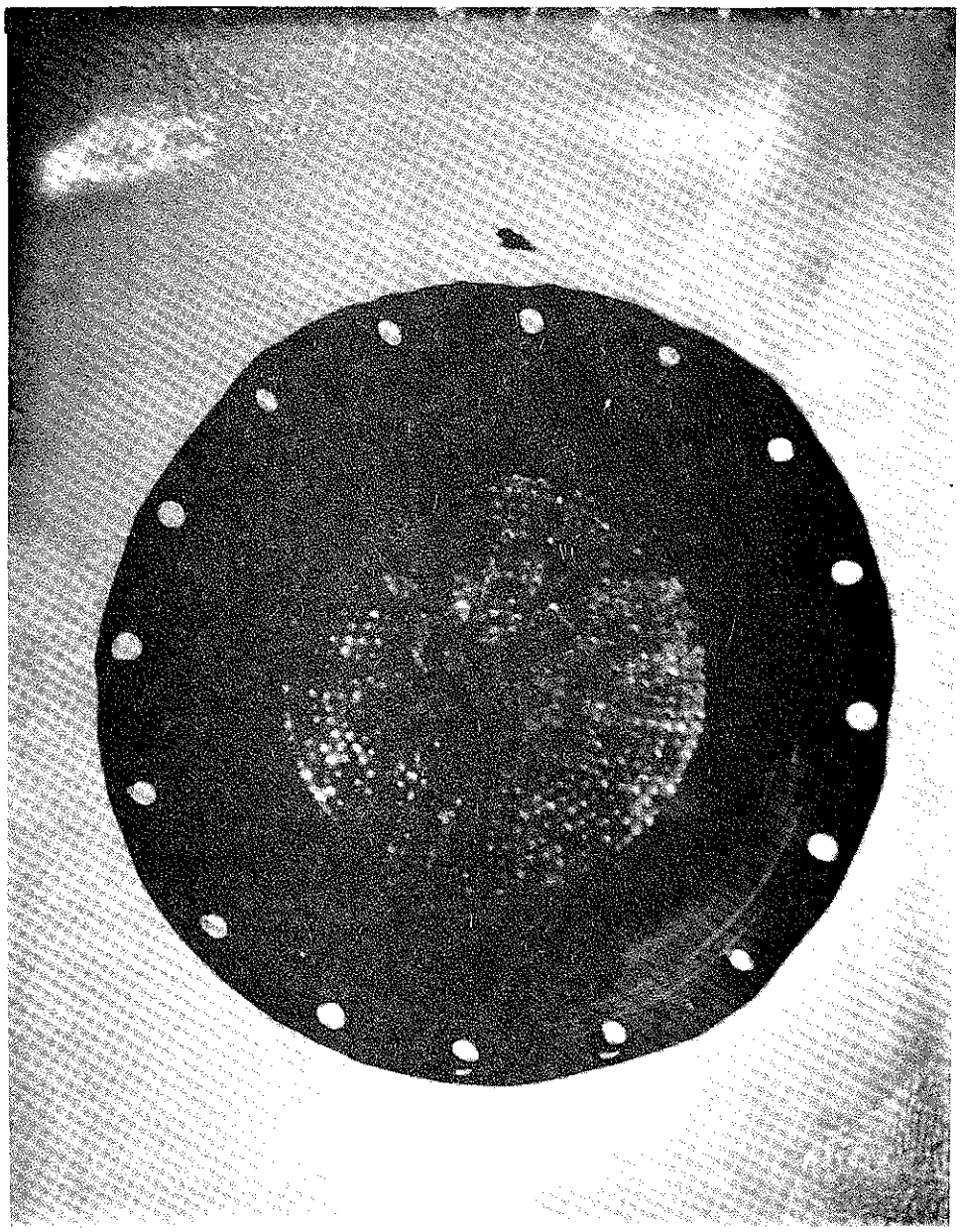

Figure 34 Anode damage from a 8.3-cm-diameter needle cathode at 1 mm with a current of 900 kA and a voltage of 100 kV.

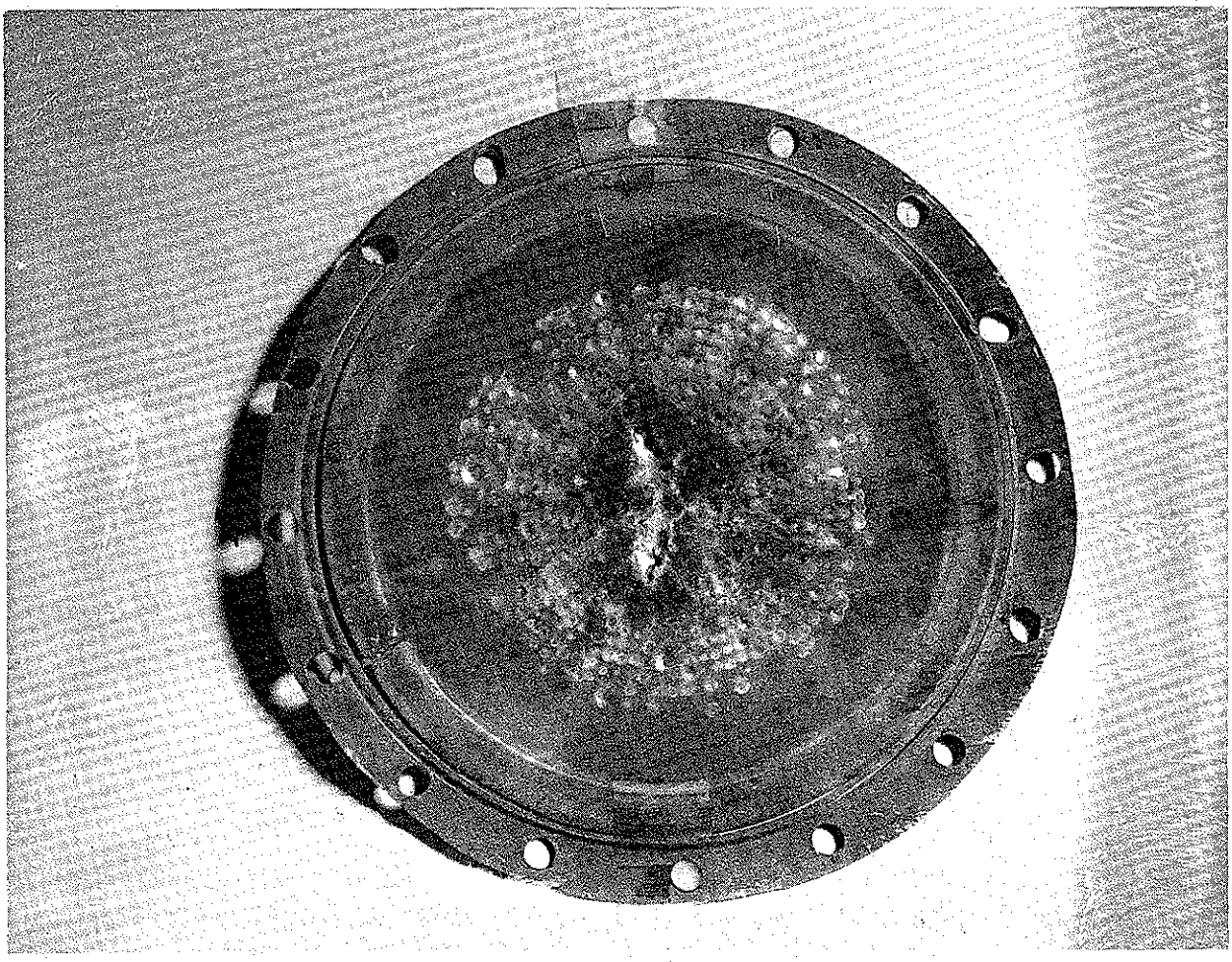

Figure 35 Anode damage from a 8.3-cm-diameter needle cathode at 1.5 mm with a current of 340 kA and a voltage of 80 kV.

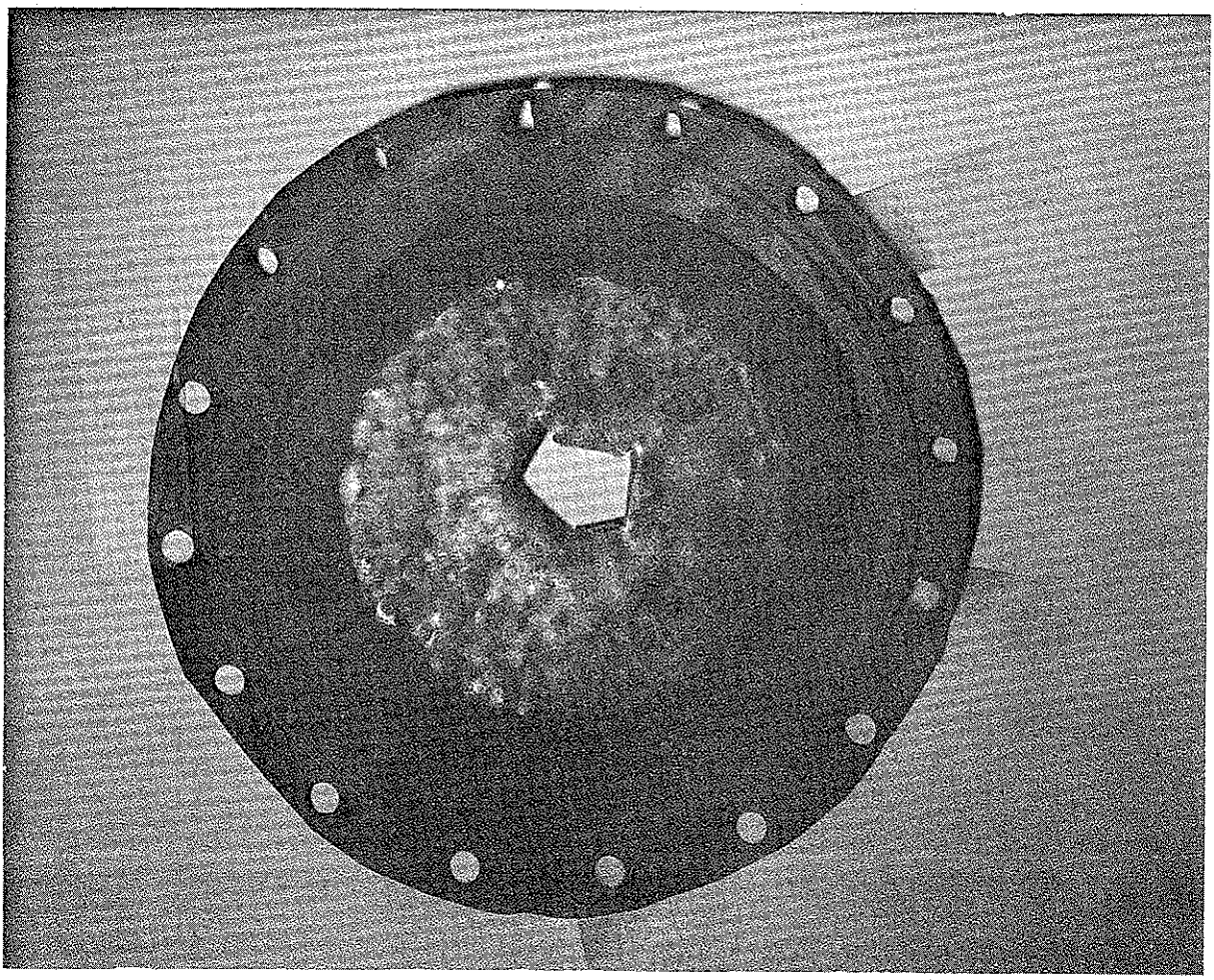

Figure 36 Anode damage from a 8.3-cm-diameter needle cathode at 2.5 mm with a current of 150 kA and a voltage of 90 kV.

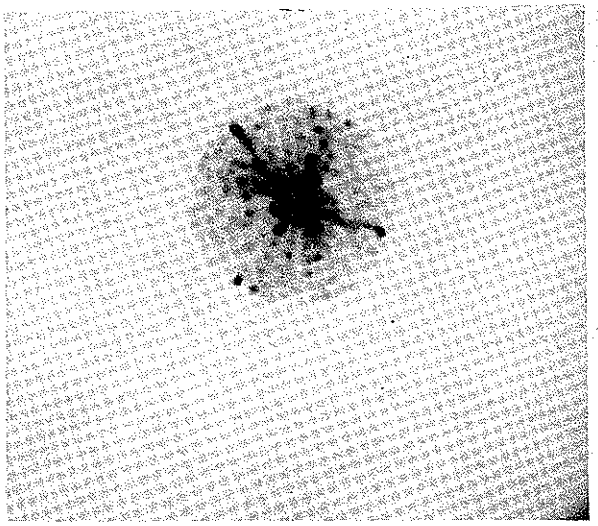

Figure 37 Radiograph from a 6.7-cm-diameter plasma cathode at 2 mm with a current of 330 kA and a voltage of 150 kV.

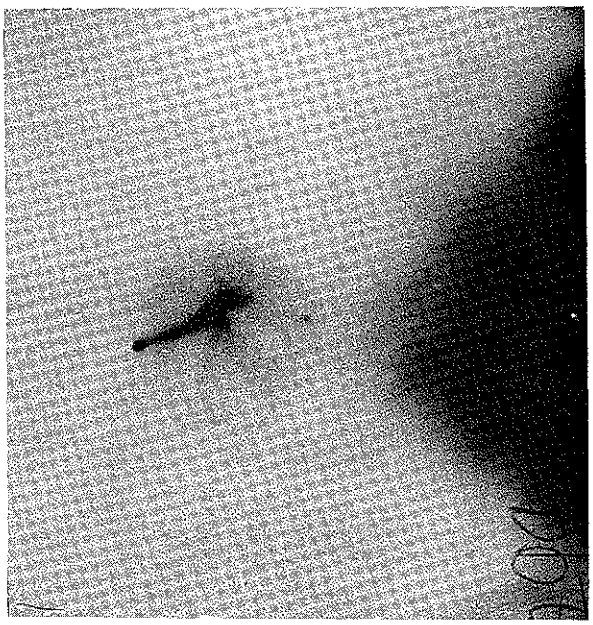

Figure 38 Radiograph from the 7600 needle cathode at 2 mm with a current of 200 kA and a voltage of 140 kV.

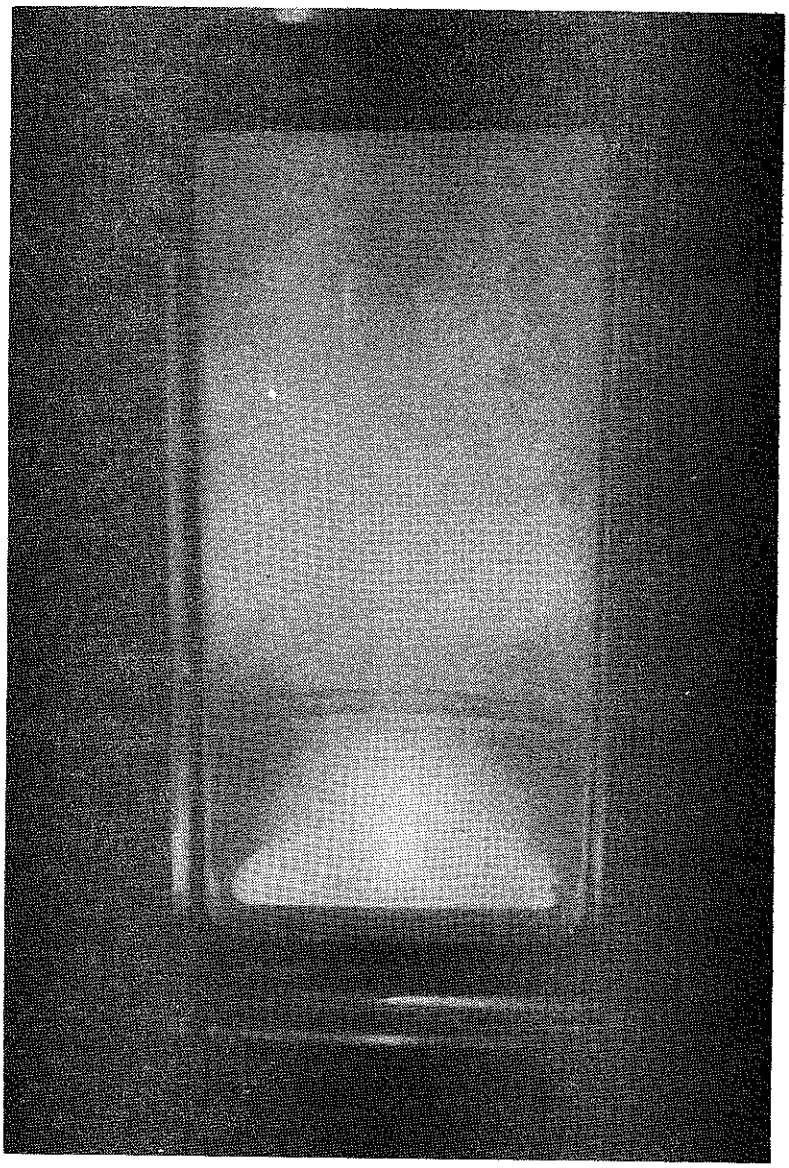

Figure 39 Pinched electron beam.

It is possible that they were affected by the geometry of the individual emitters. If these are too widely spaced, for example, the cathode may not behave as a planar emitter at close spacings, and the electric and magnetic fields near the cathode are enhanced or made nonhomogeneous. Whereas if the emitters are very closely packed, as in the 7000-needle cathode, the lack of field enhancement may result in irregular or reduced emission.

4.3.3 Diode Impedance. Figures 40 to 42 show the results of an analysis of the diode impedance as a function of cathode geometry. The cathodes used were referred to in the preceding sections.

The impedance of a large, circular parallel-plane diode is given on the space charge limited model, neglecting positive ion neutralization, by the formula

$$Z_1 = \frac{136\ d^2}{V^{1/2}\ r^2} \text{ ohms}$$

where d is the cathode anode spacing, r the radius, and V is the voltage in megavolts. The result applies when V is less than 0.5, since the calculation is nonrelavistic.

In view of the fact that the voltage dependence is weak--at higher voltages (relativistic) it should tend to disappear--no attempt was made to verify it. The analysis is designed to show whether the square dependencies on d and r are valid and what the value of the constant appears to be.

In analyzing a given test, the impedance Z can be calculated either by the current and voltage measured directly from oscilloscope traces or by measuring the gain, G, of the pulser from the input and output voltages, and using the calculated generator impedance Z_G and the formula $Z_1 = (G/2 - G)\ Z_G$. The output voltage

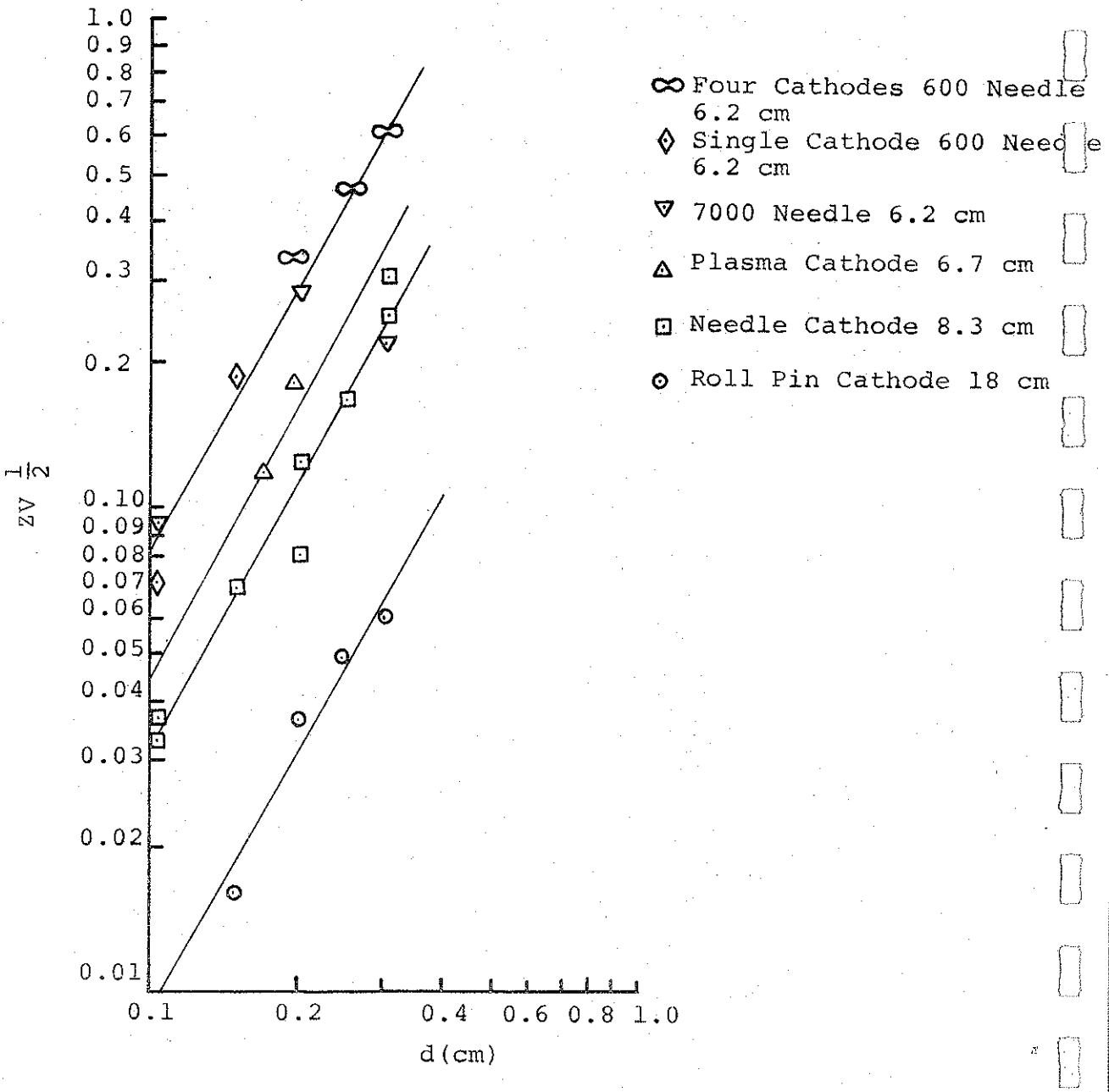

Figure 40 Diode impedance versus AK spacing.

8521

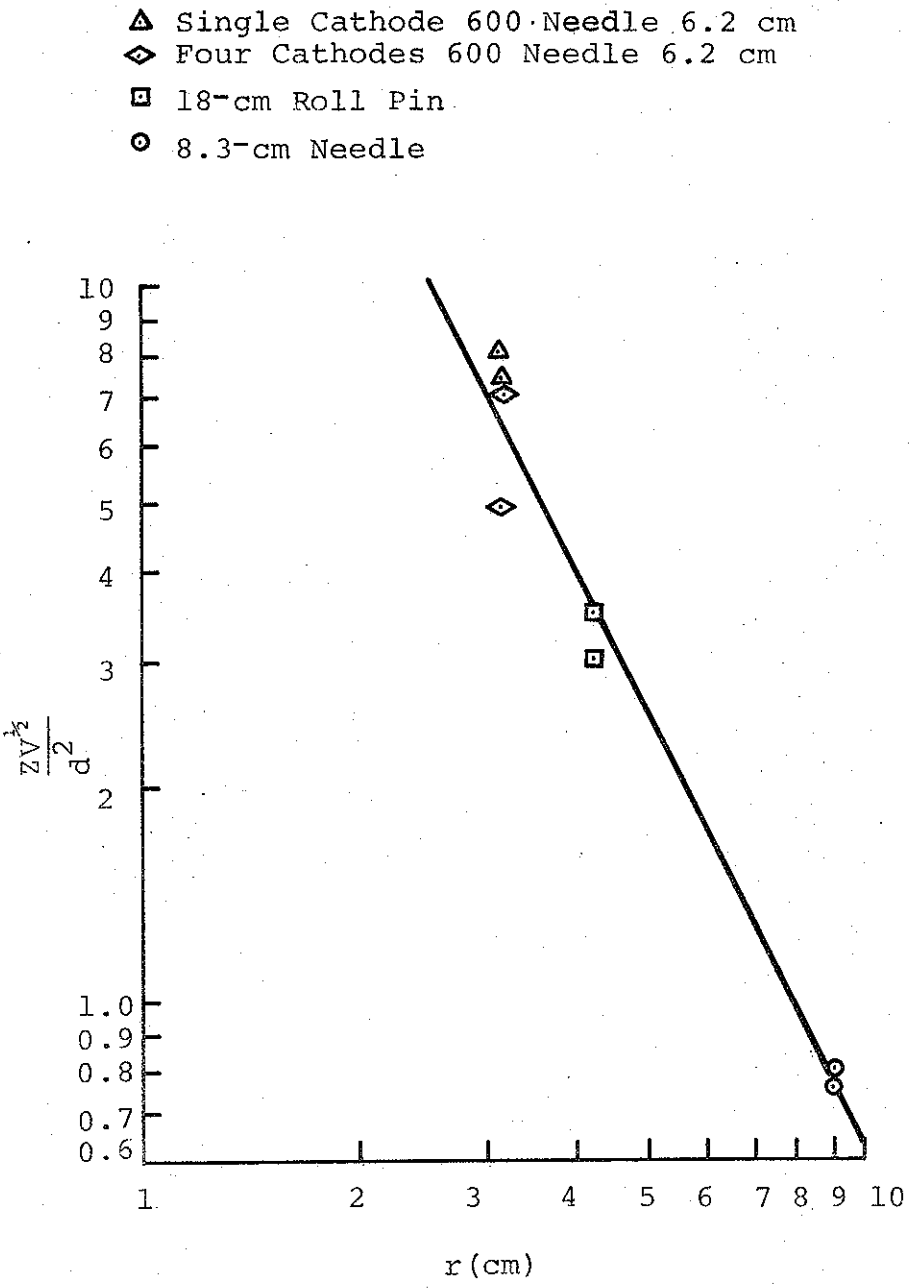

Figure 41 Effect of cathode radius - normalized for different spacing.

8441

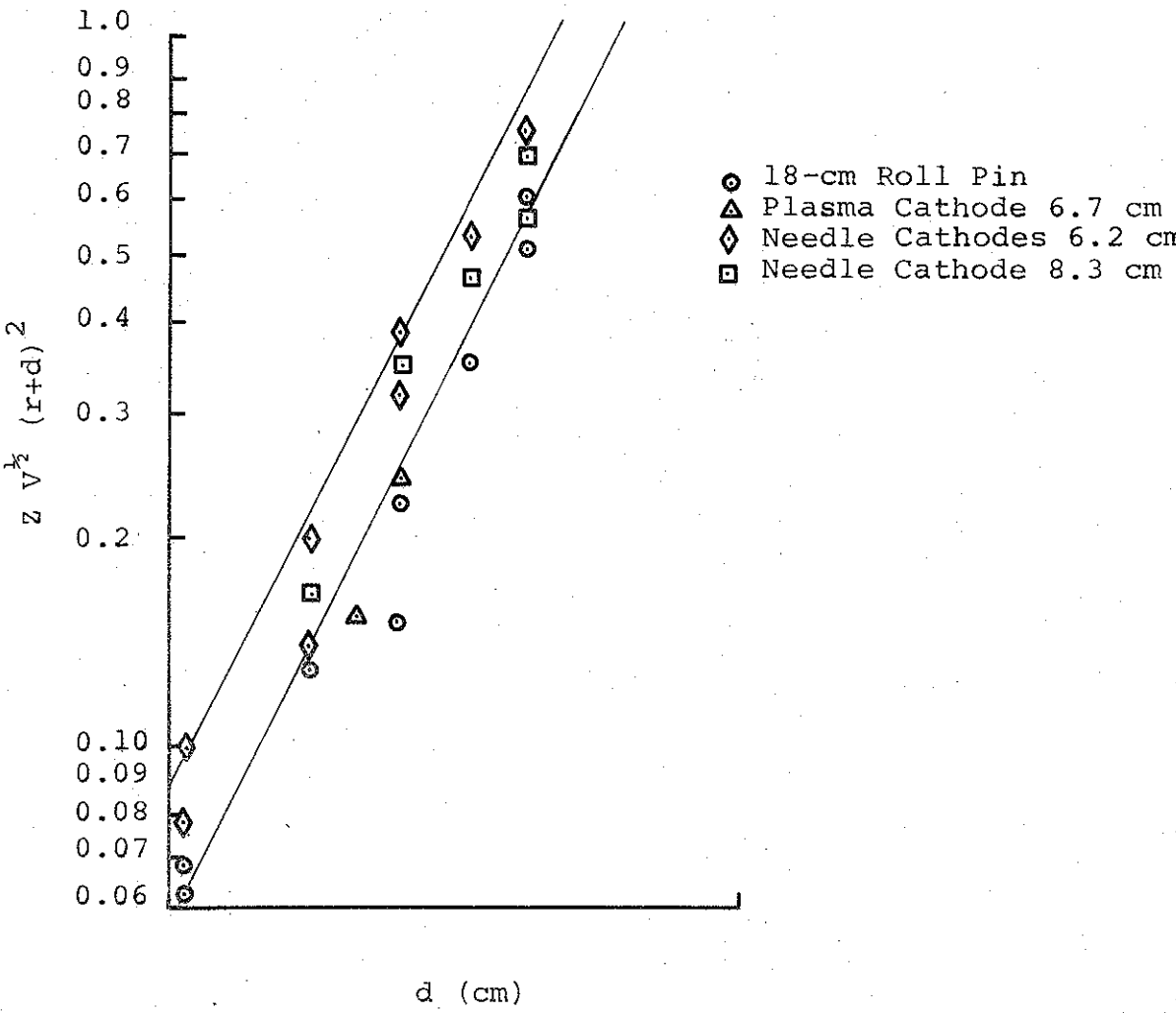

Figure 42 Impedance versus spacing--normalized for different radii.

in either case was measured at the end of the output pulse so that the inductive voltage drop on the tube was small. The current calculated by the two methods was compared and averaged. The data were rejected, however, if an agreement of better than 1.5:1 was not obtained. In some cases, there was in fact a disagreement by as much as 2:1, and where this was not attributable to errors in attenuation calculations it is probably a symptom of phase difference in current and voltage waveforms. In some cases, the impedance of the diode fell sharply toward the end of the pulse. This effect was especially noticeable at the higher charging levels, and a preliminary, but inconclusive, attempt was made to ascertain the factors influencing it.

Figure 40 shows the quantity $ZV^{1/2}$ plotted on a full logarithmic scale against the spacing d for the various cathodes. All show a general slope of about 2, with considerable experimental scatter. Each point is the average of several pulses. The experiments were performed over a long period of time, which together with phase differences, monitor calibration errors, and the difficulty of measuring the small anode spacing in a very exact and consistent manner, probably accounts for the experimental scatter. (As noted in a previous section, the current monitor was sometimes hard to read accurately.) Not shown in Figure 40 are some data for the 6.2-cm-diameter cathode, giving the impedance to be a factor of as much as 4 lower than the line drawn. There is no clear reason to invalidate these data. In other respects the impedance is the same for both types of 6.2-cm-diameter cathode, and is also the same where four parallel magnetically isolated cathodes are used.

The slope of the lines in Figure 40 appears to average about 1.9, which is probably not significantly less than 2, although a reduction of slope would be expected from the edge Effects. Beam spreading and the enhanced field at the edge of the cathode will increase the effective diameter to an extent which increases with spacing. In Figure 41 an attempt has been made to include this by plotting $ZV^{1/2}$ (r + d). At the same time, the expected dependence on cathode area has been incorporated, so that all the points should lie on one line. Though they do not, no specific tendency of the line to change position with radius--or cathode type--can be detected. The lines still have a slope of a little less than 2 and correspond to a range of Child's law constants from about 60 to 90.

Figure 42 shows the effect of cathode radius. The points represent averages of the quantity $Z_1 V^{1/2}/d^2$ obtained in experimental sequences in which d itself was allowed to vary. The line drawn has a slope of -2.0.

4.4 MYLAR-STRIPLINE ELECTRON-BEAM PROPAGATION

The development of machines having increasingly high electron-beam currents and very high ν/γ, necessitates an investigation into the applicability of present beam diagnostic and handling techniques. One reason for this is the presence in such beams of transverse energy, the kinetic energy of radial electron motion (References 1 and 2). Radial components of velocity result from the gyration of individual electrons in the large self-magnetic field of the beam. When a significant fraction of total beam energy lies in transverse motion, propagation can be seriously degraded by loss of electrons in the radial direction. In addition, transverse energy in the relatively low-energy Mylar line beam increases the

difficulty of certain existing diagnostic techniques. This difficulty is a result of the distortion of the deposition profile near the target front surface that results when a 100-to 200-keV electron having a large component of transverse velocity strikes that surface at a very oblique angle. For example, this effect would complicate the interpretation of a depth-dose measurement. This measurement is usually taken by injecting a representative part of the beam into a layered assembly of thin metal foils and then measuring the temperature rise of each foil. When electron-beam mean energy is low and transverse energy content is high, the beam energy is deposited in the foils in a very short axial distance. Because a small volume of material receives all the energy of the beam, the number of calories per gram can be high enough except at extremely low fluences to destroy the relevant foils before a temperature measurement can be made. Consequently, it becomes necessary to test and modify present techniques so as to extend applicability to this new beam region.

Another intrinsic aspect of high-current, low-energy beams is their vulnerability to their self-induced axial electric field, E_z. The current growth with time, $\partial I/\partial t$, is large at the beam front, and this induces a strong back-emf E_z (References 1 and 2). Depending upon the actual value of dI_{net}/dt in the drift chamber, this "breaking" field E_z could be as high as 100 kV in a few centimeters. Such a field could make beam generation and propagation impossible for a beam whose mean energy is in the 100-keV range. The beam does not self-stop completely, though it remains to determine what fraction of the energy is lost to the E_z field. It is anticipated that the effect of E_z will be detrimental to all ultra-high ν/γ beams.

New techniques, reported below, are being tested and developed to avoid this effect (as well as radial electron loss due to transverse energy). These techniques are pre-ionization with a linear-pinch discharge and the use of multiple cathodes.

Results of beam propagation experiments are presented in the next subsections. These include multiple cathode beam generation, Faraday cup measurements, observation of time-integrated beam cross section, and beam propagation in pre-ionized gas with weak magnetic field.

4.4.1 Results of Beam Propagation Experiments. Several techniques for beam propagation were investigated. Each of these is described in the following paragraphs.

Multiple Cathode Beam Generation. A method to reduce the effects of the induced electric field, E_z, is to use multiple cathodes. If the number of cathodes used is n, then the current flowing from each cathode is roughly* I (t)/n, where I (t) is the current waveform obtained with just one cathode. Then for each of the n electron beams obtained, the current growth rate is correspondingly reduced by the factor n and so too is the field E_z. In this way less total work on electrons is done by induced axial electric fields than would be the case if only one cathode were used. A disadvantage of the multiple cathode technique is the problem of handling n electron beams. Magnetic isolation in the diode must be made possible so that the injection of each beam is independent of the others and so that the injected beams can be propagated and possibly recombined as the application requires.

*This simple argument does not account for the change in diode inductance which results from changes in anode-cathode geometry, as when n cathodes are used instead of one. The tube impedance change results in a new total current, in addition to division among the cathodes.

An array of four magnetically isolated cathodes was used (Figure 43). The 2.5-inch-diameter, 600-needle cathodes are attached to the cathode plate and can be shimmed to vary the anode-cathode gaps between 0 and 3 mm. Figure 44 shows the anode insert plate with aluminum crossbars to provide magnetic isolation. An array of four 2-inch-diameter copper guide pipes is shown in Figure 45. This arrangement allows the option of carrying out four separate experimental measurements per shot, such as open-shutter photography, calorimetry, and net current measurement and the use of a witness plate and scintillator-photodiode detector for damage and bremsstrahlung measurement. The multiple cathode experiments were carried out when the impedance of the line was 0.1 ohm.

Initial shots with an aluminum witness plate at the anode showed the magnetic isolation to be insufficient (the four beams were magnetically attracted in the diodes and hit the witness plate at the inside edge of the four cathodes). The magnetic isolation was increased by installing aluminum sleeves in the anode insert plate to improve the magnetic shielding. After this modification the beams were observed to be fairly well centered with respect to each cathode. (At current levels of 0.8 MA the diagonal distance between beam centers was observed to be 5 inches, compared to a 5.5-inch diagonal distance between cathode centers.)

Several shots at 75-kV charging voltage were made with no guide pipes in the drift chamber to determine the interaction of the four beams. A red cinemoid witness plate placed 10 cm from the anode showed an irregular damage spot approximately 15 cm in diameter. One pulse terminated early and resulted in a hollow, ring-shaped damage spot 15 cm in outer diameter and 4 cm wide.

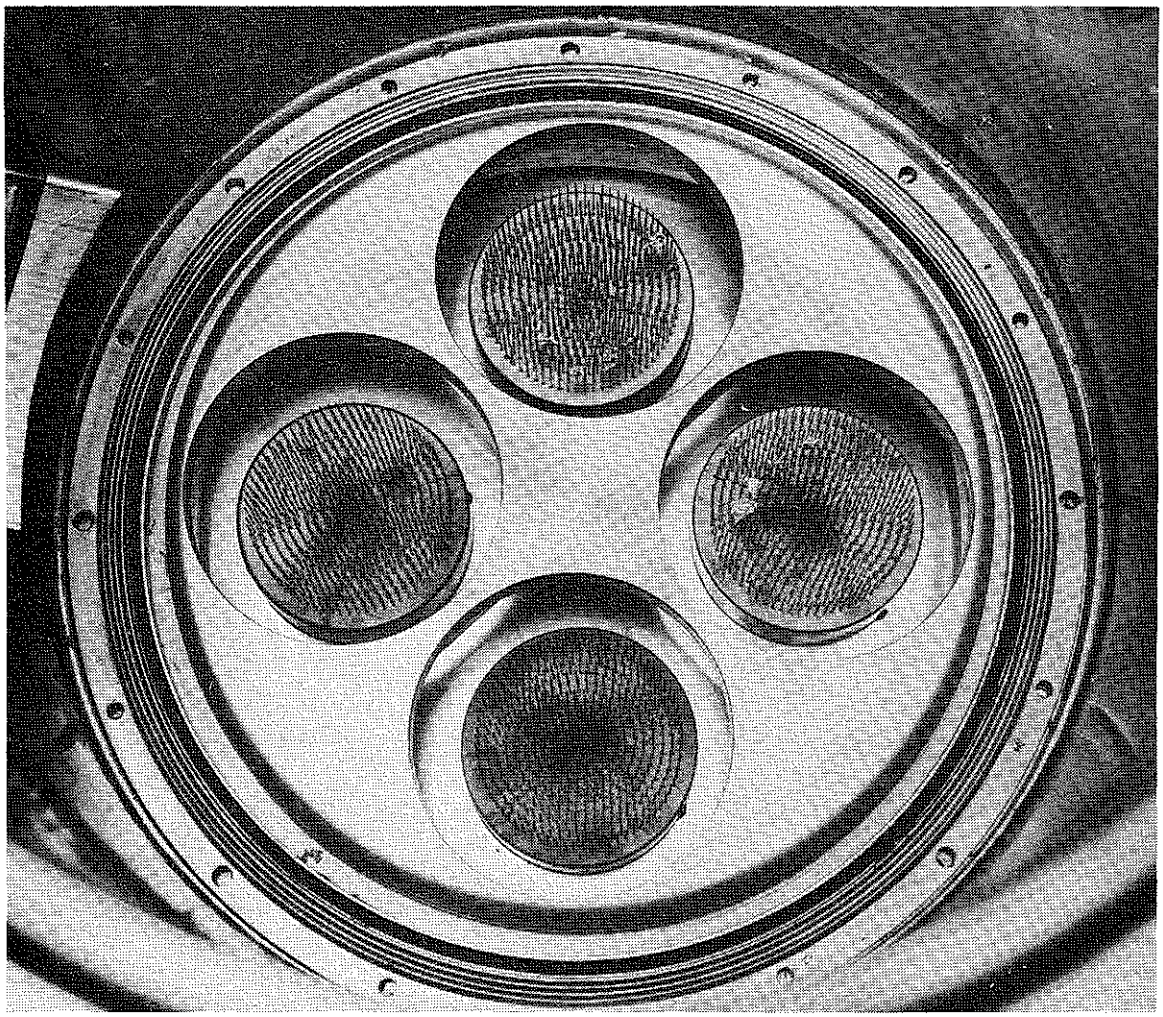

Figure 43 Array of four magnetically isolated cathodes.

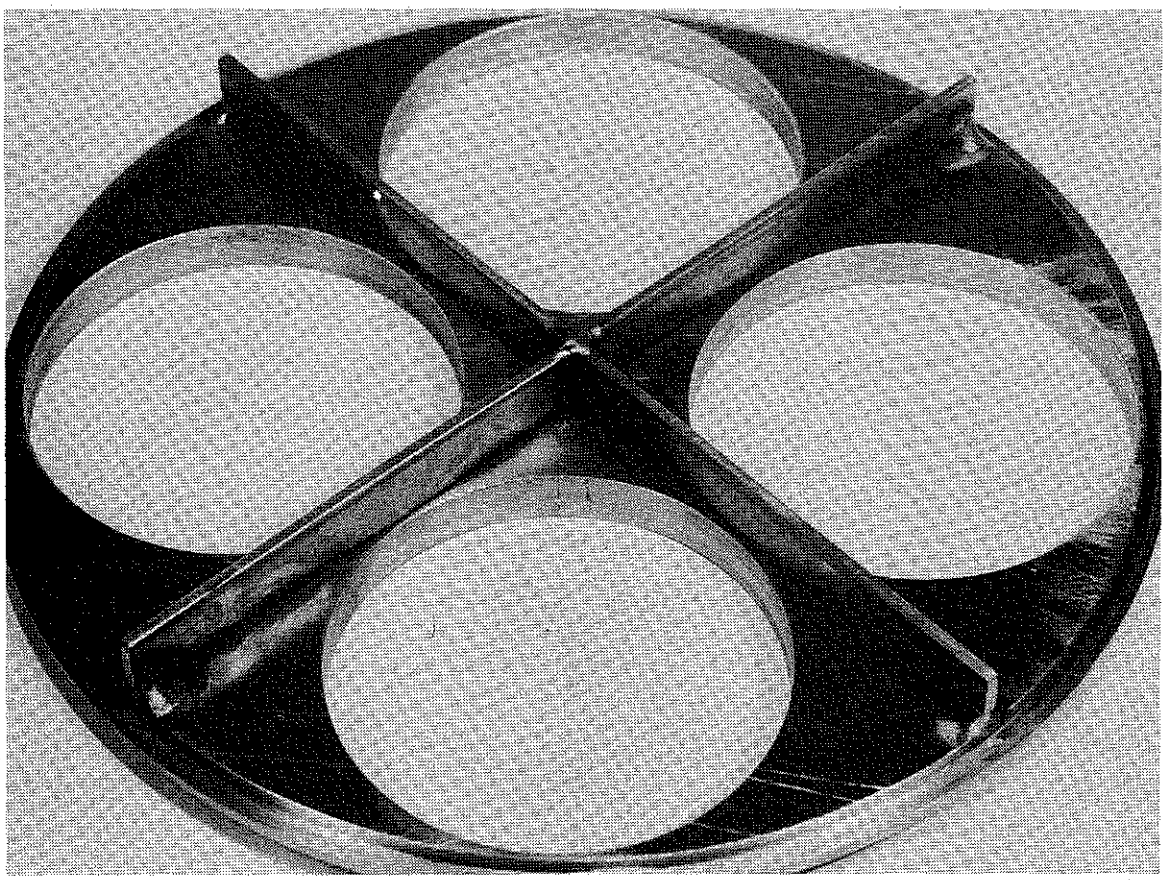

Figure 44 Anode insert plate.

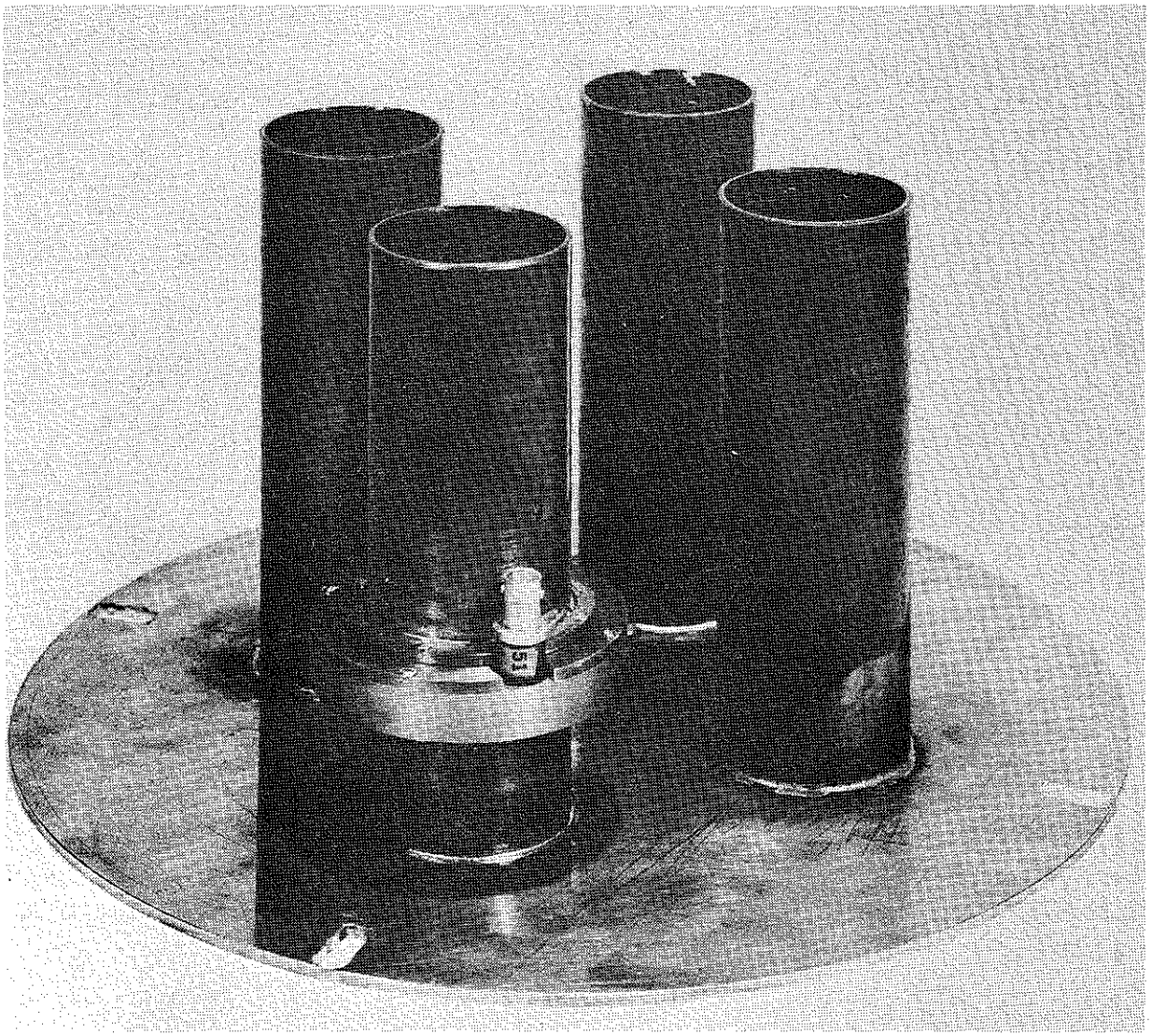

Figure 45 Copper beam-guide pipes.

From these shots we concluded that the beams were coalescing early in the pulse into a hollow ring, and that this ring gradually collapsed during the pulse to produce a circular area of damage. The damage level over the circular area was not uniform, making this beam unsuitable for sample irradiation. The four beams were also injected into the array of 2-inch-diameter guide pipes (Figure 45). Figure 46 shows results from a typical shot at 700-micron drift chamber pressure. The photodiode indicates a 90-nsec duration pulse (FWHM). The peak electron energy was 140 keV at a peak total current of 0.6 MA. The witness plate (red cinemoid) shows a hollow damage spot, which also occurred at pressures of 0.3 and 1.5 torr. This effect was interpreted as arising from the large back emf (maximum on the guide pipe axis), which stopped the beam near the center of the guide pipe. (This back emf is zero at the guide-pipe walls, which allowed the beam to propagate in this hollow mode.) We observed very little difference in damage to the cinemoid target over the pressure range 0.3 to 1.5 torr. The maximum net current was observed to decrease with pressure up to 1.5 torr (200-keV beams at 200 kA produced with the Model 730 Pulserad show a minimum net current at 0.75 torr).

The next series of shots was at 100-kV charging voltage. With the higher current generated at this charging voltage the magnetic isolation described above proved insufficient. The isolation was increased by extending the crossbars shown in Figure 44 to within 5/16 inch of the cathode plate, and the problem was solved. Preliminary shots showed that the beams produce a more uniform damage crater at the exit of the guide pipe.

The experiments described above demonstrate qualitatively that the multiple-cathode technique works and can be used to avoid the problems intrinsic to very high current, high ν/γ beam

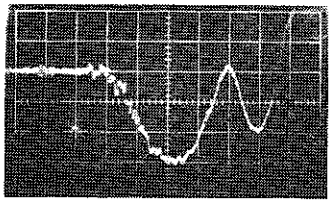

I_o 200 kA/cm
50 nsec/cm

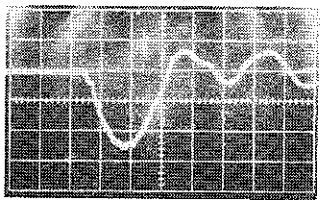

V_o 55 kV/cm
50 nsec/cm

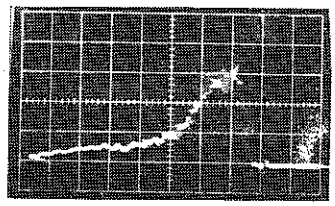

Photodiode

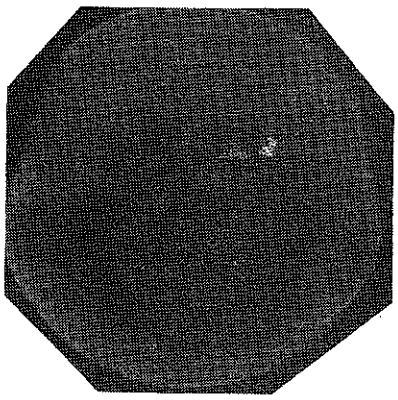

Witness Plate

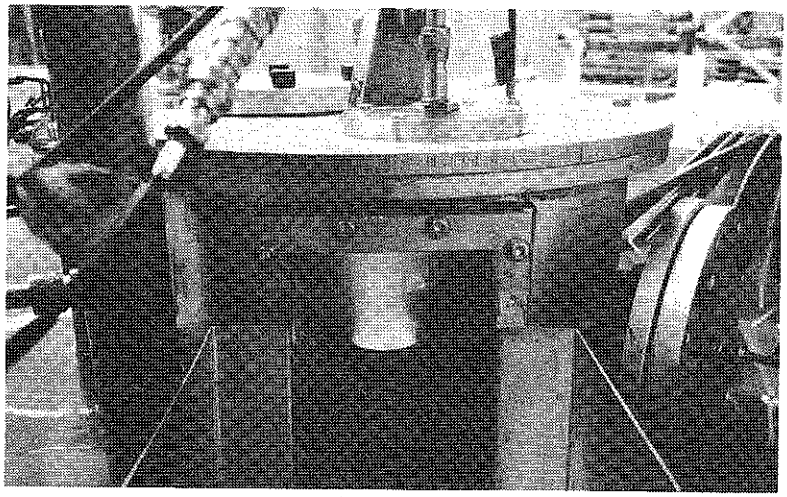

Open Shutter Photo

Figure 46 Results of a typical pulse

generation. The potentially disastrous back-emf and the transverse energy arising in the diode with a single cathode to generate a super-high-current beam can be reduced by forming several beams instead of one. In this way total beam energy can be injected and propagated in a situation in which the injection of a single-beam containing this energy would be impossible.

Faraday Cup Measurements. Using a 600-needle, 2½-inch-diameter convex cathode (24-inch radius of curvature) shots were made with 1- and 2-inch-diameter guide pipes and two guide cones into modifications of the Faraday cup reported in Reference 2. The modifications consisted of successive alterations of the existing cup, and were necessary to attain proper operation of the cup with the very-high ν/γ Mylar stripline beam. All experiments were performed after the stripline impedance was changed from 0.1 to 0.3 ohm.

It was found that pulsed-dc breakdown of drift-chamber gas occurred in the gap between the guide-pipe flange and the graphite face, over which it lay, as a result of the considerable potential of the graphite ($\approx$ 400 V) during the beam pulse (see Figure 47).

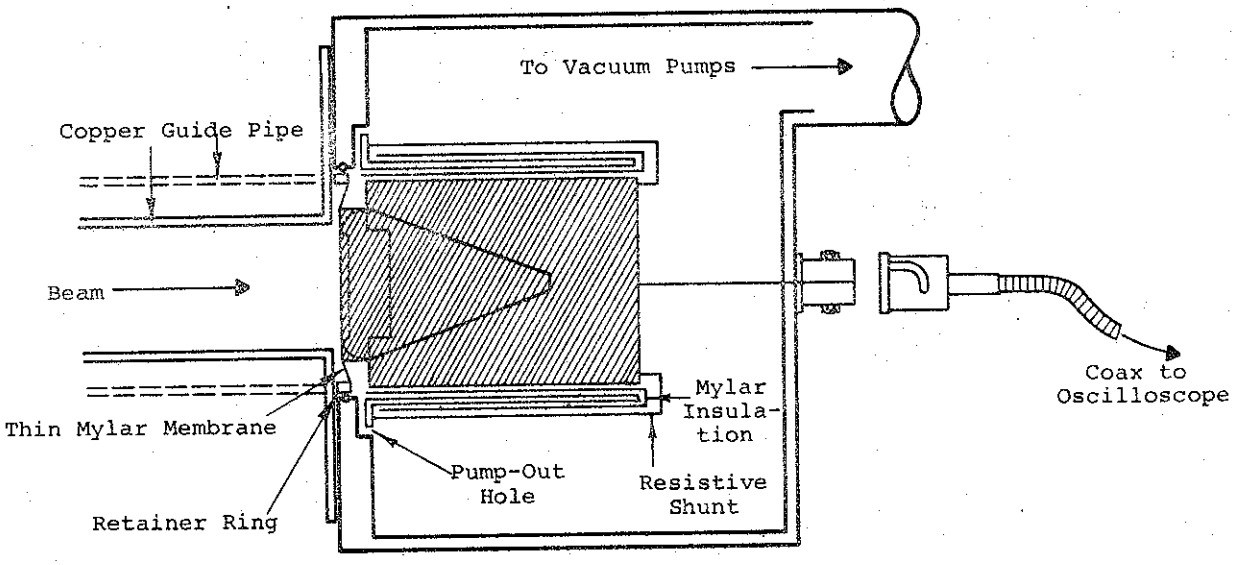

Figure 47 Faraday cup. Dashed lines indicate subsequent modifications described in the text. Shaded region is the graphite collector.

This breakdown resulted from surface damage caused by the high-current flashover and from beam repulsion caused by proximity to the high-current flashover. A breakdown did not occur in applications involving beams from the Pulserad 738 with lower ν/γ (and lower transverse energy). It appeared that the high transverse energy content of the beam from the Mylar stripline made it possible for electrons to excite or ionize the gas in the gap mentioned above. The Faraday cup modifications were primarily aimed at eliminating this flashover effect. They began with an increase in guide-pipe diameter from 1 to 1¼ inches and a rounding of the edge on the graphite face to eliminate the vulnerable gap. Although the physical evidence of flashover ceased to appear, the waveforms obtained showed no corresponding change and suggest that the flashover involved plasma currents after beam termination. The data are presented below. Reproducibility is demonstrated and interpretations relate directly to the concepts of the beam model already developed under DASA research.

Figures 48 and 49 show pairs of Faraday cup waveforms obtained with drift-chamber pressures of 50 and 100 microns in air, respectively. Details are given in the figures. The waveforms of each figure were obtained under identical conditions, except for anode-cathode spacing. Making the anode-cathode spacing larger increases diode voltage and decreases diode current, or in other words, decreases ν/γ. It is apparent from the waveforms in Figures 48 and 49 that in each case, the beam with higher ν/γ shows less beam-front loss, but more beam-body loss (generally lower-amplitude waveform) than the beam with lower ν/γ. The greater beam-body loss is a consequence of the greater transverse energy content of the higher ν/γ beam. This is direct evidence of the importance of containing transverse energy for efficient beam propagation. Note that at 1 cm from the anode only a fourth of the peak diode current is observed.

Shot 284: Peak Diode Current = ——
Peak Diode Voltage = 192.5 kV
(Anode-Cathode Gap = 1 mm)
Shot 286: Peak Diode Current = 220 kA
Peak Diode Voltage = 220 kV
(Anode-Cathode Gap = 2½ mm)
Both Shots: Beam Propagated 1 cm in
1 inch Guide Pipe at 50μ air

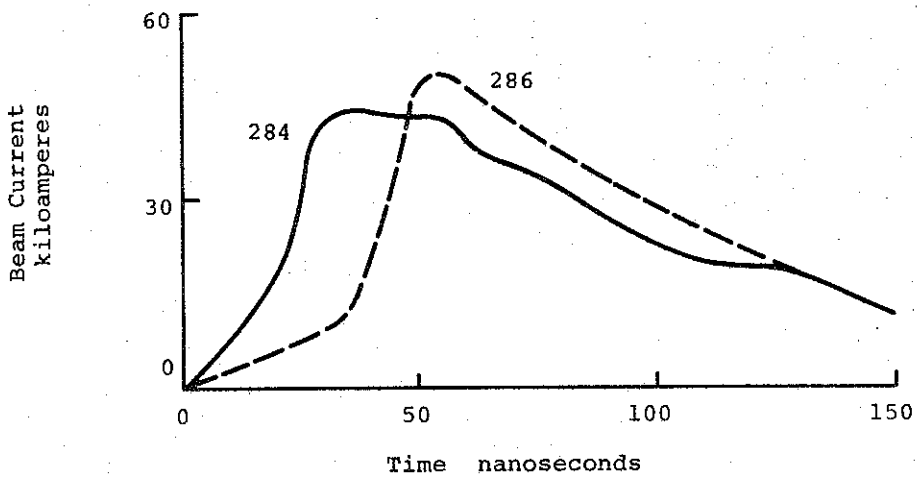

Figure 48 Faraday cup records of shots 284 and 286.

Shot 302: Peak Diode Current = 170 kA
Peak Diode Voltage = 195 kV
(Anode-Cathode Gap = 2 mm)

Shot 307: Peak Diode Current = 200 kA
Peak Diode Voltage = 189 kV
(Anode-Cathode Gap = 1½ mm)

Both Shots: Beam Propagated ½ cm in 1¼
Guide Pipe at 100 μ Air

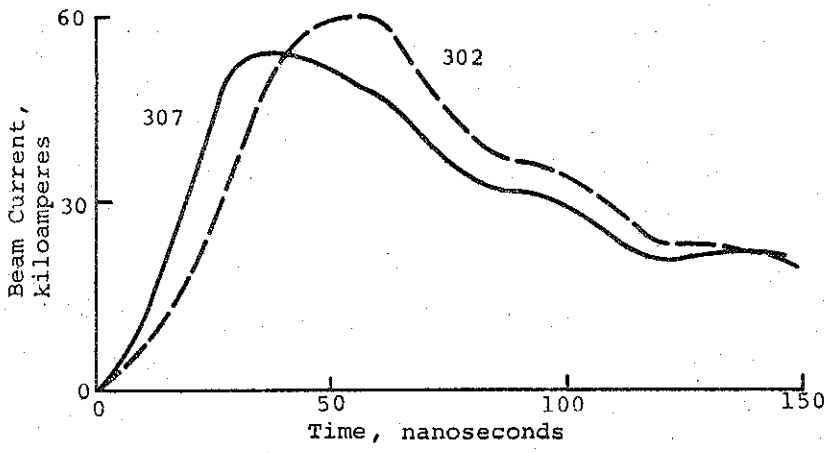

Figure 49 Faraday cup records of shots 302 and 307.

R9686

The reason that less beam-front loss is observed for the higher ν/γ beams is not yet understood. Beam-front erosion is a highly complex process involving E_z, transverse energy containment, gas-breakdown properties, gas conductivity, and gas photo-ionization rate, all of which are coupled phenomena in beam propagation. Data covering a wider range of beam and drift chamber conditions will have to be collected to understand the important effects in this case.

Figure 50 shows reproducibility of the waveform obtained at 500-micron drift-chamber pressure. The flat shoulder behind the beam front is a structure that did not appear at any of the other drift chamber pressures used: 50, 75, 100, 150, and 1000 microns in air. It suggests that maximum current neutralization occurs near 500 microns for this beam. If this is the case, azimuthal magnetic fields would remain relatively low and constant throughout the pulse. Loss due to transverse energy would degrade the primary current until it could be contained by the azimuthal magnetic field, resulting in a low-amplitude, flat waveform. Shot 282 in Figure 50 shows that all this happens in less than 1 cm of beam flight. This observation has importance in connection with present work involving propagation with a linear pinched discharge. It indicates that the entrance into the pinched-discharge apparatus must be positioned quite close to the anode.

Figure 51 shows the Faraday cup waveform of shot 313 with 1000 microns in air in the drift chamber. The beam front appears to propagate relatively well in comparison with observations at other pressures. At 1000 microns, gas breakdown occurs rapidly, but now the gas conductivity is low enough to allow for significant net current growth after breakdown (Reference 1, pages 10 through 11). Compared with the situation at 500 microns, the azimuthal magnetic field is high and the primary beam is better contained.

Shot 316: Beam Propagated 7 cm in Guide Cone Having 6.4 cm Diameter Entrance, 3.5 cm Diameter Exit
Peak Diode Current = 260 kA
Peak Diode Voltage = 208 kV

Shot 282: Beam Propagated 1 cm in 1 inch Guide Pipe
Peak Diode Current = 200 kA
Peak Diode Voltage = 191 kV

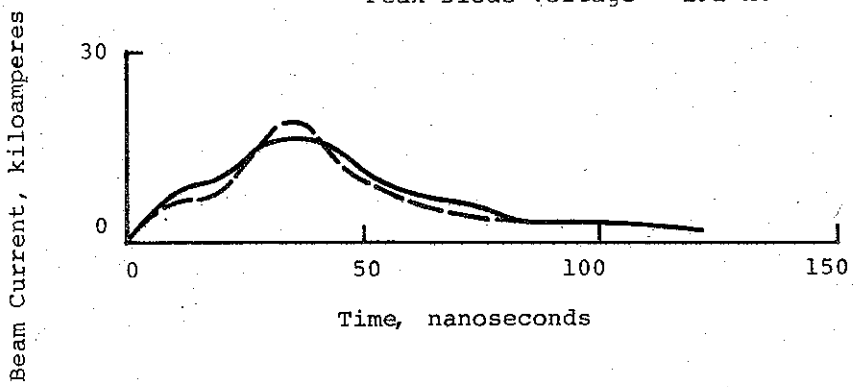

Figure 50 Faraday cup record at 500 microns.

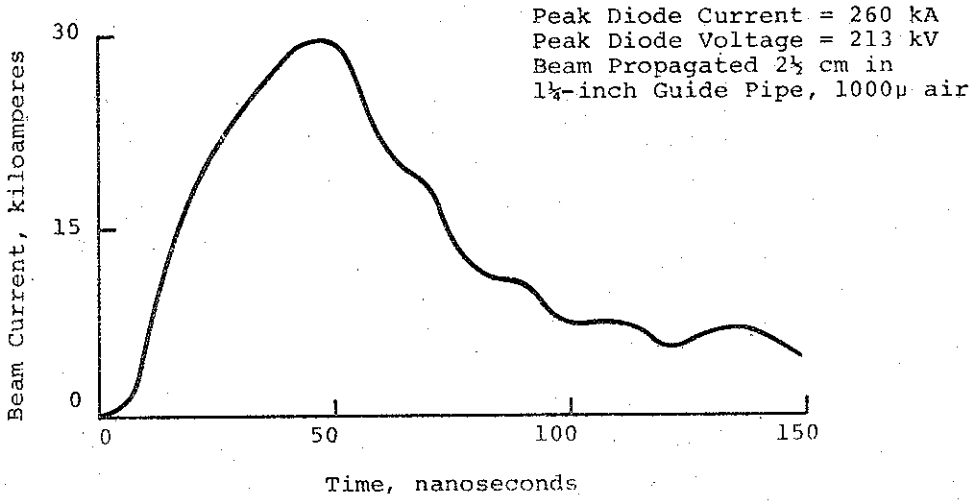

Figure 51 Faraday cup record of shot 313.

The data discussed up to this point imply that current neutralization increases up to about 500 microns and then decreases out to 1000 microns or more. This pattern and the physics responsible agree qualitatively with the results of investigations on the model 738 Pulserad beam (Reference 3, pages 65 through 68).

Figure 52 shows four waveforms obtained at 1, 2, 6, and 10 cm from the anode. Time delays have been subtracted in phasing the waveforms. Although the drift chamber pressures and other parameters were not the same for all four shots, the degrading effects of pulse dispersion and beam-front erosion with distance are evident. It is apparent from the waveforms that transport is better at 150 microns in air than at 100 or 75 microns. Also, the effect of the large-diameter entrance of the guide cone used on shot 288 is seen when that shot is compared with shot 287: a higher peak current is measured with the cone after 10 cm of propagation than with the pipe after 6 cm.

Figure 53 is included here to demonstrate reproducibility. The beam propagated only 1/2 cm before entering the Faraday cup. About 200 kA were injected in each case.

In another Faraday cup experiment a 1 mm-deep vacuum gap in the face of the graphite collector was used (Figure 47). The 0.00025-inch Mylar membrane is stretched over the raised graphite shoulder at the periphery of the face. The beam must traverse the vacuum gap before reaching the graphite collector. This experiment was motivated by the possibility that the Mylar membrane placed flat against the graphite (very thin vacuum gap) did not isolate the graphite from plasma during the pulse, since the membrane itself could become plasma. If this were the case, separating the membrane from the graphite with a vacuum gap that is wide enough

Shot No.	Centimeters Propagated	Guide Pipe Diameter (in.)	Gas Pressure	Peak Diode Current (kA)	Peak Diode Voltage (kV)
285	1	1	75	230	207
278	2	1	100	400	188
287	6	1	150	310	212
288	10	1	150	210	223

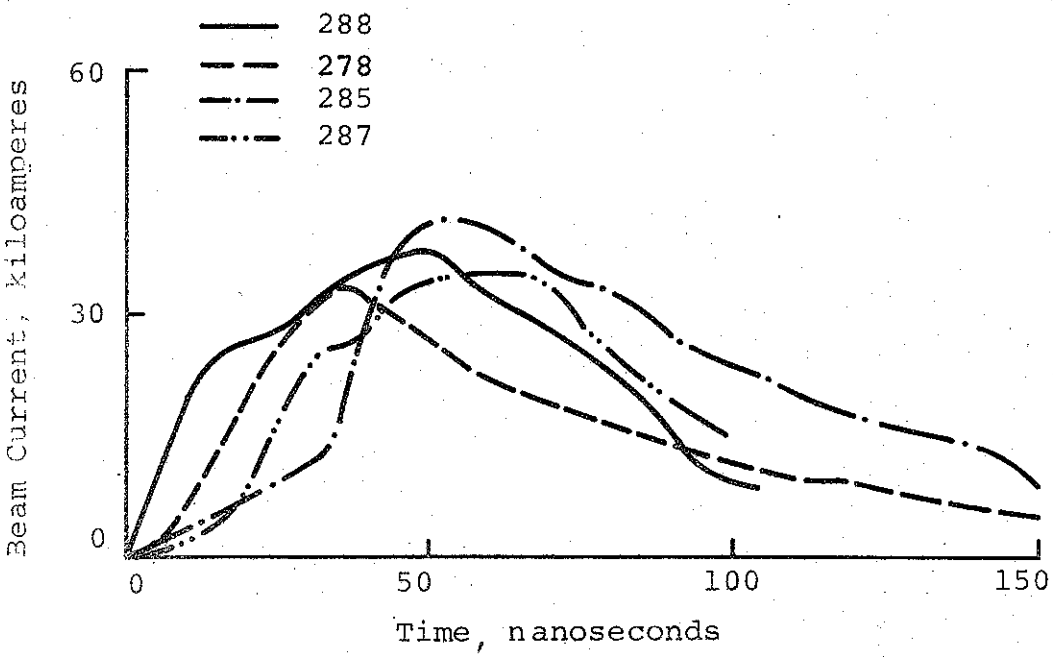

Figure 52 Faraday cup evidence of beam front erosion and pulse duration.

8494

Shot 302: Peak Diode Current = 190 kA
Peak Diode Voltage = 195 kV

Shot 303: Peak Diode Current = 200 kA
Peak Diode Voltage = 217 kV

Both Shots: Beam Propagated ½ cm in 1¼ in. Guide Pipe, 100 μ Air

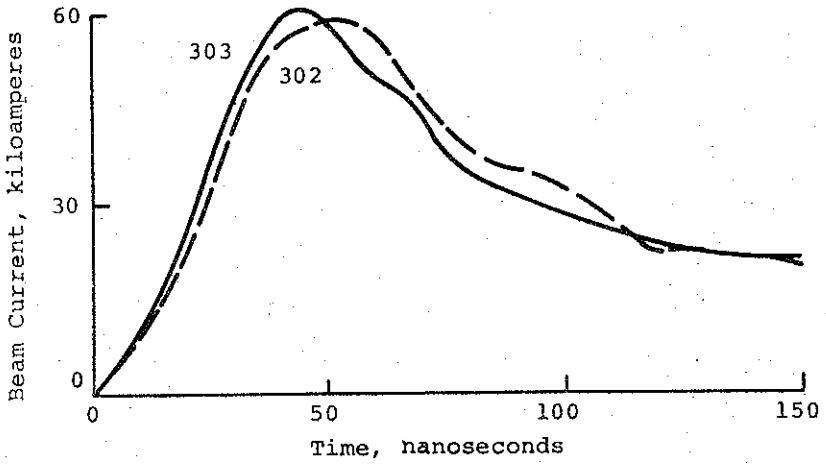

Figure 53 Example of beam reproducibility.

to successfully isolate the graphite, but not so wide that the beam must travel too far in vacuum, would have a considerable effect. Figure 54, however, shows that the effect of a 1-mm vacuum gap is to reduce the amplitude, but not change the waveform of the measured primary beam current. Further work would be needed to make the explanation of this effect more definite; however the obvious interpretation based on the present data (Figure 54) is that longitudinal electric fields induced in the vacuum gap are responsible for the reduced current.

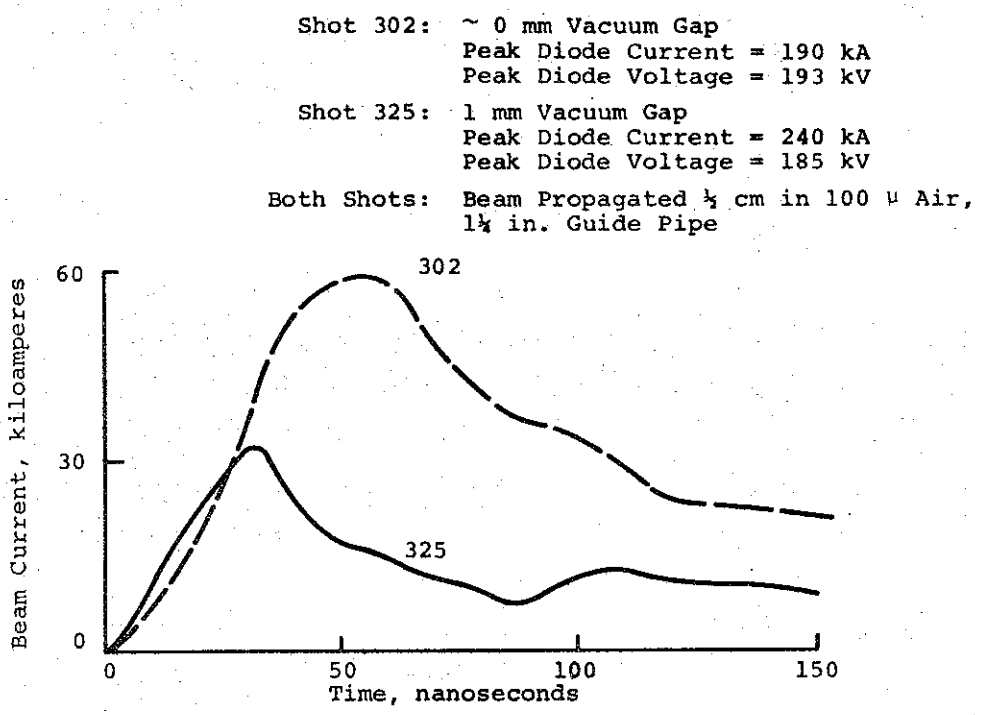

Figure 54 Vacuum gap effect on Faraday cup.

Beam Propagation in a Pre-ionized Gas. Four shots were fired into a linear discharge apparatus (Figure 55) to test the effect of injecting the beam into a pre-ionized gas. This preliminary work was carried out during a period of highly irregular and unreproducible machine performance, prior to the modifications made in early November. However, the results appear consistent with the findings of similar experiments performed later on the model 738 Pulserad (Reference 4).

A capacitor discharge circuit is used to apply a large positive voltage to the anode (see Figure 55). The gas in the apparatus is ionized by the electric field, and a linear current discharge flows from the grounded stainless-steel screen cathode to the high-voltage-anode witness plate. These are 5½ inches apart.

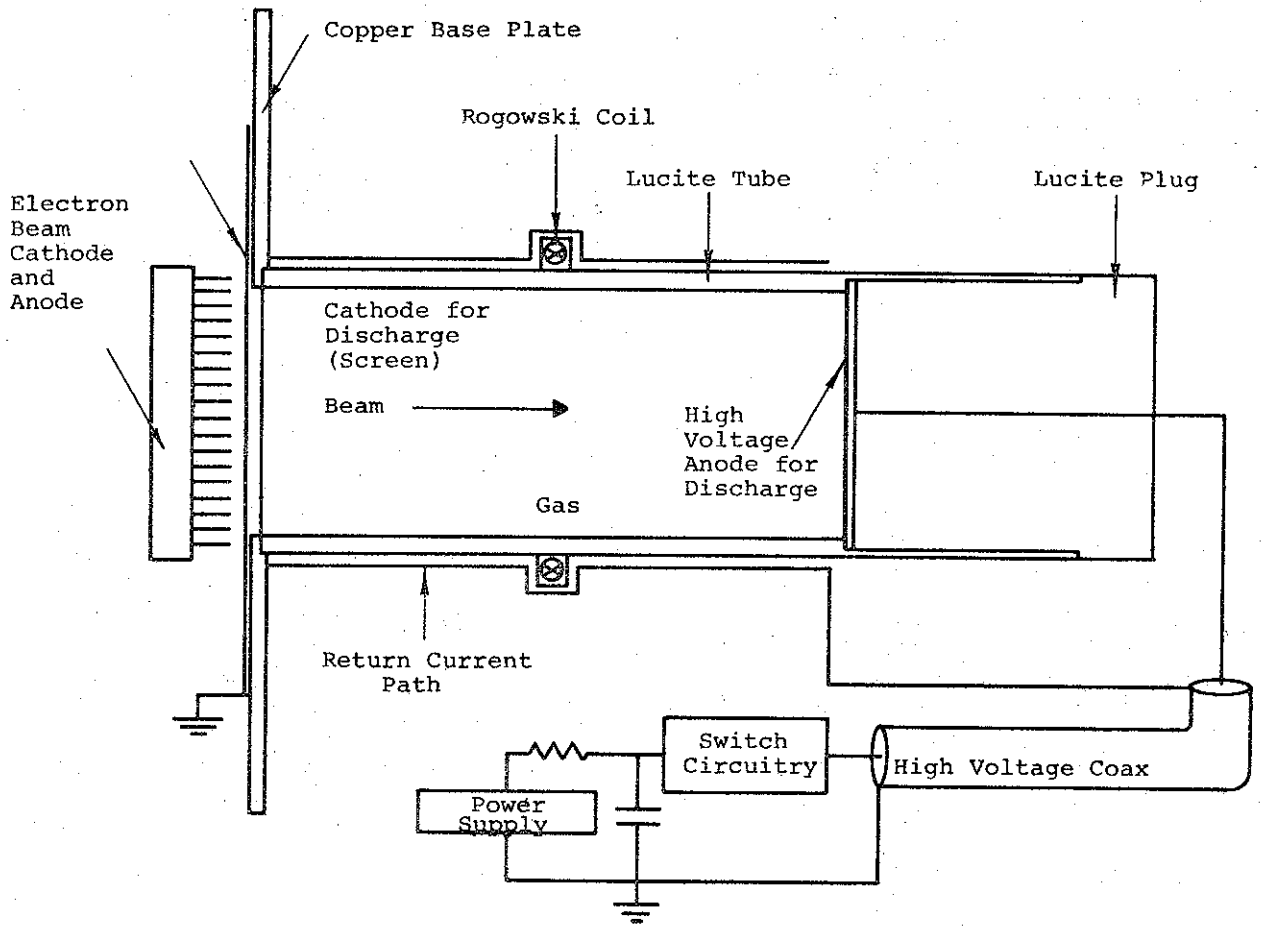

Figure 55 Linear discharge apparatus and circuitry.

In this experiment the total inductance of the circuit was high enough to prevent pinching of the discharge current. Using appropriate trigger circuitry, the electron beam is injected into the ionized gas at the desired time. In this case the discharge was triggered by a signal from a coil wound around the trigger cable of the Mylar stripline (not shown in the figure).

The gas in the discharge was air at 125-micron pressure, and the capacitor bank was charged to 10,000. Diagnostics consisted of observations of damage to the high-voltage anode (a 0.003-inch aluminum disk was replaced for each shot) and a net current trace obtained with a Rogowski coil (RC time constant = 700 μsec) around the discharge at its middle. The Tektronix 454 oscilloscope used with the coil was triggered by the diode voltage, some microseconds after the discharge was fired. A fast sweep was used so that the trace would show the discharge current level at injection, appearing as a flat trace displaced from the baseline as a result of the fast sweep. Meaningful results were obtained on the first two of the four shots fired into the discharge. Machine failure on the second two shots prevented data collection. Peak diode voltage was 110 kV and peak diode current was 0.9 MA for each of the shots. The electron beam was injected into the undischarged apparatus on the first shot. Damage to the witness plate consisted of discolorations distributed irregularly about the center, with no physical surface damage. The gas was pre-ionized for the second shot, and the Rogowski coil indicated 4.2-kA discharge current at the time of injection. Simultaneous monitoring of the Rogowski coil and machine pulse-charge signals showed that invection occurred 2.8 μsec after the discharge began. Damage to the witness plate consisted of a discoloration near the center and distinct, roughly elliptical areas of surface damage lying against the edge of the witness plate at the discharge-tube wall, with major and minor dimensions of ½ and ¼ inch, respectively.

The results are interpreted as follows: beam propagation is poor in neutral gas due to the effect of the induced electric field E_z and due to electron loss in the radial direction, a consequence of the very high ν/γ, high transverse energy beam. A small, almost insignificant fraction of the beam energy is delivered

to the witness plate, whose discoloration is due to the relatively mild heating resulting from the low incident fluence and from the discharge current itself. (Witness plate shots performed during the stripline testing which led to machine modifications showed this same effect.)

Pre-ionization alone would give free-field propagation, with no magnetic fields to contain transverse energy and would also result in very poor propagation. However, an azimuthal magnetic field was present from the discharge current. Such a field, if sufficiently strong, could prevent the radial escape of electrons with transverse energy and allow their propagation. A general fact about the type of linear discharge apparatus used here is its tendency to discharge first along the wall of the tube, due to surface effects, and subsequently discharge throughout the volume. Such is felt to be the case here. The discharge initiated along a particular segment of the wall, and although current flowed throughout the volume when the beam was injected, it was always highest along the initial narrow path at the wall. The azimuthal magnetic field was similarly greatest along this region, and beam electrons moving along paths through this region propagated successfully to the witness plate, causing the surface damage described above. Along other paths in the discharge, the magnetic field was not sufficient to contain electron transverse motion. Similar effects were observed in subsequent experiments on the Pulserad 738 (Reference 4).

These results are consistent with the ν/γ beam-propagation model developed under contract DASA-01-68-C-0096, which predicts that injection of a high ν/γ beam into an appropriate linear pinched discharge will give efficient propagation over considerable distances.

4.4.2 Conclusions. Beam research findings on the Mylar stripline have been interpreted in terms of the high ν/γ beam model developed in previous work. This model has indicated potential problems in handling ultra-high ν/γ beams and such problems have, in fact, occurred in our initial attempts to use beams with values of ν/γ not greatly in excess of that studied using the Pulserad 730. This work has served to demonstrate, however, the utility of multiple-cathode geometries and to indicate that the use of pre-ionization techniques with trapped magnetic fields will enable further evolution of beam handling methods.

SECTION 5

HIGH-VOLTAGE LINE GENERATOR DEVELOPMENT AND TESTING

The objectives of the high-voltage line project were to charge and switch, at the highest possible voltage, a Blumlein module designed to operate at electric-field energy-density levels of 1.5 MV/cm. The charging system used a separate oil-immersed Marx generator. Following this, a double Blumlein module was to be used to test a double-sided X-ray tube in which two opposing electron beams would be brought to rest in an anode much thinner than the electron range.

Before construction of the high-voltage line, a small-scale experiment was conducted to check the performance of the high-voltage leads and the interface through which the charging voltage was introduced from air to the water in the Mylar-line tank. A pulse transformer was used to charge two copper plates, 1 foot square, separated by 200 mils of Mylar to 750 kV. An inductor was used to slow the risetime of the pulse to 1.5 μsec, which is approximately what was anticipated for the line tests which were to follow. The copper-sulfate solution resistivity was adjusted to 7.5 kΩ/cm, which sufficiently graded the fields at the edge to prevent breakdown and tracking. The technique which proved acceptable for introducing the high-voltage leads consisted of using a large piece of Lucite to exclude the water from the region of the point of entry. To this was attached an oil-filled Lucite pipe which provided extra insulation to the inner polyethylene cable when this approached within the last

few feet of the generator. The same experimental system was also used to check the breakdown strength of some of the stabbed polyethylene switches used in later experiments.

At the conclusion of these tests, work began on the full-scale system. The Marx-charging system consisted of five stages, each composed of three 0.4-μF, 125-kV capacitors. A standard PI spark-gap column was used. The first two spark gaps were triggered by needle electrodes, which were pulsed with the aid of a mechanically switched cable. The Marx generator occupied a small portion of an oil-filled tank 20 feet long, 8 feet wide, and 7 feet high. The low-voltage end of the Marx generator was not grounded except by the connection to the Mylar line itself. However, it did not excurse far from ground. The low- and high-voltage lead terminals of the Marx generator were connected to lengths of stripped cable with an inner diameter of about 3/4 inch. These were brought together well beneath the surface of the oil and emerged together from the oil to travel a distance of about 12 feet to the Mylar-line tank. Each cable is capable of withstanding a voltage of about 500 kV to its sheath, and therefore the insulation between the two halves of the cable pair is adequate for a total of 1 MV. The proximity of the cables to each other, for example where they emerged from the oil surface, produces a field configuration resembling that of a single cable except at half the voltage, thus reducing the tendency to spark to ground. This method is the most convenient way of transferring such a charging voltage from a single Marx generator to a number of separated Mylar modules which might, for example, surround a large X-ray tube.

In the first series of experiments, a single-sided Blumlein was assembled in a copper-sulfate solution using the same wetting technique which had been established on the low-voltage line to avoid air bubbles. This line was then charged to high voltage but not switched. Instead, the energy was diverted with the aid of a point-point dump switch using the copper-sulfate solution as a switching medium. These tests went smoothly, except for one track which was observed at 550 kV. This track was from the high-voltage copper sheet to ground and may have been due to an unnoticed imperfection. Because of the energy dissipated, it was not possible to identify this afterwards. Measurements were taken of the resistivity of the copper-sulfate solution. It was found to be 12 kΩ-cm rather than the intended 8 kΩ-cm, a difference that should not have been crucial, however. The resistivity was adjusted, and the tracked portion was removed. The line was then tested to 750 kV without further damage.

The monitoring technique used in these tests was that of the capacitive divider--a simple copper sheet placed between appropriate Mylar sheets within the line--in combination with a resistive divider whose impedance was high enough that the associated RC decay time was much greater than the microsecond charging time of interest. The resistive divider could be encapsulated in epoxy resin and submerged under the water or could remain just outside the water, in which case encapsulation was unnecessary.

The line had been charged and dumped a number of times at 750 kV, which corresponds to an electric field of 1.5 MV/cm in the Mylar. The objective of the next phase of the testing was to demonstrate switching of the line. As for the low-voltage line, the stabbed polyethylene version of the solid dielectric switch was preferred. It was felt that accurately stabilizing the potential of the midplane trigger electrode would be more difficult

at high voltage than at low voltage, and the three-electrode-field enhancement is probably more prone to self-fire as a result of incorrect trigger electrode potential.

A three-element Mylar capacitor was provided in the main generator tank to establish the V/2 trigger potential. We did not attempt initially to provide a resistive divider outside the water because it was felt that at very high voltages it would be difficult to prevent this divider from flashing over. Stray conduction and capacitance in the copper-sulfate solution was avoided in the case of the high-voltage line by making the three-element capacity of larger area and taking great care to exclude the water from the various V/2 connections at the capacity divider and the switch trigger electrodes. When this was done, the voltage division was checked at high voltages and did indeed produce a waveform very similar to the pulse charge voltage and half as large in amplitude. However, great care was necessary to maintain this situation. For example, at one point, the line was observed to switch after the peak of the pulse charge. Reexamination of the V/2 waveform showed that it had shifted phase and was peaking later than the voltage on the Blumlein itself. It was decided to test a voltage divider similar to that used on the low voltage line consisting of long copper-sulfate resistors in air, which proved satisfactory. The alternative solution is to have an oil-immersed voltage divider. This may either occupy a small Lucite oil tank, partly submerged in the copper-sulfate solution in the main generator tank or may perhaps be installed

in the Marx tank. The latter is preferable to avoid the possibility of oil spillage in the Mylar line tank itself. The inductive voltage drop on the charging leads between the Marx tank and the line tank probably will not effect an unacceptable distortion in the V/2 waveform.

We began switching experiments into a $CuSO_4$ load using 60-mil polyethylene master switches and line switches consisting of two such polyethylene sheets in series. The master switch was positioned on top of the Blumlein only a few feet from the switch end. The connections between master switch and trigger electrodes were made with stripped cable inner conductor, which formed a well-defined, wire-over-plane transmission line of over 100-ohm impedance. Two of these trigger lines were used; they fed two switch locations which were only 1 foot apart at the end of the line.

The line was only 2 feet wide and would generally not require two switches to attain an adequate risetime. However, it was intended to show that, if required, really fast risetimes could be generated for very short square pulses. Figure 56 does indeed demonstrate such a capability. As it happened, tracking and switch-site damage necessitated cutting away portions at both ends of the Blumlein until a point was reached at which the line produced a pulse only 15 nsec long. In spite of the proximity of the switches, both fired in a multichannel fashion except on rare occasions, though one switch frequently carried more current than the other.

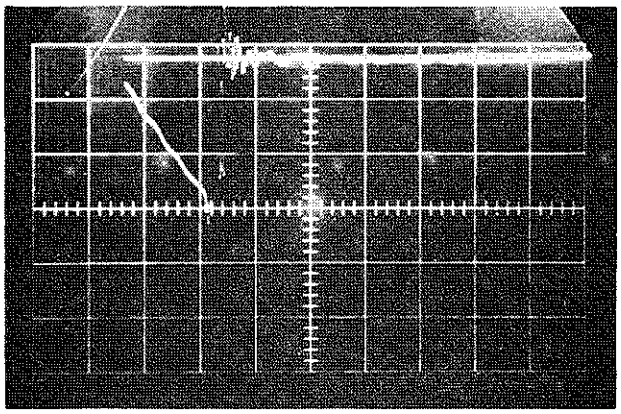

0.5 μsec/cm
140 kV/cm

a. Pulse Charge

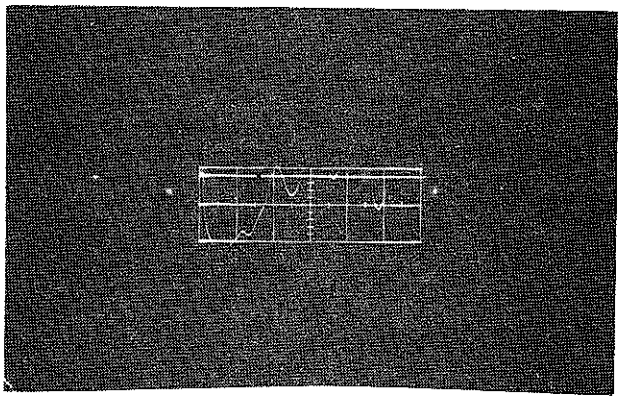

10 nsec/cm
200 kV/cm

b. Output Voltage

Figure 56 Typical high-voltage line output waveforms.

When the voltage limit of the double-layer 60-mil polyethylene-line switches was reached, the number of sheets in each switch was doubled, including the master switch. Each sheet was still stabbed, as shown in Figure 57. The voltage was then raised further. At 350 kV, a track occurred around one of the line switches causing severe damage to the line at that point (Figure 58). When the line switches are in position, the 1/4-inch-thick switch assembly fits between the middle layers of the Mylar that separates the two lines. A steel electrode passes through a hole cut in these layers to make contact with the switch. There is a large discontinuity in dielectric constant and resistivity between the polyethylene switch card and the solution that fills the gap in the divided layers of Mylar. This

a. Master Switch

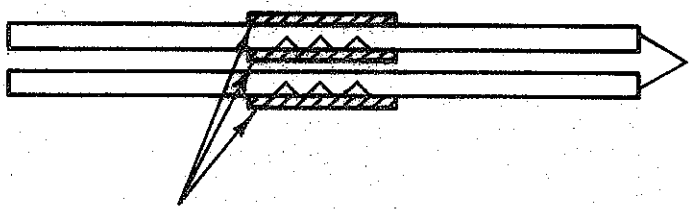

Thin aluminum disks for electrodes are used to cover stabs to exclude water.

b. Line Switch

Each card is 0,060 inch with aluminum disks as electrodes and also used to exclude water.

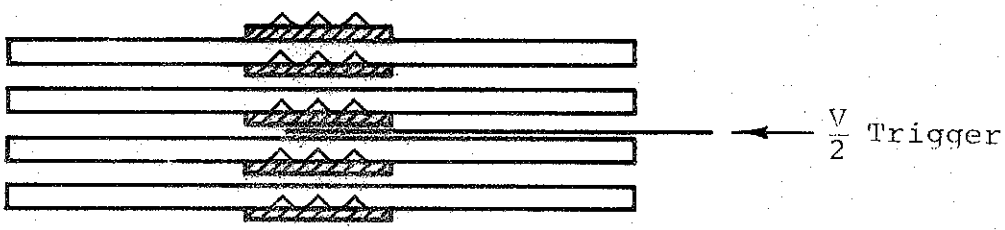

Figure 57 Switch cross sections.

5550

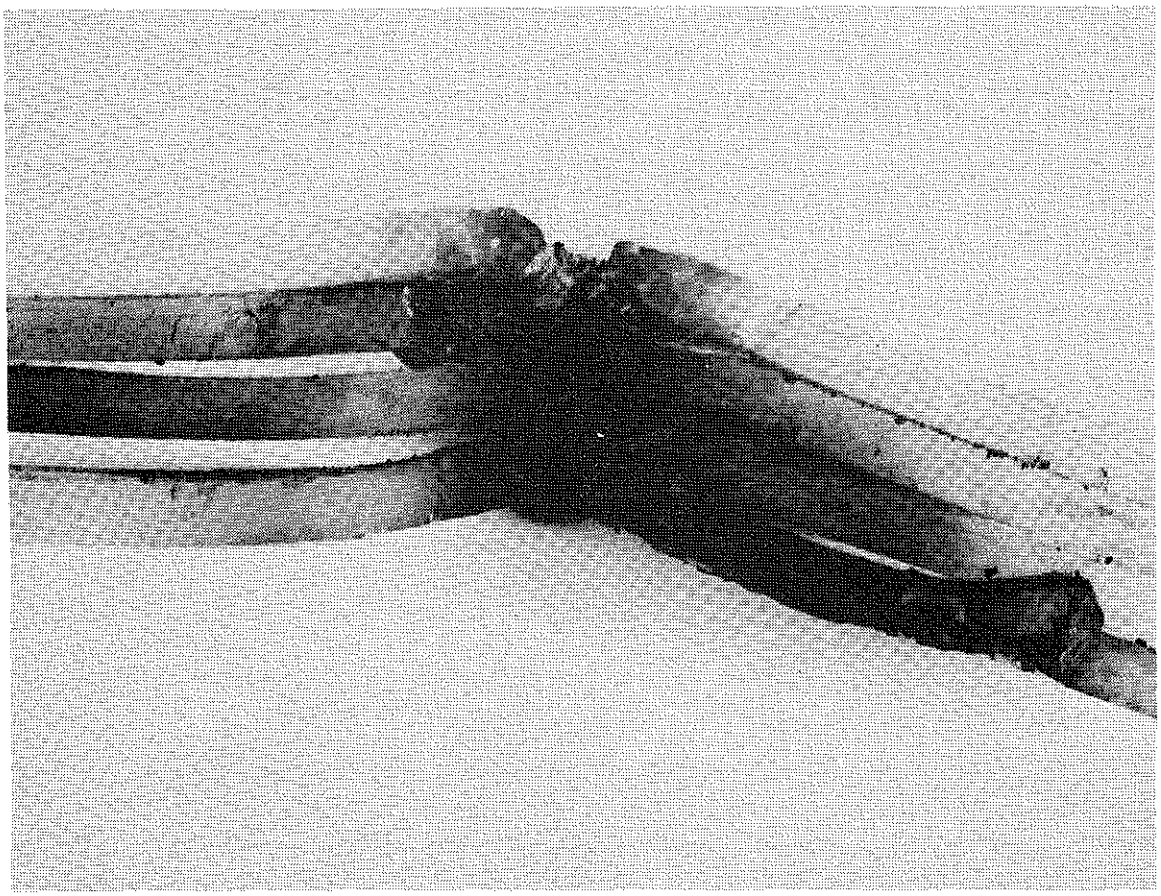

Figure 58 Double-sided line switch destroyed by arc.

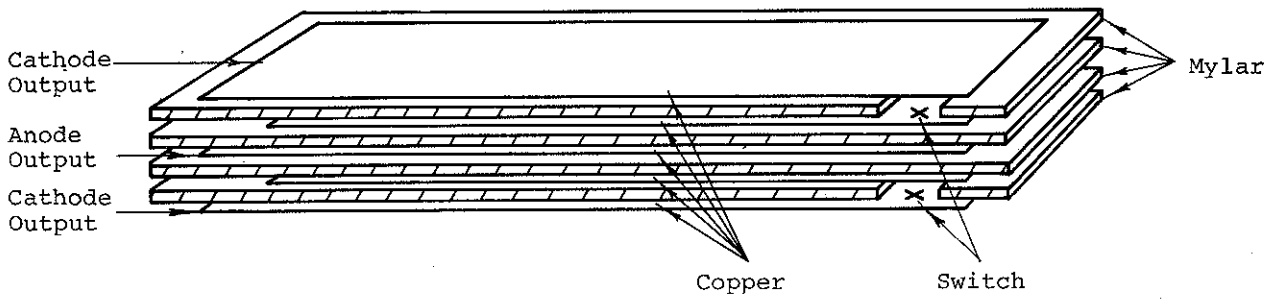

Figure 59 Double-sided high-voltage Mylar line design.

discontinuity leads to field distortion and a high stress in the water near the edges of the card. After a breakdown in this area, the edges of the cards were crudely tapered in manufacture and the problem did not recur. The line was then switched at voltages up to 450 kV without difficulty.

Next, a double-sided line was fabricated (Figure 59). This line was intended to test the double-sided tube. Since one of the questions relating to the performance of a double-sided diode is the pulse duration for which it will operate, the line was made about 20 feet long and has a pulse duration of approximately 70 nsec. The line is 2 feet wide and has an impedance of about 1-1/2 ohm. This width was chosen because at that time 10-mil-thick copper was not immediately available in greater widths. This impedance, however, is quite satisfactory for testing the performance of the double-sided diodes.

Before testing the double-sided diode, it was decided to test the two-Blumlein module in a series-switched (Marx) configuration. This test was planned because our experience in operating the first prototype line led us to believe that for a large assembly of a number of Mylar modules such as might be used to generate many megamps in a routinely operating radiation facility, the pulse charging voltage should not be much higher than about 500 kV. Above this voltage occasional tracking in the water will probably occur unless extreme care is taken. In some applications

even if the voltage on the X-ray tube is to be no more than 500 kV it may be desirable to build the lines with a high open-circuit voltage (for example, 2 MV) and mismatch them low. Although the energy transfer is slightly reduced from the case in which the line is designed approximately to match the tube, the linear current density is increased, the generator is made narrower at the expense of increased thickness, and the number of tanks and the size of the overall system are reduced. The 2-MV open-circuit voltage is most easily obtained by "Marxing" two Blumleins charged to 500 kV apiece.

The aim was briefly to demonstrate the ability of this configuration to reduce losses from interaction between the line at the switch. Included in the configuration is the feature of electrically isolated, synchronized switches, which are most desirable to avoid the complication of introducing extra dielectric spacing between the Blumleins.

The equivalent circuit for this experiment is shown in Figure 60. The lines are charged through inductances, and the V/2 trigger cables were of high impedance compared with the generator lines. They are also long enough to ensure a degree of transit-time isolation. In fact, in this experiment the cables triggering the switches led back to a master switch situated near the output end of the line. This positioning would be conveniently central in the case of a large number of modules assembled around an X-ray tube.

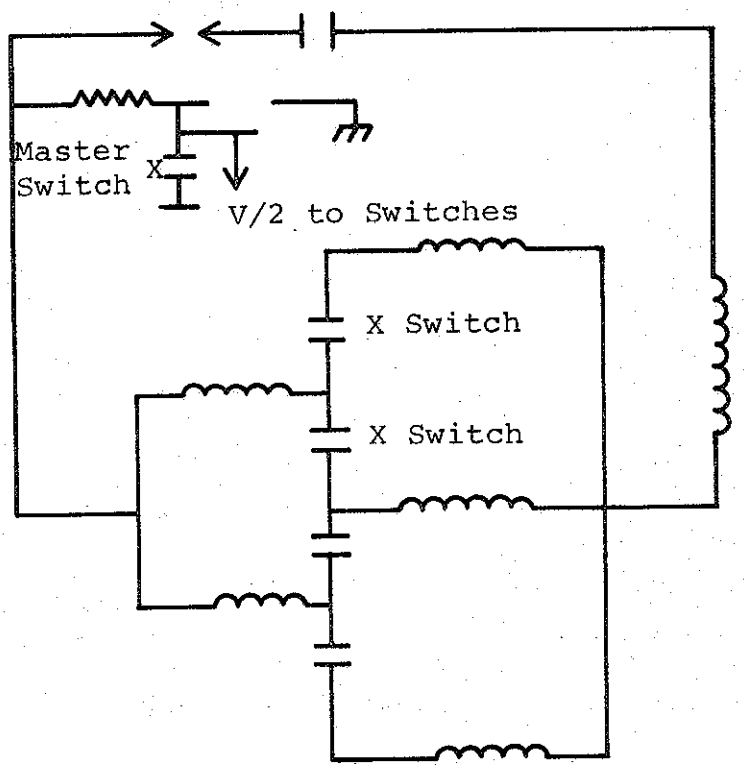

Figure 60 Series switching equivalent circuit for double-sided Mylar line.

The difference in configuration required to "Marx" the two Blumleins rather than operate them in parallel is simply that a different pair of striplines is required to be switched. Rather than restack the assembled generator, a dummy switch site was interleaved in one of the lines which would normally be unswitched. Figure 61 shows typical pulse charge and output voltage waveforms at 75 kV into a matched load. Synchronism is demonstrated by the output pulse waveform, which is measured by a capacitive divider viewing the total output voltage.

At the conclusion of this experiment, the line was converted back to its parallel configuration and experiments were begun using the double-sided diode.

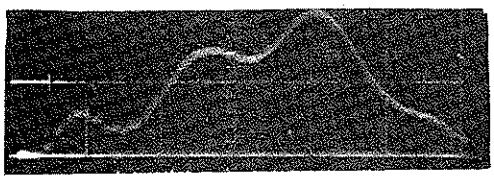

X-ray Waveform
(Photodiode Output)
When Beam is Injected
into Gas at 5 Torr

0.001-in. Al Window
10 V/cm, 10 nsec/cm

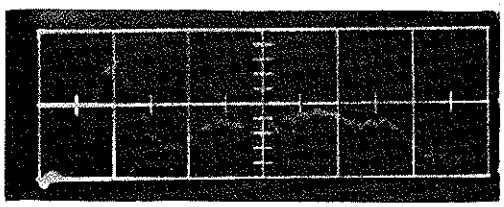

Beam Injected into
Vacuum ($<10^{-3}$ Torr)
through 0.001-in.
Al Window

20 V/cm, 10 nsec/cm

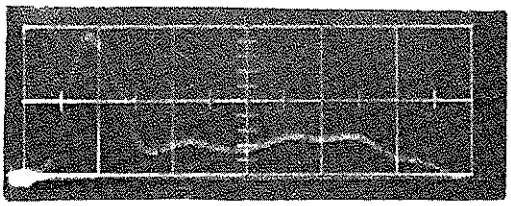

Window Thickness
Reduced to 0.00025-in.
Al
($<10^{-3}$ Torr)

20 V/cm, 10 nsec/cm

Figure 61 Effect of injecting a high ν/γ beam into a vacuum.

During subsequent experiments the line tracked at a 300-kV pulse charge at a point where an external connection was made. Repairs were made but they were unsatisfactory at 300 kV, but were satisfactory at lower pulse charges, 200 kV or less. The damage is probably attributable to excessive water exclusion at the connection. When connections are made to the line, the line is weighted with 25-pound lead bricks to ensure good electrical contact. It is probable that the line was weighted in such a way that the Mylar extending beyond the edge of the copper was squeezed together excluding the water and not providing enough resistive grading. Experience with the latest low-voltage line suggests that the high-speed transient may have contributed to failure of the line at such a location.

SECTION 6

HIGH-VOLTAGE TUBE

6.1 EVALUATION OF TWO-SIDED DIODE

In a single-sided diode, the efficiency with which X-rays are produced when an electron beam is stopped in the thick target increases as the voltage is raised. Because the electron range increases with voltage, the target thickness must also be increased, and the yield of low-energy X-rays emerging from the target, per joule of electrons dissipated therein, decreases beyond a certain voltage. If,instead of stopping the high-energy electrons in a thicker target, one stops them in a very thin target by many successive transits, the effect of target self-absorption is greatly reduced and the efficiency of the X-ray production increased.

This process was believed to have been demonstrated on the Model 730 Pulserad by allowing a high ν/γ beam to pass through a thin target into a high vacuum and create (Figure 61), by virtue of its unneutralized space charge, a potential well to act as a virtual cathode and repeatedly return electrons to the diode region. The measure of space charge associated with a given diode current might be expected to raise the tube impedance if this is space-charge limited. Tube voltage traces did in fact indicate an increased average impedance, but the time history during the pulse was obscured by inductive effects. The most informative diagnostic

available in these experiments was a scintillator photodiode combination responding chiefly to X-rays produced at the anode. It showed an enhanced dose rate--by as much as a factor of ten--for the first 10 nsec of the pulse, due probably to the increased electron interaction with the foil as well as to the increased diode impedance which leads to a higher electron energy. Indications were that the impedance returned to normal after about 10 nsec. As expected, the amplitude of the X-ray "spike" during this time was increased by decreasing the target thickness, while the dose rate for the remainder of the pulse was decreased.

Beam trapping was probably unstable on the high-vacuum side because ionized anode material was able to neutralize the potential well and remove the virtual cathode in a time of the order of 10 nsec. Substitution of a real cathode identical to the first one spaced at the same distance from the anode should avoid this instability. Both cathodes must be maintained at the same potential and supplied with current, and, hence, there must be a tube on both sides of the anode. The stripline generator provides an ideal means to drive each tube: one generator coupled to both sides is possible, but in these experiments a two-sided generator was built.

As in Pulserad 730 experiment, one of the simplest diagnostics available to study the multiple electron transit was the impedance of the double-diode system, which was expected to increase because of the extra space charge that the oscillating electrons represent. As an example, in Figure 62 the double-sided diode system is shown, in which the anode potential is V_o and the anode thickness is one-third of the penetration depth corresponding to this electron energy. The assumption is made that the electron loses one-third of its component of energy perpendicular to the target in each transit, which is

reasonable, since the total loss of energy (dE/dx) increases as the electron loses energy, but scattering also decreases the perpendicular energy at first. Based on the foregoing assumption, the electrons turn around when their distances from the cathode are given by $x = x_1$ and $x = x_2$, where the potential $V(x_1) = 1/3\ V_o$ and $Vx_2 = 2/3\ V_o$. From Poisson's equation in one dimension,

$$\frac{\partial^2 V}{\partial x^2} = 4\pi\rho = 4\pi j \left(\frac{2eV}{m}\right)^{1/2}, \quad 0 \leq x \leq x_1$$

$$\frac{\partial^2 V}{\partial x^2} = 12\pi j \left(\frac{2eV}{m}\right)^{1/2} \quad x_1 \leq x \leq x_2$$

$$\frac{\partial^2 V}{\partial x^2} = 20\pi j \left(\frac{2eV}{m}\right)^{1/2}, \quad x_2 \leq x \leq d$$

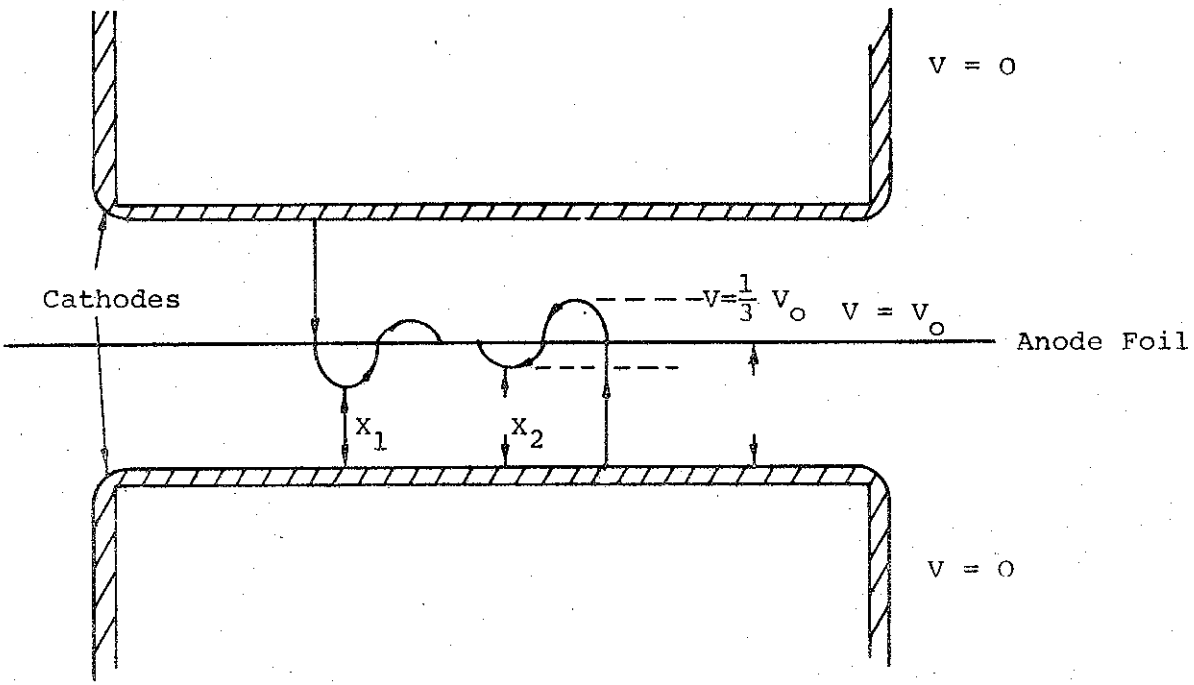

Figure 62 Electron trajectories in the double-sided diode.

where j is the current density at the cathode. The boundary conditions on $V(0)$, $V(x_1)$, $V(x_2)$, and $V(d)$ where d is the cathode-anode spacing together with the assumption of space-charge limitation

$$\left(\frac{\partial V}{\partial x}\right)_{x = 0} = 0$$

can be used with the conditions of continuity and differential ability at x_1 and x_2 to determine the six arbitrary constants, j, x_1, and x_2. The results are

$$x_1 = \frac{15d}{23} \quad x_2 = \frac{20d}{23} \quad j = \frac{529\ kV}{1350\ \pi d^2}$$

$$\text{where } k = \left(\frac{2\ eV}{m}\right)^{-1/2}$$

The value of j is 70 percent of the thick target value

$$\frac{kV}{2\ \pi\ d^2}$$

This reduction in current is less than might have been expected because the extra space charge has the effect of increasing the electric field at the anode to which the electron is then returned more promptly. In practice one would hope to use much thinner anodes than the one assumed here to simplify the calculation. The increased field at the anode should increase the space-charge neutralization by positive ions. It might also be expected to increase the rate of fall of impedance during the pulse.

The double-sided tube is shown in Figures 63 through 66. Prepulse switches were incorporated in both sides of the tube. The cathode was initially a needle design and very similar to those in use in several PI Pulserad models. Familiarity with this cathode design aided the study of the impedance as a function of target thickness, after thick target shots initially verified the independent mode of operation of the diodes. The needle cathodes were then replaced with a hollow cathode design so that the X radiation could be studied.

For future experiments, a cathode design is required that presents little attenuation to the X-rays produced, so that samples to be irradiated can be placed behind the emitter surface (perhaps on either side of the anode). It was anticipated that a thin, roughened plate of graphite, aluminum, or beryllium would provide such a cathode, since a similar design had been demonstrated on the 730.

6.2 DOUBLE-SIDED TUBE EXPERIMENTS

The first experiments were performed using the 600-needle cathodes. Low-Z foils were used for the anode since a wide range of thicknesses was available in aluminum and there was little possibility of measuring X-ray outputs through the massive cathode structure. The thickest foil (0.02 inch of aluminum) was able to stop electrons of energy as high as 500 keV. With this anode it was certain that the diodes were operating independently. Eight-mil and one-mil of aluminum provided anodes that would allow electrons to pass from one diode to another, and for the thinnest of all, 1/4-mil aluminized Mylar was used. Thus the anode thickness varied from about 1 mg/cm^2 to 137 mg/cm^2.

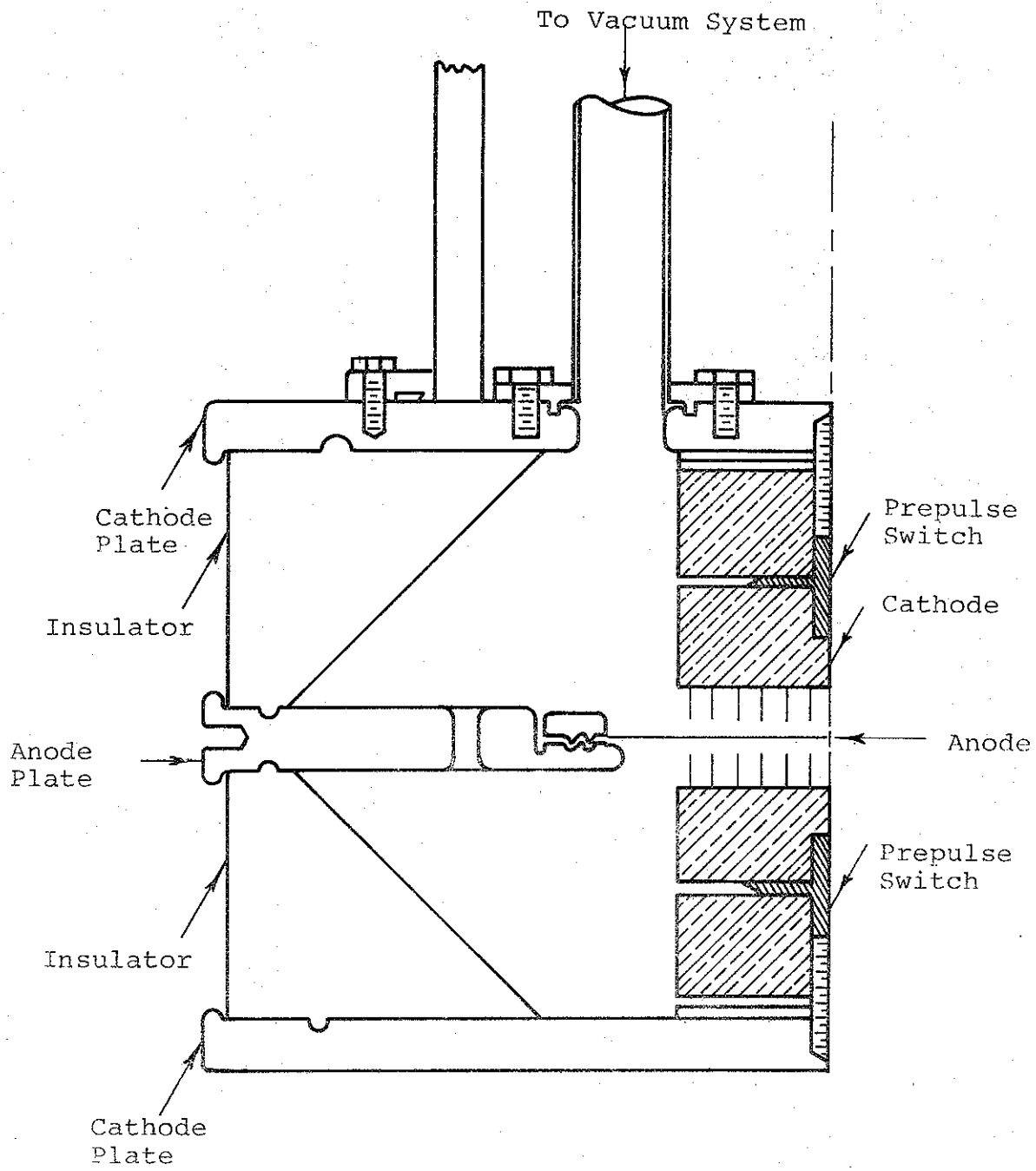

Figure 63 High-voltage line double-sided diode design

5690

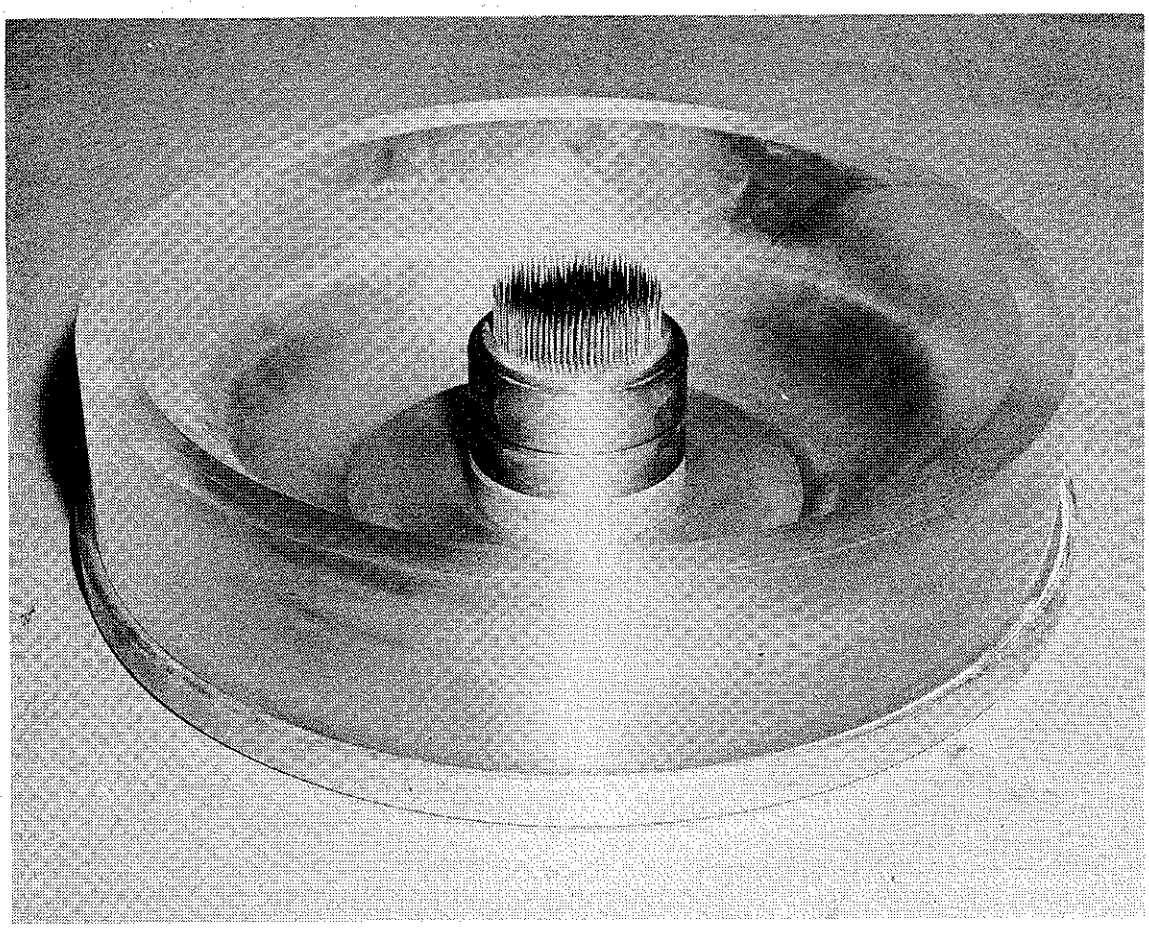

Figure 64 Bottom cathode plate with cathode in position.

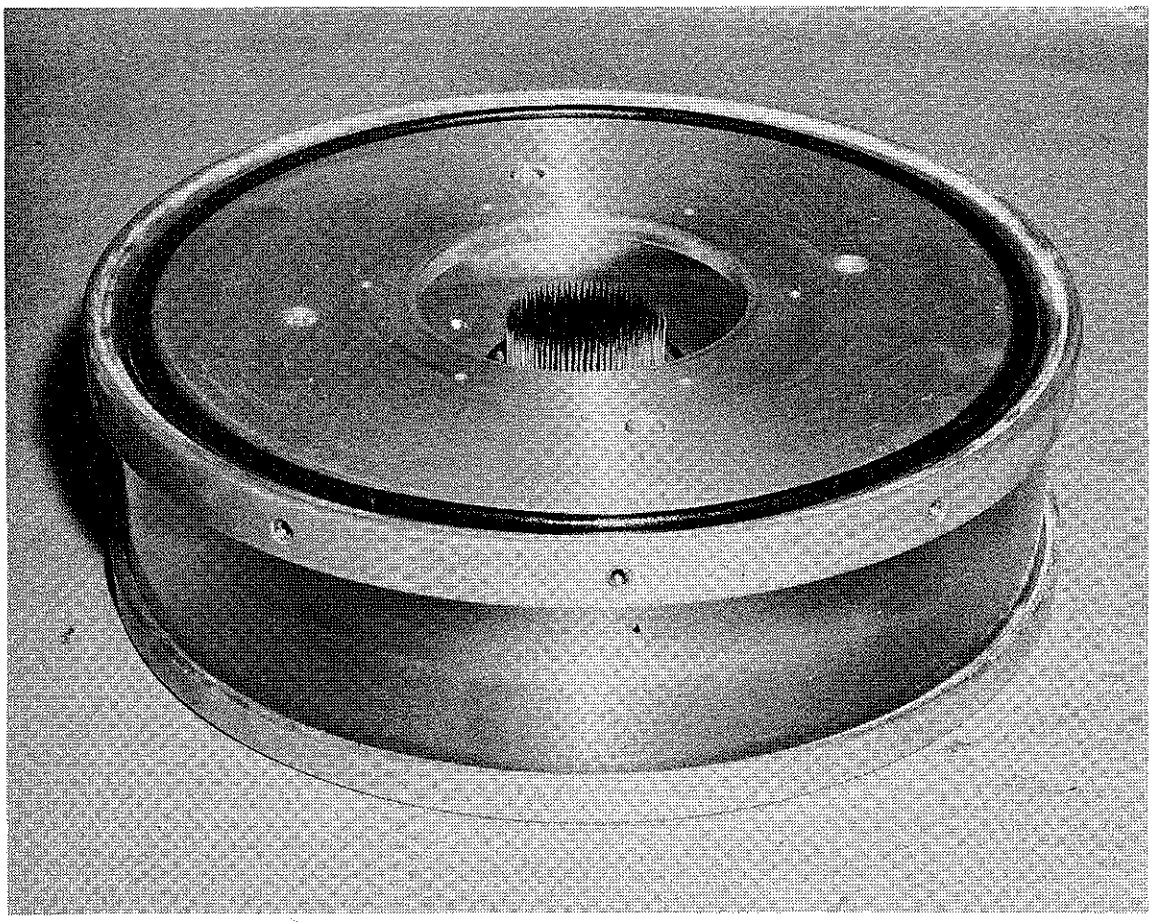

Figure 65 One cathode with anode plate in position.

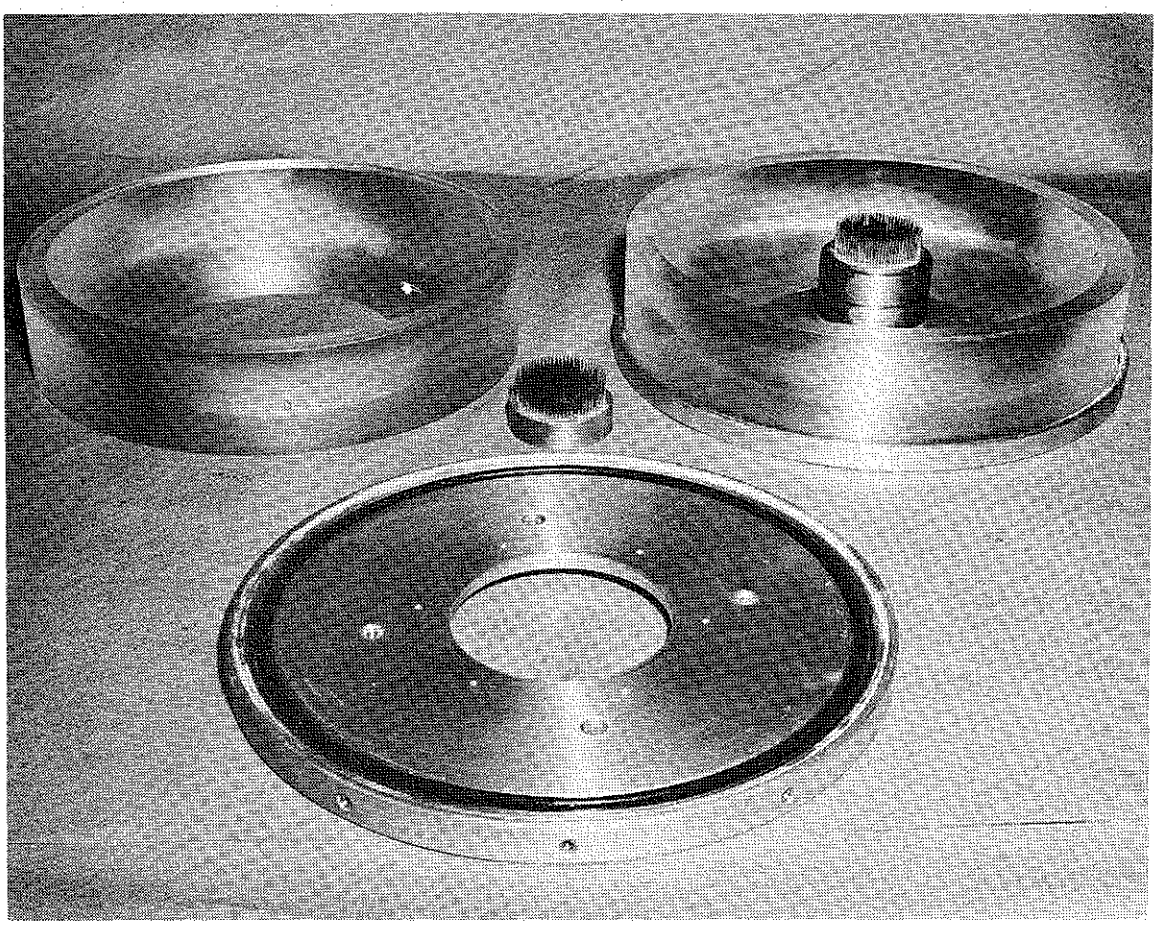

Figure 66 Tube disassembled - one cathode plate not shown.

6639

With the thick anode, and the diodes operating independently, tube behavior was diagnosed as typical. Most tests were performed with an anode-cathode spacing of 5 mm so that the tube approximately matched the line, which was charged to voltages of 150 to 300 kV. Having verified the expected diode behavior, we substituted thinner anodes. It was anticipated on the basis of the calculations described in paragraph 6.1 that a higher impedance would result when a space charge was increased by the multiple transits through the thin anodes, and that the increased electric field at the anode might speed the space charged neutralization by positive ions, resulting in an increase in the rate of fall of impedance during the pulse.

The results of the experiments with the needle cathodes are shown in the upper half of Table 1. The penetration depth for the electrons in the anode material divided by the thickness of the anode is the approximate number of times the electron should traverse the target. The table also lists the average values of the pulse charge and output voltages. Voltage and current monitors were used to determine the tube impedance at the end of pulse. The impedance was in general quite stable. The impedance is described in the table by the value of the constant k, calculated from the formula

$$Z = \frac{k\, d^2}{r^2 V^{\frac{1}{2}}}\ \Omega$$

where V is the tube voltage in megavolts, d is the anode-cathode spacing, and r is the cathode radius.

As can be seen from the data, there is, in fact, no obvious dependence of the impedance on the anode thickness. The data are somewhat scattered, but in general are consistent with the usual lowered Child's law constant, whatever the number of electron transients. This unexpected result made it apparent that the

TABLE 1

EXPERIMENTAL RESULTS FOR NEEDLE AND SCREEN CATHODES

Anode	Penetration depth thickness, mg/cm2	<pulse charge, kV>	<output, kV>	<k>
	Needle Cathode 2.5 mm A-K			
55 mg/cm^{2}Al	0.91	200	130	89
55 mg/cm^{2}Al	0.62	160	115	97
6.9 mg/cm^{2}Al	5.2	165	130	117
	Needle Cathode 5.0 mm A-K			
137 mg/cm^{2}Al	0.59	280	300	81
55 mg/cm^{2}Al	1.6	300	350	115
55 mg/cm^{2}Al	0.62	160	170	60
6.9 mg/cm^{2}Al	12.5	300	250	53
6.9 mg/cm^{2}Al	5.6	160	130	55
1 mg/cm^{2}Al-	91	300	360	118
	Screen Cathode 5.0 mm A-K			
55 mg/cm^{2}Al	0.91	200	230	108
55 mg/cm^{2}Al	0.4	120	160	134
6.9 mg/cm^{2}Al	7.1	200	240	125
6.9 mg/cm^{2}Al	3.2	120	150	110
1 mg/cm^{2}Al-	91	300	360	160
1 mg/cm^{2}Al-	52.5	210	220	100
1 mg/cm^{2}Al-	25	130	170	150
21 mg/cm^{2}Ta	2.1	215	220	110
21 mg/cm^{2}Ta	1.3	140	140	70
12 mg/cm^{2}Au	4.5	210	215	76

impedance could not be used as a confirmation of the processes occurring in the diode. It also is inconsistent with a space charge limited model for the diode. It was clearly unprofitable to proceed further without attempting to determine if the primary electrons were being absorbed by the foil or, by some mechanism, were being returned to the cathode. At the same time, it was desirable to proceed to a cathode transparent to X-rays in order to study a diode more useful in practice.

The possibility that the anode could be made extremely thin without restricting the current density by increasing the space charge suggested that the problem of containing the exploded anode material, usually severe in high current tubes, could be made quite trivial. Therefore, a cathode was devised that was thinner and even more transparent to X-ray than the roughened, low-Z plate originally intended for this application. This new cathode design consisted of a metal screen, which could be backed with just enough material to protect the sample from the anode vapor. The adaptation of this principle to the existing cathode holder is shown in Figure 67. The screen covers the aperture usually occupied by the needle holder, and there is a volume behind the screen suitable for installing TLDs.

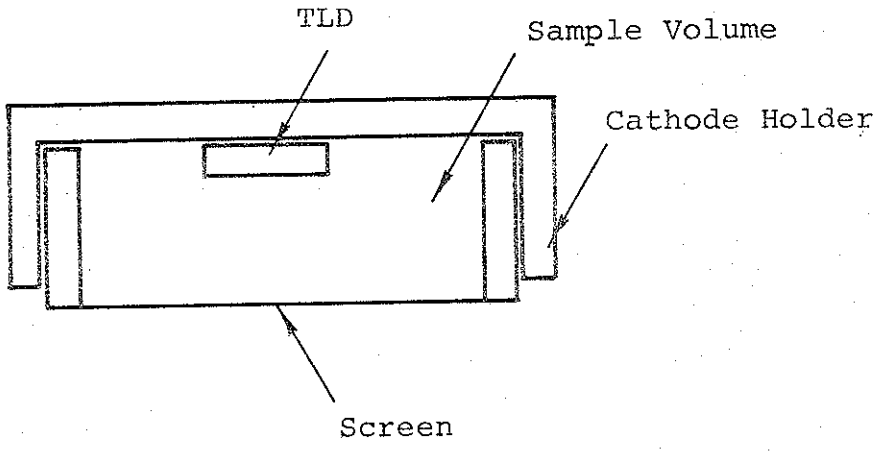

Figure 67 Screen cathode.

The screen cathode was used with as wide a range of atomic numbers as possible in the material of the anode foil. The foil thickness again varied from nearly a full electron penetration depth down to a small fraction of that depth in order to permit multiple electron transits.

The impedance observed for the screen cathode was somewhat higher than that obtained with the needle points, probably because the field enhancement of the wires was lower. However, the result of the impedance being essentially independent of anode thickness was again obtained. In addition, the X-ray intensity, while appearing to be unaffected by the anode thickness, was approximately proportional to the atomic number, consistent with the assumption that the X-rays originated only from the anode. Finally, the X-ray intensity was uniform across the anode, indicating that no pinch was occurring. From the measurements made, it cannot be completely ruled out that a significant fraction of the total current flows near or outside the cathode edge.

The results of the preliminary study of the two-sided diode are summarized as follows. The current density is approximately the same as that for a conventional diode with the same spacing. It appears that the electrons can indeed be absorbed by an anode foil very much thinner than their range and that space charged limitation does not apply. The electron streams do not pinch. Cathodes transparent to X-rays can easily be made. By greatly reducing the thickness and consequently the X-ray attenuation of both the anode and the material required to contain the anode debris, it should be possible to obtain enhanced doses of low-energy X-rays, uniform over large areas. A softer X-ray spectrum will result from any given accelerating voltage if this technique is employed. This technique is probably most suited to producing low and intermediate doses over very large areas, with considerable gains in efficiency.

REFERENCES

1. G. Yonas, P. Spence, B. Ecker, and J. Rander, Dynamic Effects of High ν/γ Beam Plasma Interactions, Physics International Company Report PIFR-106-2, August 1969.

2. G. Yonas, P. Spence, D. Pellinen, B. Ecker, and S. Heurlin, Dynamic Effect of High ν/γ Beam-Plasma Interactions, DASA 2296, April 1969.

3. G. Yonas and P. Spence, Experimental Investigation of High ν/γ Electron Beam Transport, DASA 2175, October 1969.

4. J. Benford, B. Ecker, G. Yonas, Propagation in Pre-Ionized Media, Physics International Report PIIR-10-70, December 1969.